

https://dspace.org/

Research report into the use of portable x-ray fluorescence technology at Styldrift I Mine; Western Bushveld Complex; South Africa: Identification of small-scale mineralization variation of Merensky Reef facies types using handheld XRF analyzer and statistical correlation analyses between platinum group elements and base metals for the purpose of underground stope cut optimization

Moodley, Yusavia

2017

http://hdl.handle.net/10539/23617

Moodley, Yusavia (2017) Research report into the use of portable x-ray fluorescence technology at Styldrift I Mine; Western Bushveld Complex; South Africa, University of the Witwatersrand, Johannesburg, <http://hdl.handle.net/10539/23617>

Downloaded from a DSpace repository. https://dspace.org/

Research Report into the Use of Portable X-ray Fluorescence Technology

at Styldrift I Mine; Western Bushveld Complex; South Africa

Yusavia Moodley

Student Number: 0612589A



School of Engineering and the Built Environment

University of the Witwatersrand

Johannesburg, South Africa

A research report submitted to the Faculty of Engineering and the Built Environment, University of the Witwatersrand, Johannesburg, in partial fulfilment of the requirements for the degree of Master of Science in Engineering.

2017

Declaration

I declare that this research report is my own unaided work. The research covers work undertaken at Styldrift I Mine which is part of the Bafokeng Rasimone Platinum Mine Joint Venture. It is being submitted for the Degree of Master of Science in Engineering by advanced coursework and research to the University of the Witwatersrand, Johannesburg. It has not been submitted for any degree or examination to any other University.



_____

Yusavia Moodley

Signed on the 20th day of April 2017

Table of Contents

Acknowledgements ..... **i**

Abstract ..... **ii**

List of Figures ..... **iii**

List of Tables ..... **vi**

List of Terms ..... **vii**

Chapter One: Introduction **1**

1.1 The Bushveld Complex 1

1.2 Mine Background and History 1

1.3 The Research Aim 3

1.4 The Research Objectives 4

Chapter Two: Literature Review **6**

2.1 Merensky Stratigraphy 6

2.2 Merensky Regional Facies Classification 8

2.3 Merensky Local Facies Classification 9

2.4 The Merensky Mineralisation 13

2.5 Portable X-ray Fluorescence (pXRF) Technology 19

2.6 Application of pXRF in the Mining and Minerals Industry 21

2.7 Using Copper/Nickel as PGE Pathfinders 25

Chapter Three: Methodology **29**

3.1 QAQC of Laboratory Data 29

3.1.1 Laboratory Data Accuracy Analysis 29

3.1.2 Laboratory Data Precision Analysis 30

3.2 pXRF Calibration 32

3.3 Hypothesis One: pXRF Accuracy Test 34

3.3.1 Sample Selection 34

3.3.2 Sample Preparation 34

3.3.3 Sample Analysis 35
3.3.4 Result Interpretation 35
3.4 Hypothesis Two: Copper and/or Nickel as a proxy for PGE content 38
3.4.1 Multivariate Data Analysis 38
3.5 Investigation into the Use of the pXRF in an Underground Environment 39
Chapter Four: Results 40
4.1 QAQC of Laboratory Data 40
4.1.1 Accuracy of Laboratory Data 40
Table 3: Percentage Bias per Standard and Element Analysed 40
4.1.2 Precision of Laboratory Data 41
4.1.3 Data Validation 45
4.2 pXRF Calibration 45
4.3 Hypothesis One: pXRF Accuracy Test 49
4.4 Hypothesis Two: Copper and/or Nickel as a proxy for PGE content 58
4.4.1 Multivariate Data Analysis 58
i. Lateral Zone Analysis 66
ii. Lithology Analysis 66
iii. Stratigraphic Analysis 69
iv. 3E Grade Analysis 71
4.4.2 Regression of the Merensky Footwall 73
4.5 Investigation into the Use of the pXRF in an Underground Environment 74
Chapter Five: Discussion 85
Chapter Six: Recommendations and Conclusion 91
6.1 Recommendations 91
6.2 Conclusion 92
References 93
Appendix 96
7.1 Appendix A: CRM Certificates 96

7.2 Appendix B: CRM Result Graphs 101

7.3. Appendix C: Niton XL3T GOLDD pXRF Specifications 120

7.3 Appendix D: Drillholes Analysed for pXRF Accuracy Test 121

Acknowledgements

Thank you to Royal Bafokeng Platinum for providing financial assistance towards this qualification as well as allowing me the opportunity to gather and analyse data at Styldrift I Mine. I am thankful to my supervisor, Professor Richard Minnitt, for guidance towards this study. I am appreciative of the technical and academic advice, support and encouragement provided to me by Mayshani Dahya and my husband, Shaun Naidoo.

Abstract

The Merensky Reef vertical grade distribution is highly variable within Styldrift I Mine. The variable nature of the Merensky Reef mineralisation necessitates regular and timeous updating of the planned mining cut with sampling information so that the optimum can be applied during mining operations. The current geochemical assay analysis that is used for the analysis of platinum group elements (PGEs) has been proven to be accurate and precise however it is expensive with long turn-around times from the laboratory. Portable X-ray fluorescence (pXRF) technology has been tested as an alternative to measure the platinum group element content along the Merensky Reef. pXRF technology cannot accurately measure PGE content directly. Copper and nickel are detectable by the pXRF analyser and, like PGEs, copper and nickel mineralisation peaks along Merensky Reef horizon. Copper and nickel were therefore tested as potential pathfinder elements to target PGE mineralisation along the Merensky Unit. The testing of the pXRF analyser was undertaken by analysing the accuracy of the results it produces as well as determining if a regression between copper/nickel to PGE content is possible along the Merensky Unit. The pXRF did not produce results of adequate accuracy as a consistent significant bias was detected with pXRF results which were consistently lower than laboratory results. Calibration of the pXRF using site specific samples was not sufficient to overcome the bias. Regressions from copper/nickel to PGEs were tested for the Merensky Footwall which could be isolated as a single data population. Significant outliers exist that do not fit the regression analysis due to the inconsistent PGE modes of occurrence along the Merensky Unit. Application of the pXRF to the study area therefore does not meet the required conditions. An underground trial of the pXRF has indicated that peaks in pXRF copper and nickel results often, but not always, coincide with peaks in PGE mineralisation. The pXRF can therefore be used as a low confidence indicator of PGE mineralisation however the user must be aware of the limitations of the instrument. pXRF analysis cannot be used reliably therefore geochemical assay analysis remains the most reliable method to analyse PGE content at Styldrift I Mine.

List of Figures

Figure 1. Geological map of the Bushveld Complex indicating the three major limbs and stratigraphic zones (Padiachy, 2015) 1
Figure 2. BRPM JV operations comprised of North, South (BRPM) and Styldrift mines (RBPlat, 2016). 2
Figure 3. Location of Western Limb mines indicating Merensky Reef outcrop in red, (taken from RBPlat, 2010) 3
Figure 4. Generalised stratigraphy of a). Rustenburg Layered Suite (left) and b). Upper Critical Zone (right) (taken from Smith, Basson and Reid, 2004)..... 6
Figure 5. Generalised stratigraphy of Styldrift I (Vermeulen, 2010)..... 7
Figure 6. Bushveld Complex Western Limb facies types (RBPlat, 2016)..... 8
Figure 7. Merensky Reef facies domain across the BRPM JV with Styldrift I mining area outlined in red (taken from Vermeulen, 2010) 9
Figure 8. Merensky Reef intersection drilled in the Abutment Facies (Smith, 2014)..... 10
Figure 9. Merensky Contact Reef drilled in the Central Reef Facies (Smith, 2014) 11
Figure 10. Potholed Merensky Reef intersection drilled in the Terrace Facies (Smith, 2014) 12
Figure 11. Normal reef intersection with pegmatoid developed between the Merensky Top and Bottom Reef Chromitite Stringers (Smith, 2014)..... 13
Figure 12. Generalised stratigraphy and grade distribution of the Merensky Reef across mines on the western and eastern limbs of the Bushveld Complex (taken from Smith, 2014)..... 14
Figure 13. Variable grade distributions within the Central Reef Facies of BRPM (taken from Smith, 2014) 15
Figure 14. 4PGE (4E), sulphur (S), copper (Cu) and nickel (Ni) mineralisation trend along BRPM Merensky Reef intersection (taken from Smith, 2014) 18
Figure 15. 4PGE (4E), sulphur (S), copper (Cu) and nickel (Ni) mineralisation trend along BRPM Merensky Reef intersection (taken from Smith, 2014) 18
Figure 16. Fluorescence and scatter from X-ray interaction with a sample (Brouwer, 2010)..... 19
Figure 17. Typical exterior of a portable XRF machine (taken from United States Patent, 2011) 20
Figure 18. pXRF analyser during the X-ray fluorescence process (Thermo Scientific, 2015)..... 21
Figure 19. Plutonic Gold Mine geologist visual mineralisation intensity logging ('As logged') versus pXRF mineralisation classification ('Schema') (Gazley et al., 2014)..... 23
Figure 20. Yttrium/titanium versus zircon/titanium plot of pXRF results (Zhang and Lentz, 2016)..... 24
Figure 21. Yttrium/titanium versus zircon/titanium plot of pXRF results (Zhang and Lentz, 2016)..... 25
Figure 22. Thermo Scientific study on samples indicates positive correlations between pathfinder and target elements..... 27

Figure 23. Scatter plot of an indirect relationship showing the residual (difference between the actual and predicted value) (Clark and Harper, 2000) 28
Figure 24. Drillhole sampling and QAQC procedure 31
Figure 25. Thermo Scientific Niton XL3T GOLDD pXRF analyser used for investigation 32
Figure 26. Laboratory prepared homogenous pressed pellets used to test accuracy and precision of handheld XRF 33
Figure 27. Core being cleaned with plastic brush to remove dust and foreign particles prior to handheld XRF analysis 34
Figure 28. pXRF sample spacing intervals across a geological sample 35
Figure 29. Methodology of Hypothesis One 37
Figure 30. Methodology of Hypothesis No. 2 (Determining if a quantifiable relationship exists between copper and/or nickel and PGE) 38
Figure 31. Methodology of pXRF underground trial 39
Figure 32. Platinum Twinstream Results (Leg 1 versus Leg 2); outliers indicated in red 42
Figure 33. Palladium Twinstream Results (Leg 1 versus Leg 2); outliers indicated in red 43
Figure 34. Gold Twinstream Results (Leg 1 versus Leg 2); outliers indicated in red 43
Figure 35. Copper Twinstream Results (Leg 1 versus Leg 2) 44
Figure 36. Nickel Twinstream Results (Leg 1 versus Leg 2); outliers indicated in red 44
Figure 37. Pressed pellet pXRF copper results versus laboratory results 46
Figure 38. Pressed pellet pXRF nickel results versus laboratory results 46
Figure 39. Pressed pellet pXRF copper versus laboratory results per pressed pellet sample analysed 47
Figure 40. Pressed pellet pXRF nickel versus laboratory results per pressed pellet sample analysed. 48
Figure 41. Drillhole No.1 pXRF Results versus Laboratory XRF Results 50
Figure 42. Drillhole No.2 pXRF Results versus Laboratory XRF Results 51
Figure 43. Drillhole No.3 pXRF Results versus Laboratory XRF Results 52
Figure 44. Drillhole No.4 pXRF Results versus Laboratory XRF Results 53
Figure 45. Drillhole No.5 pXRF Results versus Laboratory XRF Results 54
Figure 46. Copper Versus Laboratory 3E Grade Content 58
Figure 47. Nickel Versus Laboratory 3E Grade Content 59
Figure 48. Magnified data (log transformed and +3 constant) – copper/nickel versus 3E (left) indicating at least two data populations (right) 61
Figure 49. Copper grade frequency distribution within Styldrift I; Central Reef Facies 62
Figure 50. Nickel grade frequency distribution within Styldrift I; Central Reef Facies 63

Figure 51. 3E grade frequency distribution within Styldrift I; Central Reef Facies 64
Figure 52. Spatial plotting of Population One and Population Two Boreholes 66
Figure 53. Copper Versus 3E grade content coded by lithological type 67
Figure 54. Lithological sub-populations within the Copper versus 3E mineralisation populations 68
Figure 55. Nickel Versus 3E grade content coded by lithology of the sample 68
Figure 56. Lithological sub-populations within the Copper versus 3E mineralisation populations 69
Figure 57. 3E Versus Copper/Nickel (left) and resulting footwall trends (right) 70
Figure 58. 3E Versus Copper/Nickel (left) and resulting grade trends (right) 72
Figure 59. Merensky Footwall 3E versus Cu regression with outliers indicated in red 73
Figure 60. Merensky Footwall 3E versus Ni regression with outliers indicated in red 74
Figure 61. Section No. 1 Copper and Nickel pXRF Results versus Laboratory 3E Results 76
Figure 62. Section No. 2 Copper and Nickel pXRF Results versus Laboratory 3E Results 77
Figure 63. Section No. 3 Copper and Nickel pXRF Results versus Laboratory 3E Results 78
Figure 64. Section No. 4 Copper and Nickel pXRF Results versus Laboratory 3E Results 79
Figure 65. Section No. 5 Copper and Nickel pXRF Results versus Laboratory 3E Results 80
Figure 66. Section No.1 Laboratory 3E versus pXRF Copper (left) and Nickel (right) 82
Figure 67. Section No.2 Laboratory 3E versus pXRF Copper (left) and Nickel (right) 82
Figure 68. Section No.3 Laboratory 3E versus pXRF Copper (left) and Nickel (right) 83
Figure 69. Section No.4 Laboratory 3E versus pXRF Copper (left) and Nickel (right) 83
Figure 70. Section No.5 Laboratory 3E versus pXRF Copper (left) and Nickel (right) 83
Figure 71. Standard Certificates G1, G2 and G3 96
Figure 72. Standard Certificates G4, G6 and G8 97
Figure 73. Standard Certificates G9, G10 and G11 98
Figure 74. Standard Certificates G13 and blanks G20 and G21 99
Figure 75. Standard Certificates G24, G25 and AMIS0151 100
Figure 76. Platinum results of standards AMIS0151, G1, G10 and G13 101
Figure 77. Platinum results of standards G2, G21, G24 and G25 102
Figure 78. Platinum results of standards G3, G4, G6 and G8 103
Figure 79. Platinum results of standard G9 and blanks G11, G20 and AMIS0350 104
Figure 80. Palladium results of standards AMIS0151, G1, G10 and G13 105
Figure 81. Palladium results of standards G2, G21, G24 and G25 106
Figure 82. Palladium results of standards G3, G4, G6 and G8 107
Figure 83. Palladium results of standards G9, G11, G20 and AMIS0350 108
Figure 84. Gold results of standards G1, G13, G2 and G24 109

Figure 85. Gold results of standards G3, G8, G9 and blank AMIS0350 110
Figure 86. Gold results of blanks G11 and G20 111
Figure 87. Copper results of standards G1, G13, G2 and G21 112
Figure 88. Copper results of standards G3, G4, G6 and G8 113
Figure 89. Copper results of standards G9 and blanks G11, G20 and AMIS0350 114
Figure 90. Copper results of blank G10 115
Figure 91. Nickel results of standards AMIS0151, G1, G13 and G2 116
Figure 92. Nickel results of standards G25, G24, G3 and G4 117
Figure 93. Nickel results of standards G6, G8, G9 and blank G10 118
Figure 94. Nickel results of blanks G21, G11, G20 and AMIS0350 119
Figure 95. Drillhole No.1 used for Core Analysis 121
Figure 96. Drillhole No.2 used for Core Analysis 122
Figure 97. Drillhole No.3 used for Core Analysis 123
Figure 98. Drillhole No.4 used for Core Analysis 124
Figure 99. Drillhole No.5 used for Core Analysis 125

List of Tables

Table 1: Merensky mineral groups and types (Schouwstra et al. 2000) 16
Table 2: Breakdown of sample types in the drillhole dataset 29
Table 3: Percentage Bias per Standard and Element Analysed 40
Table 4: Precision statistics for drillhole dataset used for investigation 42
Table 5: Sample occurrences where pXRF result is greater than laboratory result 55
Table 6: F Test Statistics and Variance Comparisons between pXRF and laboratory datasets per drillhole (unequal variance highlighted in red) 55
Table 7: T Test Statistics and Mean Comparisons of pXRF Versus Laboratory Results (population differences highlighted in red) 56
Table 8: F Test Statistics of Population 1 and Population 2 65
Table 9: T Test Statistics of Population 1 and Population 2 65
Table 10: Data populations and associated lithologies 67
Table 11: Sample occurrences where pXRF result is greater than laboratory result 84
Table 12: Niton XL3t GOLDD pXRF Analyser specifications (Thermo Scientific, 2017) 120

List of Terms

Term	*Definition*
3E	Sum of platinum, palladium and gold assay values.
4PGE	Sum of platinum, palladium, rhodium and gold assay values.
Blank	Certified reference material with trace grades of the element of interest. Blanks are inserted into sample batches with the objective of testing possible laboratory contamination.
Bulk Modal Analysis	Mineralogical study to determine the mineral composition of a rock type.
BRC	Bottom Reef Chromitite – The lowermost Merensky Chromitite which is approximately 2 cm thick.
Certified Reference Material	Control sample of a known grade which is added to a sampling batch to test the accuracy of the laboratory analysis.
Contamination	The addition of foreign sample material to a sample during laboratory analysis which negatively affects the accuracy of the sample result.
Control Samples	Quality control samples inserted in a sample batch to test accuracy of the laboratory analysis.
CRM	Certified Reference Material - Control sample of a known grade which are added to sampling batches to test the accuracy of the laboratory analysis.
Lead Collection Fire Assay	Geochemical assay method commonly used to analyse platinum group elements. Lead is used as a collector of the elements being analysed.
Lower Detection Limit	The lowest quantity which an analytical method can detect the concentration of the element of interest.

Merensky Reef	The economically feasible stope cut along the Merensky Chromitite and its overlying and underlying stratigraphic units (i.e. Merensky Pyroxenite and underlying Footwall lithologies, e.g. Footwall One).
Merensky Unit	The Merensky Reef Chromitite and associated overlying and underlying stratigraphic zones which may or may not be economically feasible to mine.
PGE	Platinum group elements, i.e. platinum, palladium, rhodium, iridium, ruthenium and osmium.
Power Function	Method to identify twinstream outliers that is based on the Thompson and Howarth precision curve.
Pressed Pellet XRF	Geochemical assay method using X-ray Fluorescence to analyse base metals including copper and nickel. This method uses pulverised, homogenous sample material to prepare hardened disks which are then inserted into the XRF machine.
Primary Samples	Geological core samples that are submitted for laboratory analysis (exclusive of quality control samples).
pXRF	Portable (handheld) X-ray fluorescence analyser.
Standard	A certified reference material of known element concentration that is inserted to test the accuracy of a laboratory analysis.
Trace Element Analysis	Mineralogical study to determine the trace element composition of a minerals within a rock type.
Twinstream Analysis	Splitting of a sample into two separate streams or legs each of which are analysed separately to test the precision of the laboratory analysis.

Chapter One: Introduction

1.1 The Bushveld Complex

The Bushveld Complex is the world's largest layered igneous intrusion covering an area of 65 000 km^2 and reaching a thickness of up to 7 km. It is separated into three major exposed limbs namely the Western, Eastern and Northern limbs (Figure 1) and hosts approximately 80% of the world's platinum group element (PGE) deposits. The PGE deposits are mainly enriched in a major stratigraphic zone called the Upper Critical Zone within three horizons known as the Merensky Reef, Upper Group 2 (UG2) and Platreef (Cawthorn, 1999).

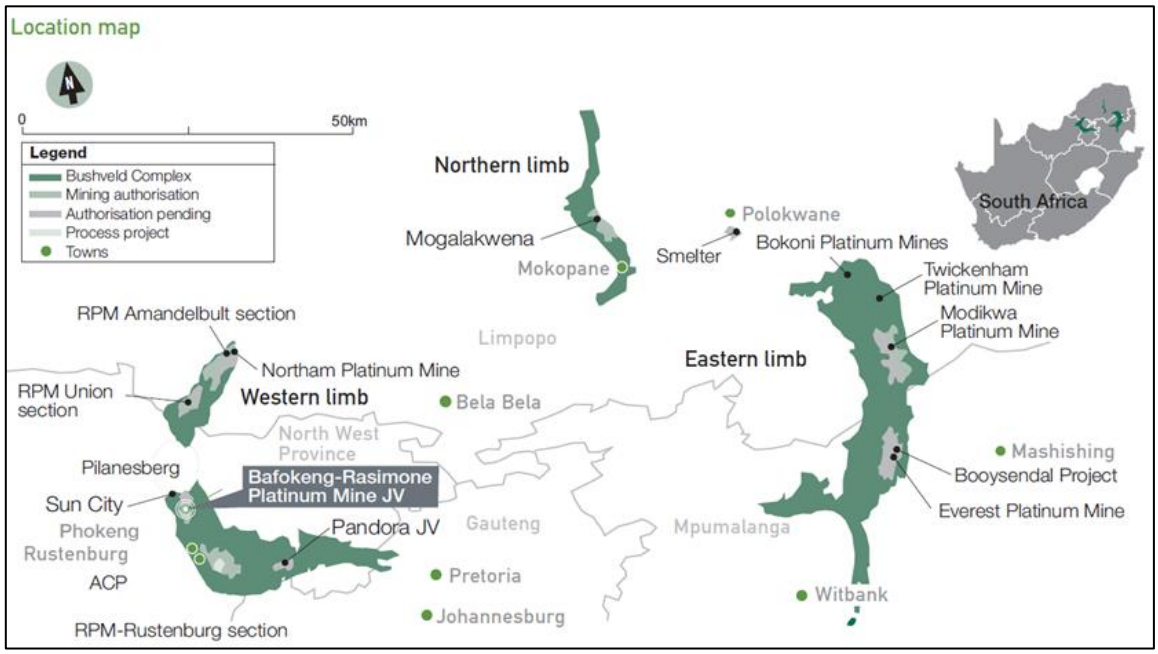

Figure 1. Geological map of the Bushveld Complex indicating the three major limbs and stratigraphic zones (Padiachy, 2015)

1.2 Mine Background and History

The BRPM JV (Bafokeng Rasimone Platinum Mine Joint Venture) is a joint venture between Royal Bafokeng Platinum (RBPlat), the majority shareholder and Anglo American Platinum. It is located 30 km northwest of the town Rustenburg in the North West Province of South Africa on the Boschkoppies, Styldrift and Frischgewaagd farms. Geologically it occurs south of the Pilanesberg Alkaline Complex on the western limb of the Bushveld Complex. It is found atop the only shallow PGE bearing reserves remaining in South Africa. The BRPM JV consists of North and South Shafts which

comprise the Bafokeng Rasimone Platinum Mine (BRPM), Styldrift I Mine and Styldrift II Project (Figure 2).

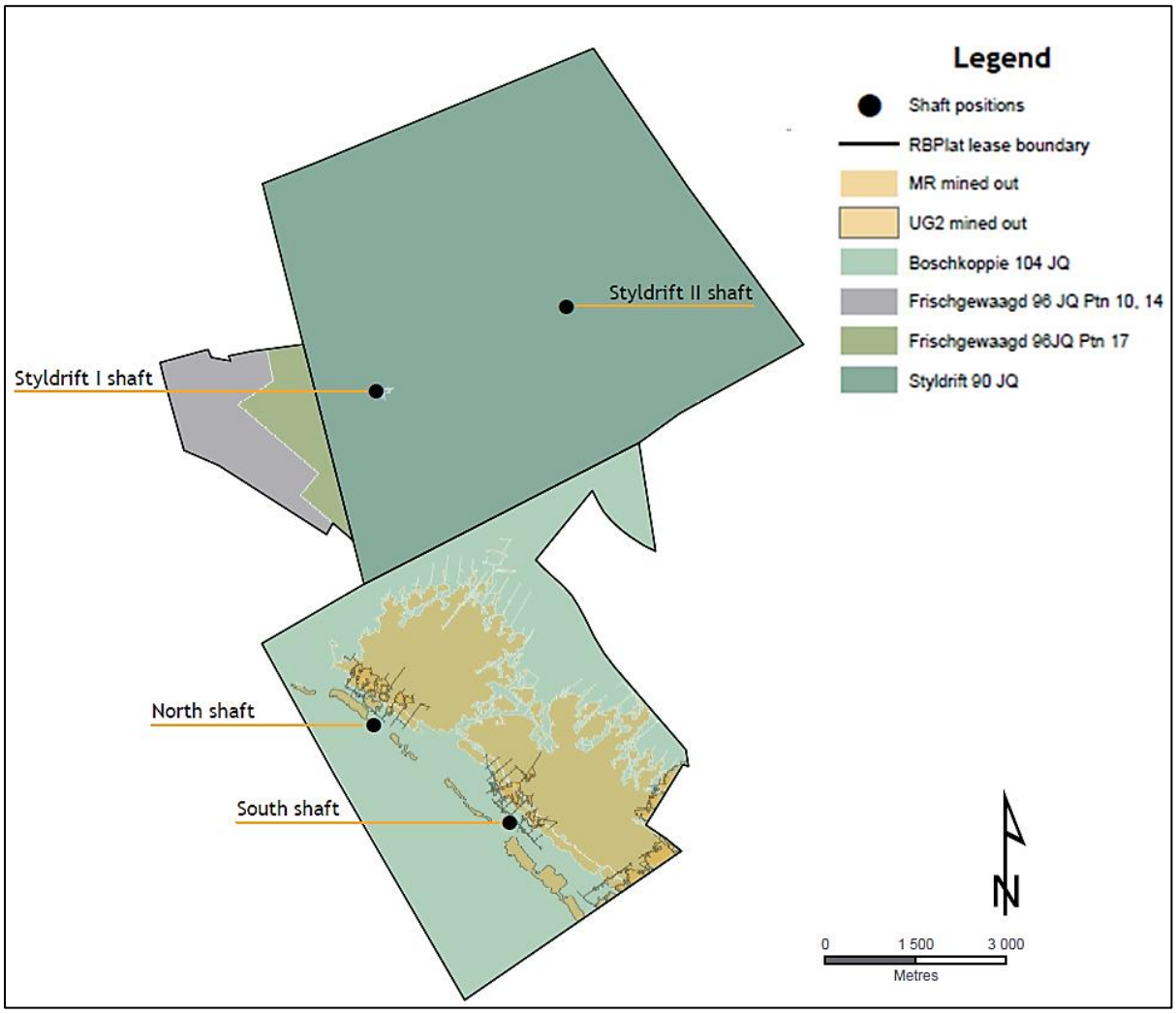

Figure 2. BRPM JV operations comprised of North, South (BRPM), Styldrift I Mine and Styldrift II Project (RBPlat, 2016)

The first platinum exploration in the area was undertaken in 1950 but was soon abandoned by 1956 as the area was considered too complex for mining operations at the time. Exploration resumed in 1993 by Anglo American Platinum. A successful exploration campaign resulted in open pit mining at BRPM in 1997 followed by underground operations (North and South Shafts) in 1998 which are ongoing today. Styldrift I is in the project phase and is scheduled to ramp up to steady state production in 2020 (Padiachy, 2015).

The mineable reef horizons of economic interest to the BRPM JV are the PGE bearing Merensky Reef and UG2 Reef (Figure 3) both of which occur stratigraphically within the Upper Critical Zone of the

Rustenburg Layered Suite (Cawthorn, Eales, Walraven, Uken and Watkeys, 2006). BRPM extracts both the Merensky and UG2 reef horizons. Styldrift I is planned for the mining of Merensky Reef only.

The Merensky Unit within Styldrift I is highly variable. Characteristics such as the Merensky Unit thickness, stratigraphic positioning and grade distribution are inconsistent across the area (Lionnet and Lomberg, 2006; Cawthorn, 2010). Bord and pillar method is planned in areas of thicker Merensky Reef while conventional mining is planned in narrow reef areas (RBPlat, 2016).

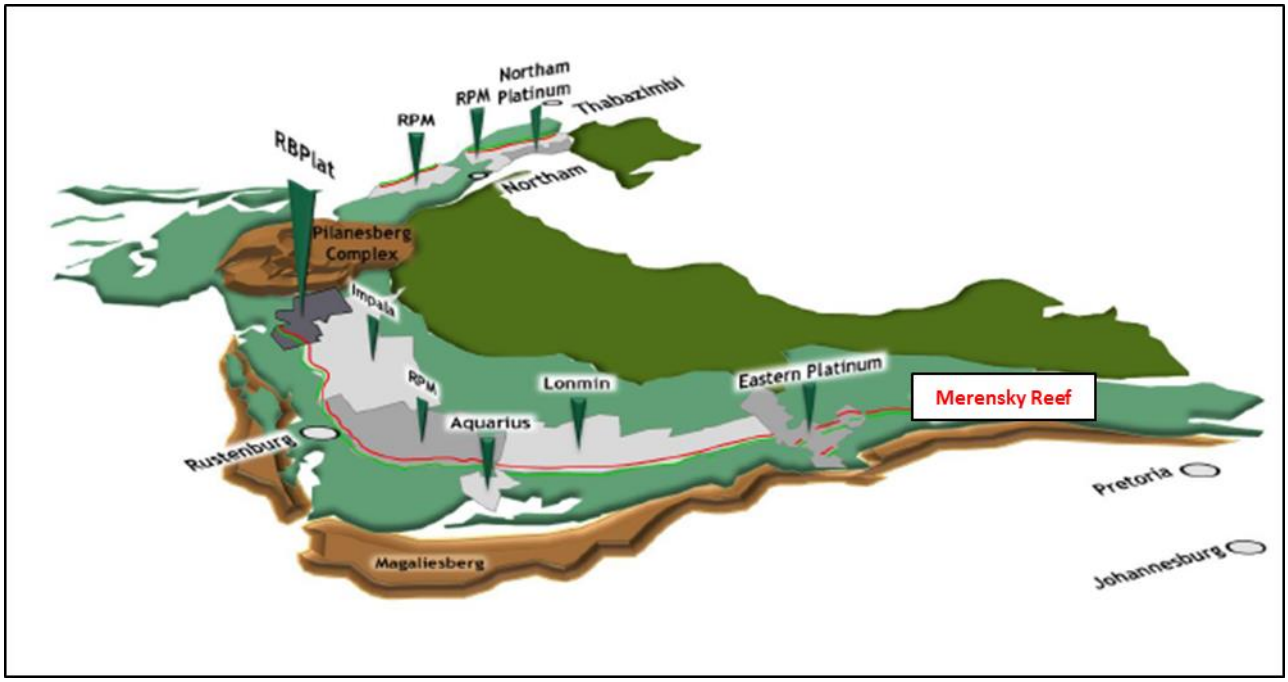

Figure 3. Location of Western Limb mines indicating Merensky Reef outcrop in red, (taken from RBPlat, 2010)

1.3 The Research Aim

The vertical Merensky Reef grade distribution within Styldrift I is highly variable therefore timeous, accurate and regular measurement of the PGE mineralisation is required. The PGE mineralisation results are used to update the applied stope cut underground to ensure that the most optimal cut (i.e. best cut) is extracted during mining.

Routine underground sampling is currently used to quantify 4PGE, copper and nickel grades. Sampling is undertaken by chip sampling along the length of the Merensky Unit at 10 – 15 cm sample intervals taken vertically. The samples are submitted to the laboratory for analysis. PGEs undergo geochemical

assay analysis using lead collection fire assay method. Base metals, copper and nickel, are analysed by pressed pellet X-ray Fluorescence (XRF).

Laboratory analysis is a trusted method to obtain PGE results as accredited laboratory facilities are used. Rigorous quality assurance and quality control (QAQC) procedures are used during the sampling process and to assess the laboratory analysis once results have been received (Moodley, 2015). However, laboratory sampling poses the following problems:

- High turn-around times of laboratory sample analysis and subsequent QAQC of laboratory results often takes up to six to eight weeks before laboratory results may be applied to update the stope cut. The ground from which the samples were taken may be partially or fully mined before the stope cut is updated to the best cut using the laboratory assay data.
- Laboratory sampling is expensive with costs such as transportation of samples, laboratory analysis costs and the purchasing of certified reference materials (CRMs) for QAQC purposes. Premium prices are charged for decreased turn-around times of results.

The aim of this investigation is to test an alternative sampling method that may either fully or partially replace the current standard of laboratory analysis to alleviate the aforementioned problems associated with laboratory sampling.

1.4 The Research Objectives

The application of portable X-ray fluorescence (pXRF) technology is common across the automotive, jewellery, cement, oil, plastic, pharmaceutical and food industries. Use of the pXRF analyser within the mineralogical, exploration and mining industries has also been growing in line with other industries (Fisher, Gazley, Baensch, Barnes, Cleverley, and Duclaux, 2014). The main objective of this study is to test pXRF technology as an alternative method to laboratory sampling to delineate PGE mineralisation underground.

Direct pXRF analysis of precious elements such as PGEs and gold produces erroneous results. At low levels, these elements cannot be accurately quantified by direct pXRF analysis (Hall, Buchar and Bonham-Carter, 2011; Thermo Scientific, 2012; Hall, Page and Bonham-Carter, 2013; Le Vailant, Barnes, Fisher, Fiorentini and Caruso, 2014). However, pathfinder elements may be analysed to target the element of interest. A pathfinder element is an element which can be measured using pXRF technology and has a relationship or correlation to the target element (Charnley and Lentz, 2016; Fisher *et al.,* 2014; Thermo Scientific, 2012; Zhang and Lentz, 2016).

The objectives of the study are to test the two requirements for successful use of pXRF technology in the study area which are separated into Hypothesis One and Hypothesis Two. The final objective of the study is to test the pXRF in the underground environment. A brief description of each objective is listed:

i. Hypothesis One (H1)

The pXRF is required to produce accurate results if it is to replace laboratory sampling. Accurate sampling results allow for correct stope cuts to be applied underground. The use of data that is not representative will result in the application of a sub-optimal stope cut. The null and alternate hypothesis statements of the Hypothesis One test are listed as $H1_0$ and $H1_1$ respectively.

$H1_0$: The pXRF produces accurate copper/nickel results

$H1_1$: The pXRF does not produce accurate copper/nickel results

ii. Hypothesis Two (H2)

Copper and nickel is required to be an accurate consistent proxy for PGE content to successfully apply pXRF technology within the study area using pathfinder elements. The null and alternate hypothesis statements of the Hypothesis One test are listed as $H2_0$ and $H2_1$ respectively.

$H2_0$: Copper and/or nickel can be used to predict 3E content

$H2_1$: Copper and/or nickel cannot be used to predict 3E content

iii. Underground pXRF Trial

The underground environment has unique conditions including higher temperatures and pressures due to the depth of the mine. The rock surface is often damp, jagged and covered with dust due to blasting. A practical underground trial is therefore required to test everyday use and possible limitations which may be experienced by the user. An analysis of the underground data taken using the pXRF is required to determine if the results can be used.

Chapter Two: Literature Review

2.1 Merensky Stratigraphy

The Bushveld Complex intruded into the floor rocks of the Transvaal Supergroup. It is subdivided into four major rock suites called the Lebowa Granite Suite, Rashoop Granophyre Suite, Rustenburg Layered Suite and Rooiberg Group. The PGE enriched horizons occur within the Upper Critical Zone of the Rustenburg Layered Suite (Figure 4) (Cawthorn *et al.*, 2006; Kinnaird, 2016).

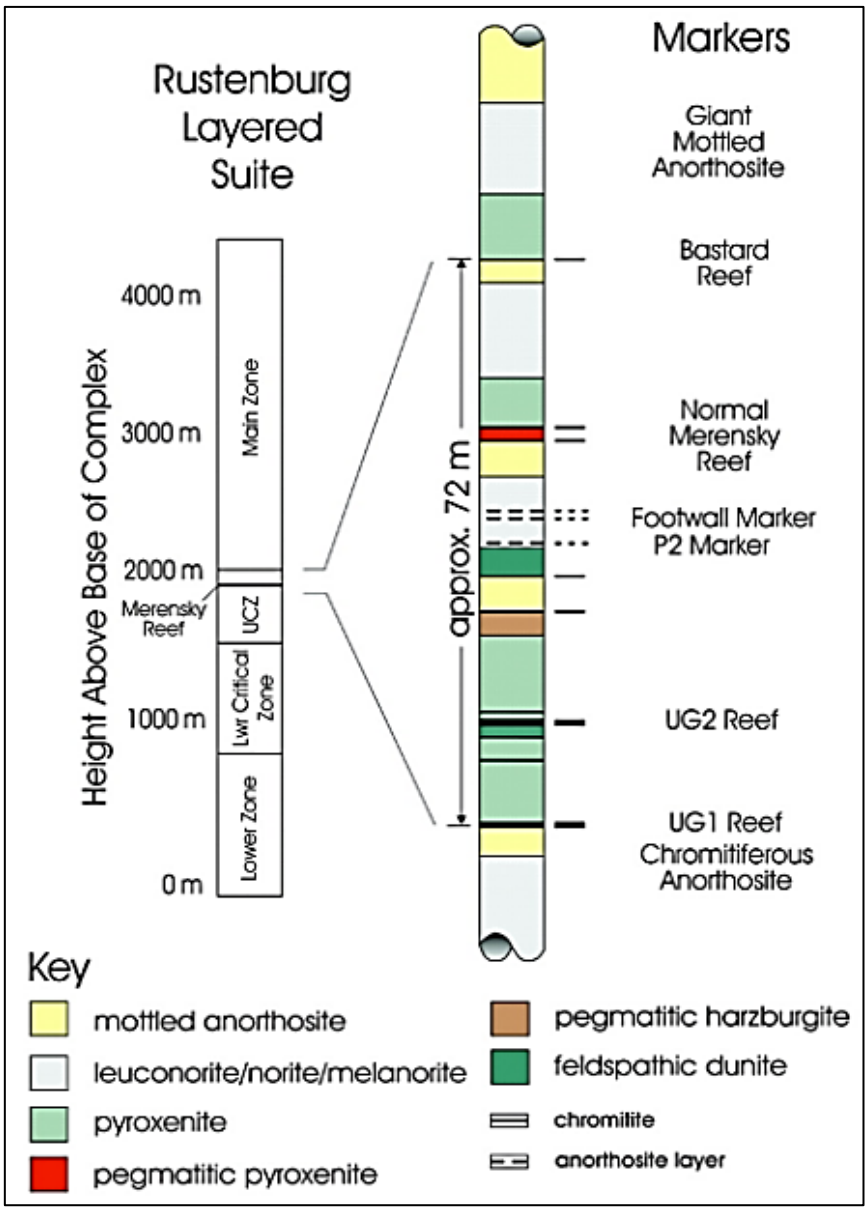

Figure 4. Generalised stratigraphy of a). Rustenburg Layered Suite (left) and b). Upper Critical Zone (right) (taken from Smith, Basson and Reid, 2004)

The Upper Critical Zone consists of well-developed cyclical units, the names of which have been modified by RBPlat from the nomenclature system developed by Leeb du Doit (1986). The stratigraphic layers which underlie the lower most Merensky Chromitite (known as the Bottom Reef Chromitite - BRC) are called footwall layers. The footwalls range from Footwall 14 ('FW14') upwards to Footwall 1 ('FW1'). The immediate pyroxenitic hangingwall which overlies the top most Merensky chromitite is termed the 'Merensky Pyroxenite'. The lithologies overlying the Merensky cyclical unit are called hangingwall layers. The generalised stratigraphy of the Styldrift I is depicted in Figure 5.

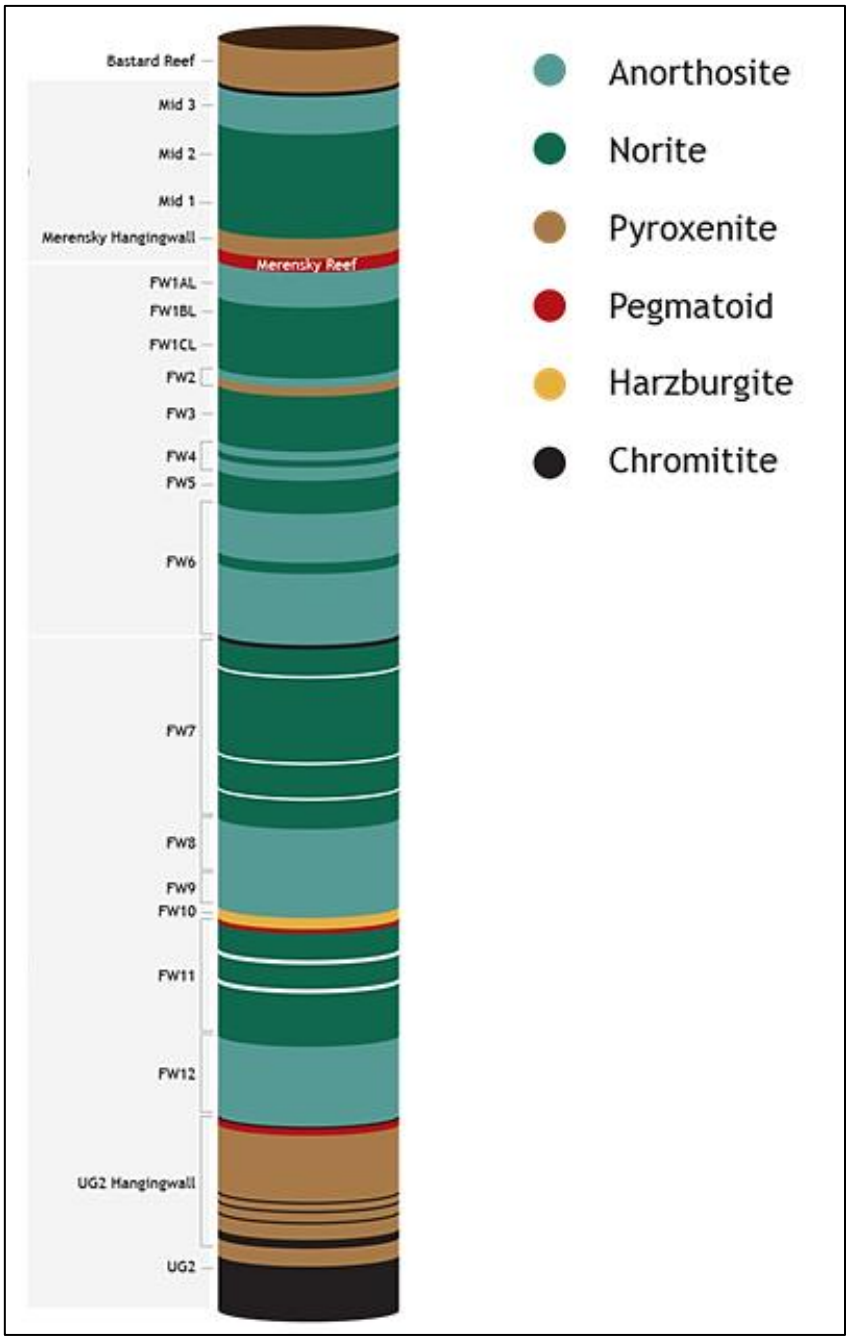

Figure 5. Generalised stratigraphy of Styldrift I (Vermeulen, 2010)

2.2 Merensky Regional Facies Classification

The Merensky Reef was discovered by Dr Hans Merensky and Andries Lombaard in 1925 (Wagner, 1929). Soon after the discovery, distinguishing features of Merensky facies types were identified by Wagner (1929) who then subdivided the western limb of the Bushveld Complex into the Swartklip Facies to the north east and the Rustenburg Facies to the south west and are roughly divided by the Pilanesberg Alkaline Complex (Figure 6). These facies classifications are still used today (Viljoen, 1994; Vermeulen, 2010).

There is a marked thinning of the vertical separation or middling distance between the Merensky Reef and UG2 reef towards the Swartklip facies (Viljoen, 1994). The Swartklip facies contains prominent feldspathic harzburgite layers in the Merensky footwall. These layers are referred to as Pseudo Reef due to its close resemblance to the Merensky Reef. It is poorly developed in the Rustenburg Facies (Vermeulen, 2010).

A pothole is an elliptical to sub-circular feature where the reef transgresses into underlying stratigraphic units (Lee, 1996). Merensky Reef potholes within the Swartklip facies are generally small and cause minimal disturbance to mining activities. Potholes within the Rustenburg facies are large, frequently occurring and often disturb mining activities (Smith, Viljoen, Schouwstra, Roberts, Schalkwyk and Gutzmer, 2013).

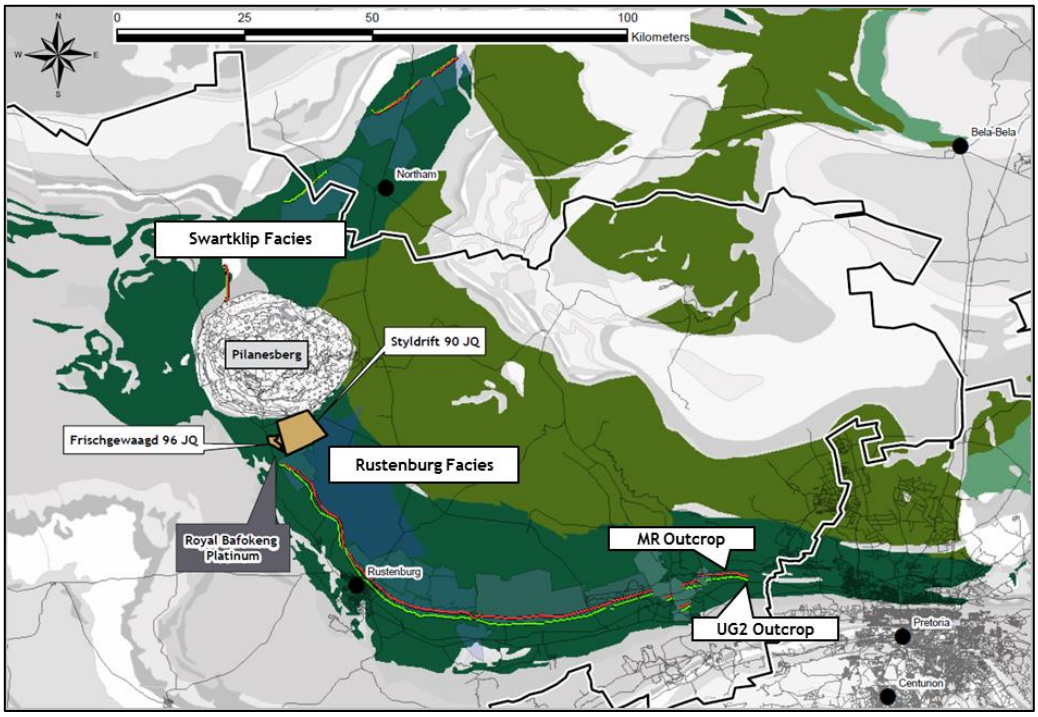

Figure 6. Bushveld Complex Western Limb facies types (RBPlat, 2016)

2.3 Merensky Local Facies Classification

Research has been undertaken to classify the facies within the BRPM JV on a smaller local scale. This has been undertaken due to the highly variable nature of the Merensky Reef within the BRPM JV (Lionnet and Lomberg, 2006; Moodley, 2008). The classification is largely controlled by the underlying Merensky footwall and the stratigraphic position of the Merensky reef. Lithological and structural characteristics have been considered to a lesser extent. Moodley (2008) identified eleven facies types which strike in a north-west to south-east direction. This has since been refined to six facies by Vermeulen (2010) with the terrace facies being subdivided into three categories depending on the immediate footwall lithology underlying the BRC (Figure 7).

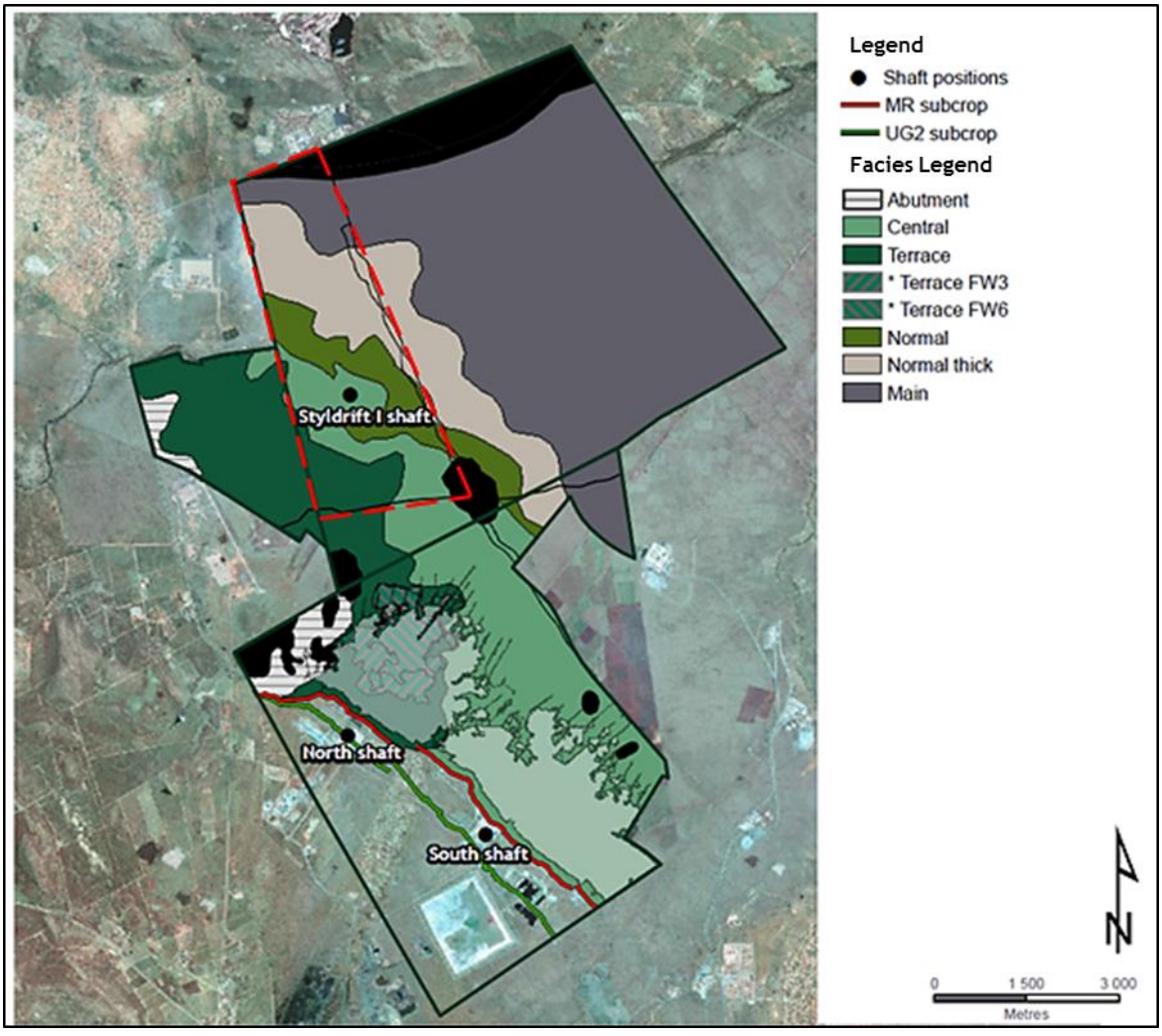

Figure 7. Merensky Reef facies domain across the BRPM JV with Styldrift I mining area outlined in red (taken from Vermeulen, 2010)

A brief explanation of each facies is provided below as described by Moodley (2008) and Vermeulen (2010):

1. Abutment

   This is structurally disturbed facies is characterized by ductile shearing and folding of the Merensky Reef stratigraphy. Iron replacement ultramafic pegmatoid is a common structural intrusion within this area (Figure 8). The Merensky grade distribution within this facies is erratic due to the geological features which have disturbed the original reef profile.

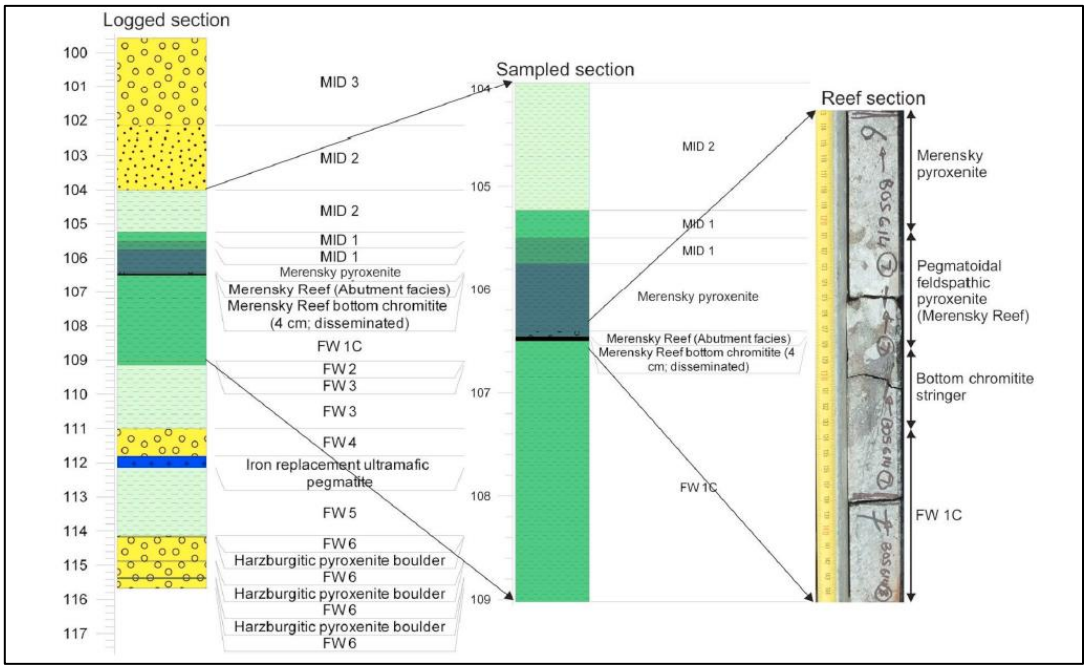

Figure 8. Merensky Reef intersection drilled in the Abutment Facies (Smith, 2014)

2. Central

   The Merensky Reef of the central facies consists mainly of contact Merensky Reef. Contact Merensky Reef is the occurrence of a 2 cm Merensky Reef chromitite overlying a fully developed anorthositic footwall called Footwall One A Lower (FW1AL). The 2 cm Merensky chromitite is overlain by Merensky Pyroxenite. A typical Merensky contact reef intersection is depicted in Figure 9. Normal reef may occur within this facies albeit to a lesser extent. Normal reef comprises a 15 cm pegmatoidal feldspathic pyroxenite and may also contain one or two 2 cm chromitite bands (Merensky top and bottom reef chromitites). This facies tends to be stable as potholing is encountered less frequently than in neighbouring facies such as the terrace facies.

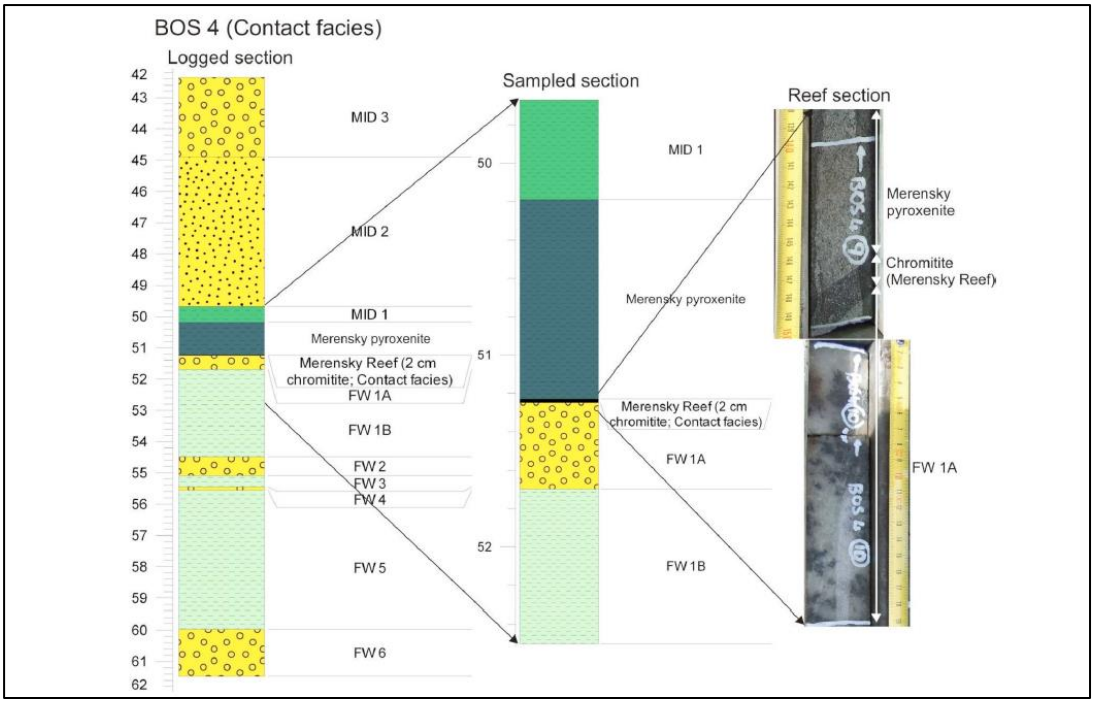

Figure 9. Merensky Contact Reef drilled in the Central Reef Facies (Smith, 2014)

3. Terrace

Potholing of the Merensky Reef is the defining characteristic of the terrace facies. The sizes and shapes of the potholes are irregular. The Merensky Reef commonly settles on the underlying stratigraphic footwalls known in mining terms as Footwall 3 and Footwall 6 (Leeb du Toit, 1986). A well-developed pegmatoidal feldspathic pyroxenite is present below the potholed Merensky Reef (Figure 10). In some areas, an additional pegmatoidal feldspathic harzburgite is developed resulting in reef thicknesses of up to 1.5 m. The abundant potholing in the area results in highly variable Merensky Reef mineralisation trends. Padiachy (2015) has divided the terrace facies into three sub-facies namely terrace, terrace FW3 and terrace FW6. Previous studies (Lionnet and Lomberg, 2006; Moodley, 2008) sub-divided this facies further into several other sub-facies based on which footwall the reef has potholed onto.

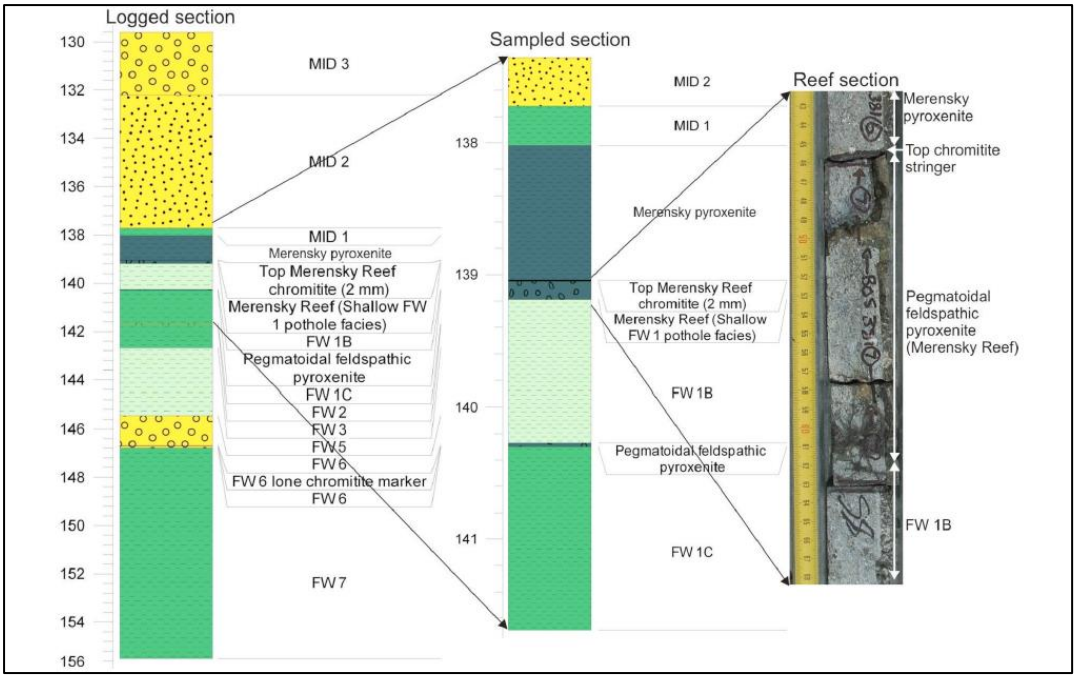

Figure 10. Potholed Merensky Reef intersection drilled in the Terrace Facies (Smith, 2014)

4. Normal Reef

   Merensky Pyroxenite thicknesses range from 1.5 m to 3.5 m within this facies type. The Merensky Reef consists of a pegmatoidal feldspathic pyroxenite and a 2 cm chromitite layer at the top and/or at the bottom (Figure 11). The occurrence of the top and bottom chromitite layers is inconsistent. Mineralisation is generally confined to the pegmatoidal feldspathic pyroxenite of the Merensky Reef.

5. Normal Thick

   This facies is lithologically similar to the Normal Reef Facies however the mineralisation trend differs. Mineralisation is confined to the upper portion of the pegmatoidal feldspathic pyroxenite. The change in mineralisation correlates with a sudden thickening of a lower lying lithological unit called Footwall 10.

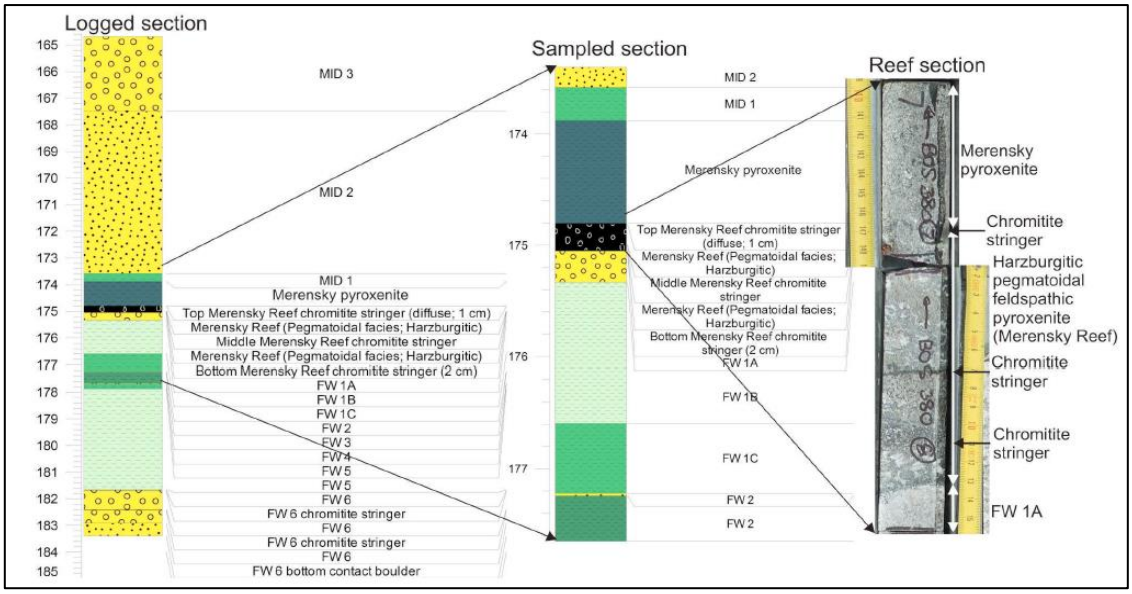

Figure 11. Normal reef intersection with pegmatoid developed between the Merensky Top and Bottom Reef Chromitite Stringers (Smith, 2014)

6. Main Reef

   Merensky Pyroxenite in this area is unusually thick at approximately 7 m. The Merensky Reef in this area is a pegmatoidal feldspathic pyroxenite interlayered by feldspathic pyroxenite. The mineralisation occurs at the top of pegmatoidal feldspathic pyroxenite. Like the normal reef, the Merensky Reef within the main reef facies is inconsistently bound by a top and/or bottom reef chromitite.

Smith (2014) notes that the central and shallower terrace facies (Terrace and Terrace FW3) are consistent with the southern Rustenburg facies while the deeper terrace facies (Terrace FW6), normal, normal thick and main facies are consistent with the northern Swartklip facies. Five facies types (terrace, central, normal, normal thick and main) occur within the Styldrift I area resulting in a highly variable orebody which displays characteristics of both regional facies types, Rustenburg and Swartklip.

2.4 The Merensky Mineralisation

According to Lomberg (2014), the Merensky Reef can be broadly defined as a zone of mineralisation within or closely associated with the ultramafic cumulate which occurs at the base of the Merensky Unit. The boundaries of the economically feasible stope cut or mineralised reef horizon are characterized as 'hard' or 'soft' by Glacken and Snowden (2001). The former refers to a clearly visible boundary or sharp contact where a change in lithology of the economic horizon and

underlying/overlying lithologies is evident. The latter refers to mineralisation that is gradational and cannot be recognised visually. The mineralisation of the Merensky Reef belongs to the latter group as mineralisation peaks along thin chromitite stringers and dissipates into the overlying hangingwall and underlying footwall units.

Mineralisation is not consistently vertically distributed along the Merensky Reef across the Bushveld Complex. Figure 12 shows the differences in the grade distributions at various mines across the Bushveld Complex. Generally, the grade is not restricted to any lithology or stratigraphic zone. Instead it is distributed over various units while peaking along the chromitites and pegmatoidal feldspathic pyroxenite, (Cawthorn, 2010; Lomberg, 2014). Striking variations of the grade distribution have been observed within the currently mined central reef facies of BRPM (Lionnet and Lomberg, 2006; Moodley, 2008; Cawthorn, 2010; Vermeulen, 2010). The various Merensky grade distributions found at BRPM are depicted in Figure 13. Mineralisation peaks and troughs in areas of thicker reef poses a challenge in applying a stope cut to mine optimally because several centimetres of barren material can introduce significant dilution (Cawthorn, 2010).

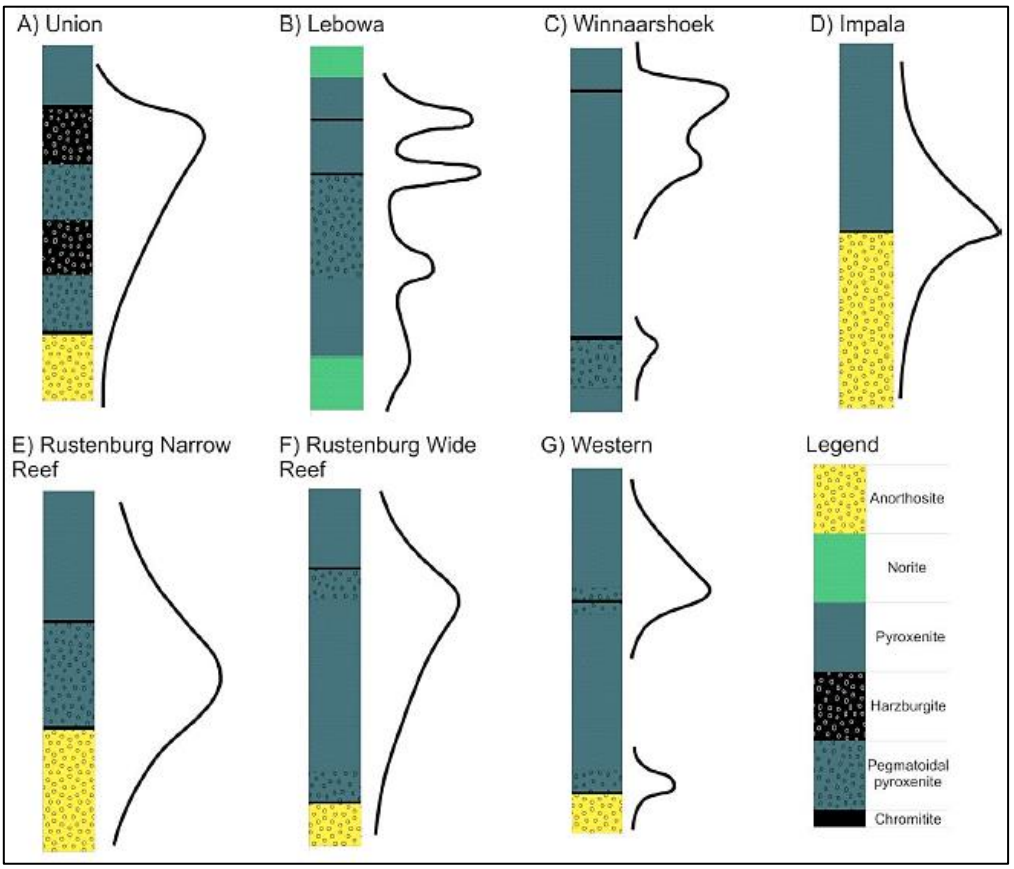

Figure 12. Generalised stratigraphy and grade distribution of the Merensky Reef across mines on the western and eastern limbs of the Bushveld Complex (taken from Smith, 2014)

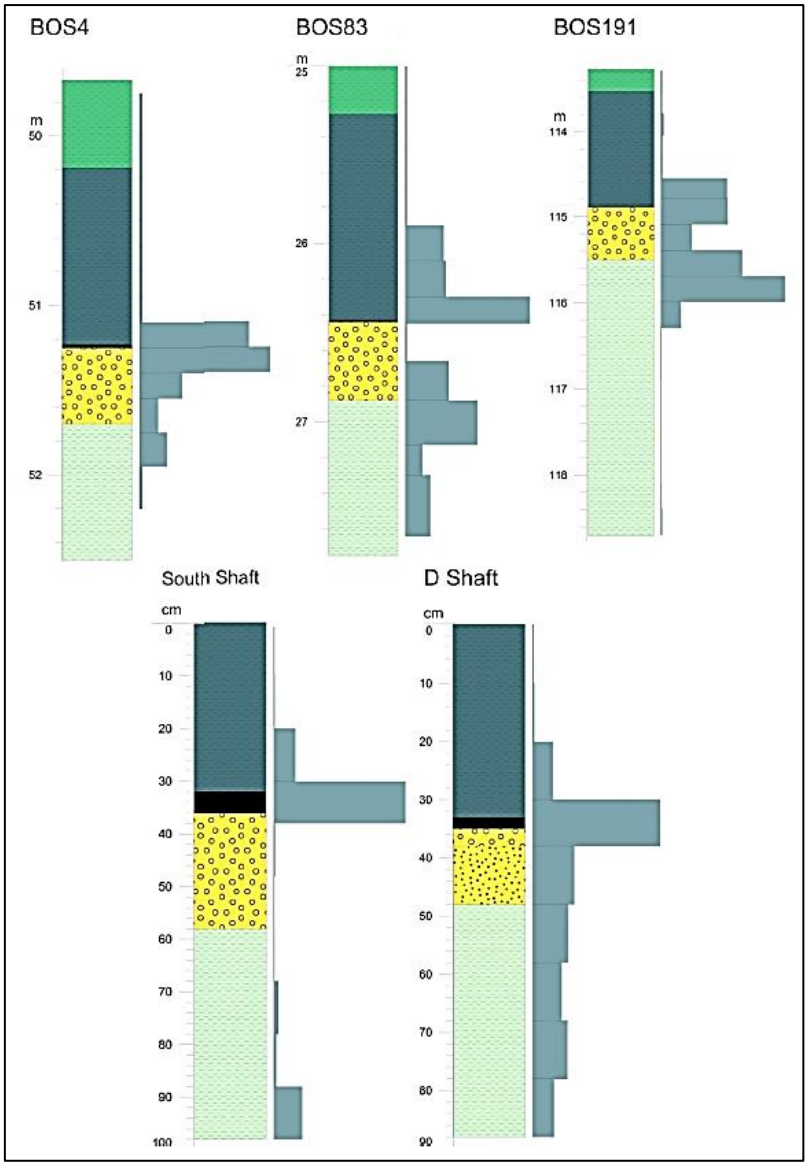

Figure 13. Variable grade distributions within the Central Reef Facies of BRPM (taken from Smith, 2014)

Merensky lithologies comprise complex mineralogy consisting mainly of silicates. The most abundant silicates are known as primary silicates while less abundant silicates are known as secondary (Schouwstra, Kinloch and Lee, 2000). The PGE-bearing minerals occur in trace amounts in the form of sulphides, arsenides, bisumuthotellurides and alloys. The mineralogical groups and types found within the Merensky Unit are listed in Table 1.

Table 1: Merensky mineral groups and types (Schouwstra *et al.* 2000)

Mineral Group		Abundance	Mineral Examples	Formula
Primary Silicates	Pyroxenes	Major	Enstatite	$MgSiO_3$
			Bronzite	$(Mg,Fe^{2+})_2\ (SiO_3)_2$
			Augite	$(Ca,Na)(Mg,Fe^{2+},AlFe^{3+},Ti)[(Si,Al)_2O_6]$
	Feldspar	Major	Anorthite	$CaAl_2Si_2O_8$
			Labradorite	$(Ca,Na)[Al(Al,Si)\ Si_2O_8]$
			Andesine	$(Na,Ca)[Al(Si,Al)\ Si_2O_8]$
	Olivine	Major	Forsterite	Mg_2SiO_4
			Fayalite	Fe_2SiO_4
Secondary Silicates	Amphibole	Minor	Magnesiohornblende	$(Ca_2)(Mg_4Al)(AlSi_7O_{22})(OH)_2$
			Riebeckite	$(Na_2)(Fe_3^{2+},Fe_2^{3+})Si_8O_2\ 2(OH)_2$
	Micas	Minor-trace	Annite	$KFe_3^{2+}(AlSi_3O_{10})(OH)_2$
			Phlogopite	$KMg_3(AlSi_3O_{10})(OH,F)_2$
	Chlorite	Minor-trace	Clinochlore	$(Mg,Fe^{2+})_5Al(AlSi_3O_{10})(OH)_8$
	Clay	Minor-trace	Talc	$Mg_3(Si_4O_{10})(OH)_2$
	Serpentine	Minor	Antigorite	$(Mg,Fe^{2+})_3(Si_2O_5)(OH)_4$
			Dickite	$Al_2(Si_2O_5)(OH)_4$
Other	Spinels	Minor	Chromite	$FeCr_2O_4$
	Oxides	Trace	Magnetite	Fe_3O_4
	Carbonates	Trace	Calcite	$CaCO_3$
Ore Minerals	Sulphides	Minor-trace	Pentlandite	$(Fe,Ni)_9S_8$
			Pyrrhotite	$Fe_{1-x}S$
			Chalcopyrite	$CuFeS_2$
			Pyrite	FeS_2
	PGE-sulphides	Trace	Braggite	(Pt,Pd,Ni)S
			Cooperite	(Pt,Pd,Ni)S
			Laurite	RuS_2
	PGE-arsenides	Trace	Sperrylite	$PtAs_2$
	PGE-bismuthotellurides	Trace	Moncheite	$(Pt,Pd)(Bi,Te)_2$
	PGE-alloys	Trace	Isoferroplatinum	Pt_3Fe
			Tetraferroplatinum	PtFe
	Au-minerals	Trace	Electrum	(Ag,Au)

Mineralogical studies of Merensky mineralisation have been undertaken laterally in an attempt to identify zones or domains based on the PGE mineralisation types. PGE mineralisation in the northwest region of the western Bushveld Complex (Swartklip Facies) is characterized mainly by alloys while the southeast region (Rustenburg Facies) is characterized by sulphides, tellurides and arsenides (Viljoen, 1999; Cawthorn, Merkle and Viljoen, 2002). Smith (2014) found that the major Merensky Reef sulphide mineralogies at BRPM are pyrrhotite, pentlandite, chalcopyrite and pyrite (in order of decreasing abundance).

Previous research has shown that sulphides are the most common PGE bearing mineral along the Merensky Unit. Based on this finding, it is generally accepted that PGEs have a strong correlation with sulphur and base metals such as copper and nickel as both PGEs and base metals are hosted largely within sulphides (Mostert, Hofmeyr and Potgieter, 1982; Schwellnus, Hiemstra and Gasparrini, 1976; Prichard, Barnes, Maier and Fisher, 2004; Thermo Scientific, 2012; Smith, 2014). Smith (2014) has demonstrated that within BRPM a generally strong correlation does indeed exist between the PGEs and sulphides with strongest associations found between pyrite, chalcopyrite and pentlandite. Pyrrhotite has the weakest association. In line with this, Smith (2014) also observed a strong association between 4PGE, sulphur, copper and nickel in the Merensky Reef grade distribution at BRPM (Figure 14).

However rare exceptions to the PGE and base metal sulphide association were observed where peaks in PGE content did not coincide with peaks in copper/nickel or sulphur (Figure 15). This is likely to be observed due to the presence of other PGE bearing minerals such as arsenides, tellurides, alloys as well as alteration of the sulphide mineralogy. Smith (2014) undertook a petrographic study of samples from BRPM and found that at least two events have resulted in the PGE bearing mineralogy seen in the Merensky Reef of the area:

1. Initial sulphide forming event where a sulphide liquid entered the magma chamber, displaced the already present residual silicate liquid and collected PGEs. The exact relative timing of this event could not be determined in the study. In this case PGEs would be closely associated with other base metals which occur within the sulphide mineralogy.
2. Later alteration event due to post-magmatic hydrothermal fluid influx causing existing sulphides to become altered (rimmed or completely replaced) by other minerals such as talc, amphibole, chlorite, epidote and so on. In such cases the PGEs may not be closely associated with base metals that are also associated with sulphides.

In the initial event, PGEs are closely associated with base metal sulphides and the elements hosted within it such as sulphur, copper and nickel. In cases of the latter event, the PGEs may not be closely associated with copper and nickel as it may be hosted in minerals which do not contain significant or any copper and/or nickel. Alteration is observed to increase upwards into the hangingwall of the Merensky Unit within the Central Reef Facies.

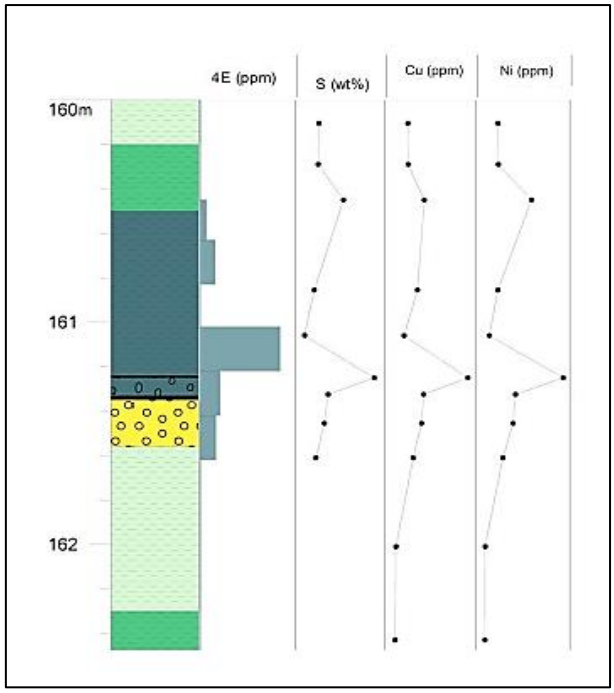

Figure 14. 4PGE (4E), sulphur (S), copper (Cu) and nickel (Ni) mineralisation trend along BRPM Merensky Reef intersection (taken from Smith, 2014)

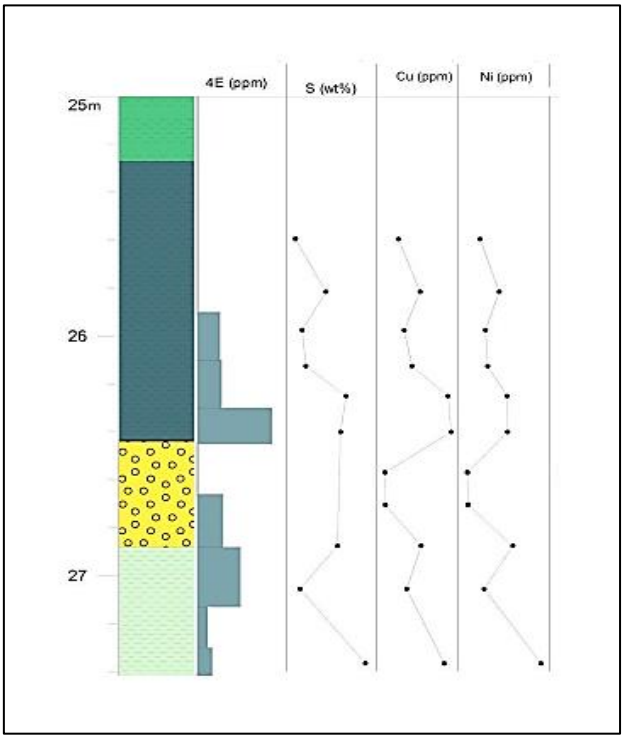

Figure 15. 4PGE (4E), sulphur (S), copper (Cu) and nickel (Ni) mineralisation trend along BRPM Merensky Reef intersection (taken from Smith, 2014)

2.5 Portable X-ray Fluorescence (pXRF) Technology

X-ray fluorescence (XRF) technology is a fast, non-destructive method used to analyse element types and concentrations in samples. This method offers broad and dynamic detection limits ranging from parts per million to percentages. An X-ray can be described as a beam of photons with energy. When an X-ray is produced, each element that is present in the sample reacts by emitting fluorescent X-ray radiation (excitation) with a unique energy and colour. The unique nature of the emitted fluorescence allows the element to be identified. This is the first qualitative step which means that the element has been identified but its quantity is unknown. The content of the element is then determined by measuring the intensity of the emitted energy (colour) of the particular element to be measured. This is the quantitative step of the analysis (Brouwer, 2010).

Three main interactions occur when an X-ray interacts with matter. These are fluorescence, Compton scatter and Rayleigh scatter (Figure 16). The X-ray photons which are absorbed by the sample and emitted back with unique energies and colours of the elements in the sample is the fluorescence. A fraction of the photons is scattered back from the sample. Compton scatter refers to scattering with a loss of energy and Rayleigh scattering refers to scattering with no loss of energy. The fluorescence and scatter are dependent on the thickness, density and composition of the sample as well as the energy of the incoming X-ray. It is therefore important that samples are free of foreign material or water during analysis as these factors may alter the interaction of the X-ray with the sample material producing inaccurate results (Brouwer, 2010; Hall *et al.*, 2011).

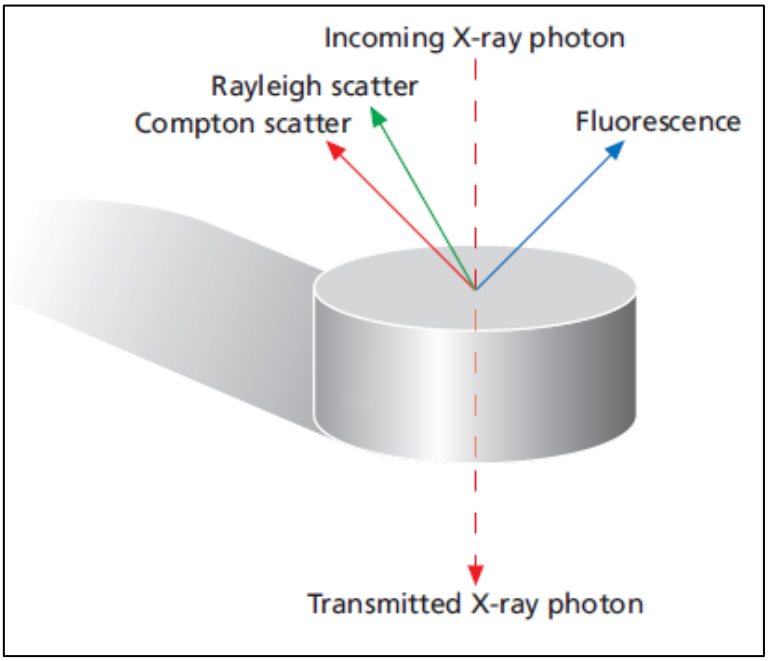

Figure 16. Fluorescence and scatter from X-ray interaction with a sample (Brouwer, 2010)

Advances in semi-conductor technology and instrument compaction have resulted in rapid development of pXRF technology (Hall, *et al.* 2011). The pXRF analyser is a lightweight battery operated instrument which emits X-rays from an internal source. The X-ray travels to the sample through a 1.5cm^2 window lens. Figure 17 depicts the typical exterior of a pXRF analyser. The user can control the pXRF analyser through interface buttons and view results on a small touch screen on the top of the machine. When the pXRF window is placed on a sample, the forward wall comes into contact with the sample triggering the contact switch which acts as a safety interlock. The trigger switch is used to start an analysis when the machine is in the correct position. The snout houses a shutter which enables the analyser to produce an X-ray (United States Patent, 2011).

The internal working mechanisms of the pXRF are depicted in Figure 18 and include an X-ray source, detector, signal processor and a central processing unit (CPU). The X-ray florescence resulting from the interaction of the X-ray beam and sample is analysed by the detector. The CPU stores result data from analyses which can be downloaded in Excel sheet format (United States Patent, 2011; Thermo Scientific, 2015).

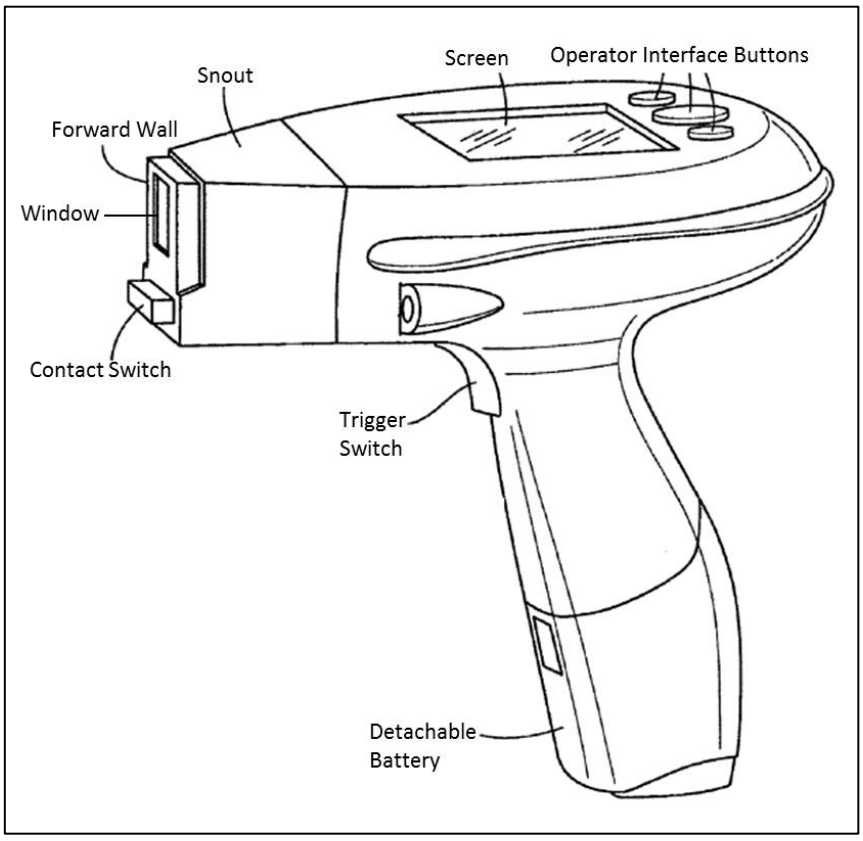

Figure 17. Typical exterior of a portable XRF machine (taken from United States Patent, 2011)

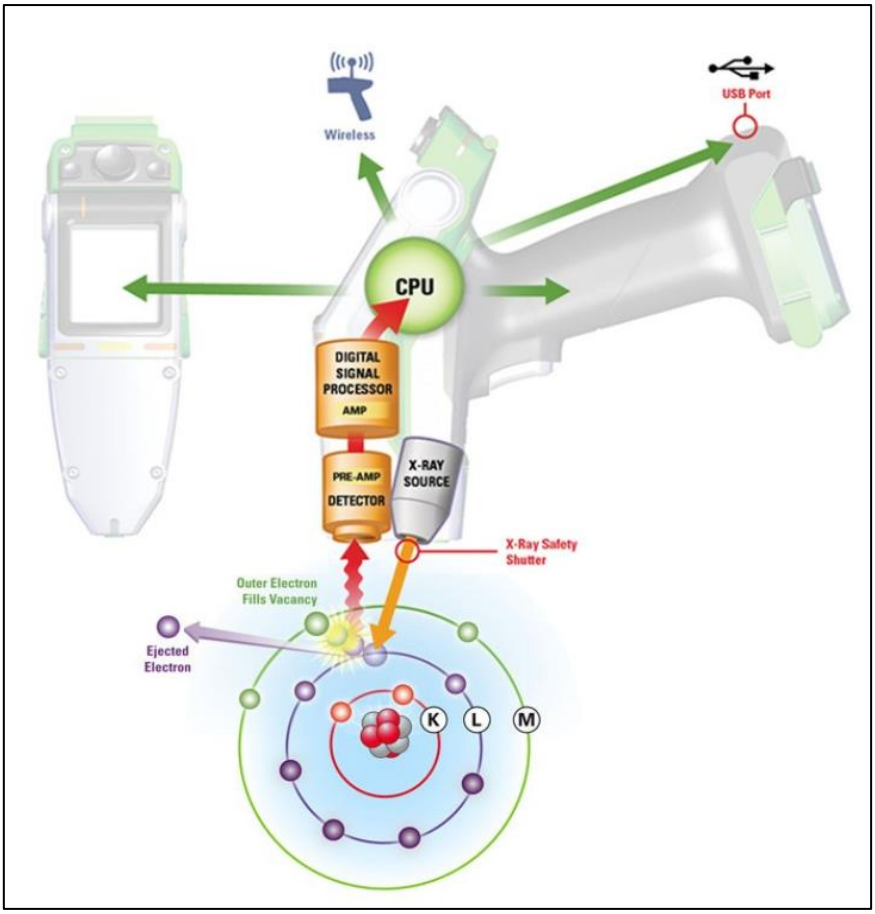

Figure 18. pXRF analyser during the X-ray fluorescence process (Thermo Scientific, 2015)

2.6 Application of pXRF in the Mining and Minerals Industry

The application of the pXRF to a geological matrix such as soil, rock or ore is more complex due to the heterogeneity of the sample (Brouwer, 2010; Hall *et al*., 2011; Hall *et al*., 2013, Charnley and Lentz, 2016). As a result of the rock matrix, calibration of the pXRF is required prior to analysis of samples (Hall *et al*., 2011; Hall *et al.,* 2013; Le Vailant *et al*., 2014; Fisher *et al.,* 2014). The calibrations applied to the pXRF analyser depend on each orebody, the elements that are being analysed and the mineralogical matrix in which the elements occur. Each site should therefore determine unique calibrations that are to be determined using site specific samples (Hall *et al*., 2011; Hall *et al*., 2013; Fisher *et al.,* 2014).

The analysis reading duration affects both the precision and accuracy of the result (Hall *et al*., 2011; Hall *et al*., 2013; Fisher *et al*., 2014). Short reading durations of less than twenty seconds produce inaccurate as well as imprecise results for some elements. It is recommended that analysis reading durations should be between twenty seconds and sixty seconds (Fisher *et al*., 2014).

Hall *et al.* (2011) notes that there has been growth in the use of the pXRF in mining and mineral exploration however the advertised quality of the machine is often lacking in terms of the quantities of an element that the machine is able to detect (the lower detection limit) as well as the accuracy of the results. However according to Fisher *et al.* (2014) It has been difficult to analyse the reliability of pXRF data because there is often a lack of information about if and how the pXRF analyser was calibrated and how data was collected. To limit these factors, it is recommended that all pXRF work that is undertaken be carefully tracked and documented for the purpose of QAQC. The Australian Joint Ore Reserves Committee (JORC) has responded to the general lack of quality control applied during pXRF analysis by adding required measures to be taken during pXRF analysis to the Australian mineral resource and reserve reporting code (Arne, Jeffress, Sergeev and Margerson, 2014). The measures include documenting details such as the pXRF make and model, analysis reading durations and calibration methods used. Quality assurance analyses on the data must be undertaken to ensure that it is acceptable for use and public reporting.

The pXRF has been tested and successfully applied to mine sites. Three case studies of the successful application of pXRF technology are summarized:

i. Plutonic Gold Mine; Western Australia

Geologically, Plutonic Gold Mine occurs on the Yilgarn and Pilbara cratons. Geological drillhole logging at Plutonic Gold Mine requires documenting the lithology and degree of mineralisation. Mineralisation on the mine is correlated to alteration of the rocks. Seven mineralisation categories exist which are based on the alteration intensity.

The logging of the mineralisation over time was inconsistent as various logging geologists viewed the degree of mineralisation differently. The pXRF was used to as a tool to standardize the categorization of the mineralisation. A newly developed mineralisation classification schema based on gold content was developed.

pXRF technology cannot reliably measure gold therefore arsenic and copper were used as pathfinder elements. Drillholes were analysed by the pXRF and arsenic/copper results were successfully regressed to gold content. Each drillhole was re-categorized using the newly formulated mineralisation classification schema largely removing discretionary logging of mineralisation, two examples of which are illustrated in Figure 19.

The authors note that the method of using the pXRF to determine the mineralisation intensity should be used as a guideline only and should not totally replace the geologist's interpretation (Gazley, Tutt, Fisher, Latham, Duclaux, Taylor and de Beer, 2014).

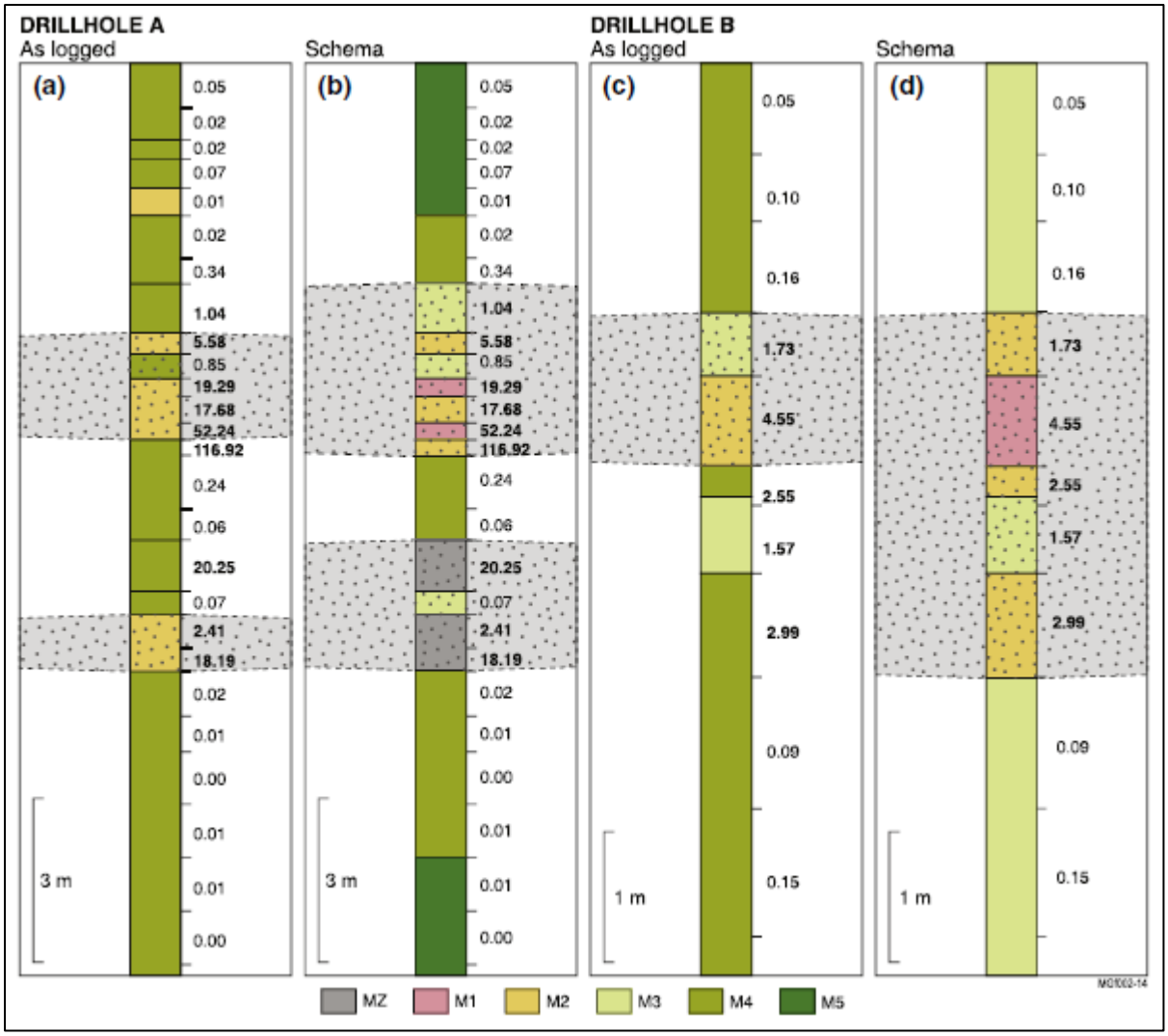

Figure 19. Plutonic Gold Mine geologist visual mineralisation intensity logging ('As logged') versus pXRF mineralisation classification ('Schema') (Gazley *et al*., 2014)

ii. Mount Pleasant; New Jersey; USA

Mount Pleasant is located in New Brunswick in the eastern USA (New Jersey). The deposit consists of two highly altered mineralised zones called the Fire Tower Zone and the North Zone. The Fire Tower Zone is enriched in tungsten, molybdenum and bismuth while the North Zone is enriched in tin, copper, zinc and indium. Rock identification is difficult due to the highly altered and weathered nature of the deposit (Zhang and Lentz, 2016).

Identifiable rock samples of the various rock units were analysed using pXRF technology. The elements titanium, zircon, niobium, yttrium and thorium were analysed as these are effectively detected by the pXRF and are generally unaffected by alteration so they can be used as a

geochemical signature of the original rock type (Charnley and Lentz, 2016; Zhang and Lentz, 2016). Plots of the elements analysed were successfully used to distinguish rock types by distinct geochemical populations (Figure 20).

However, one group of rocks (granite suite) could not be distinguished using pXRF results only. This was due to the geochemical similarity of the rock types within this group. Using both pXRF and field mapping data, the rock units were distinguished (Charnley and Lentz, 2016; Zhang and Lentz, 2016). pXRF results and mapping data can therefore successfully be used to differentiate altered rock types within the Mount Pleasant deposit.

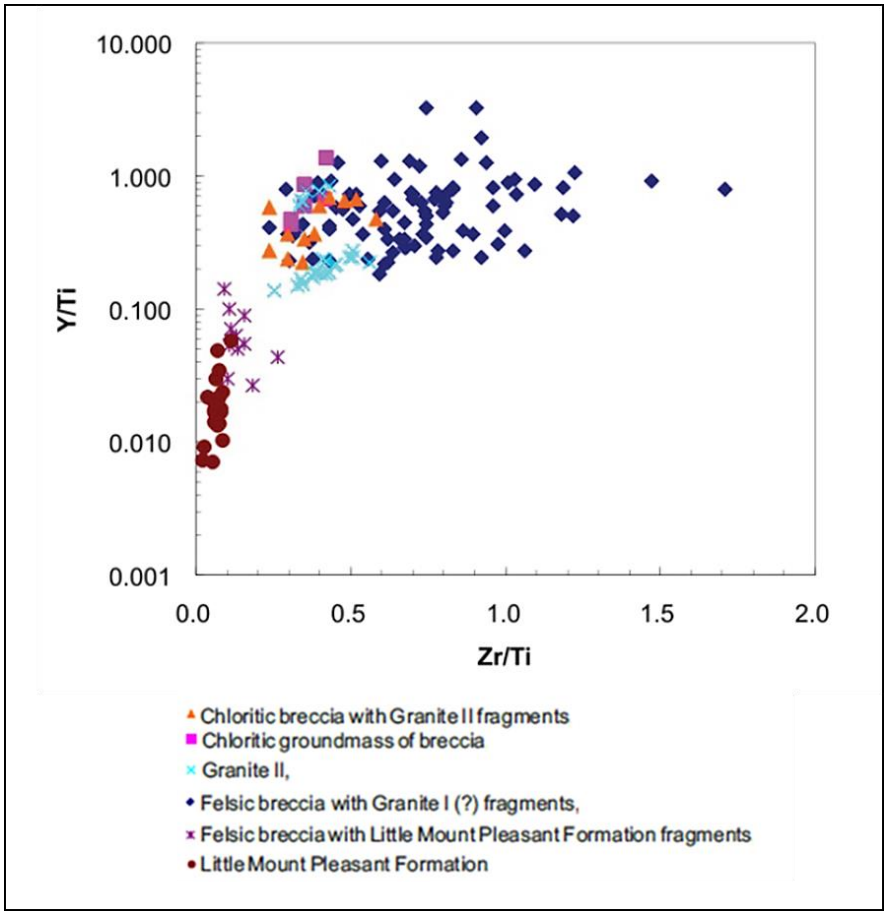

Figure 20. Yttrium/titanium versus zircon/titanium plot of pXRF results (Zhang and Lentz, 2016)

iii. Nickel Sulphide Exploration; Yilgarn Craton; Western Australia

The Yilgarn Craton of Western Australia hosts the Perseverance, Miitel and Wannaway nickel sulphide deposits. Le Vailant *et al.* (2014) conducted a pXRF study on samples surrounding these deposits to determine if the pXRF could be used to identify potential areas for geological prospecting. Split core samples were analysed at the laboratory for a range of elements (silicon,

sulphur, potassium, calcium, titanium, chromium, iron, nickel, copper, zinc, arsenic, strontium and zirconium). The remaining split core samples were analysed using the pXRF.

Le Vailant *et al.* (2014) stress the importance of calibration when using the pXRF. Twenty-eight matrix matched reference materials were analysed by pXRF. The pXRF results were plotted against the laboratory results of the sample to determine the correct calibration equations as illustrated in Figure 21 . The slope and intercept produced were used to calibrate the pXRF machine prior to analyses. Le Vailant *et al.* (2014) found that precision of pXRF sample analysis increased with longer analysis durations. It is recommended that the analysis duration should be between 20 – 60 seconds.

The research indicated that the pXRF and laboratory results were well correlated. In particular, nickel, chromium, titanium and zirconium were of adequate quality to be used an effective guide for future prospecting of nickel sulphides. The researchers recommend that laboratory analysis should be used subsequent to pXRF analysis to verify results.

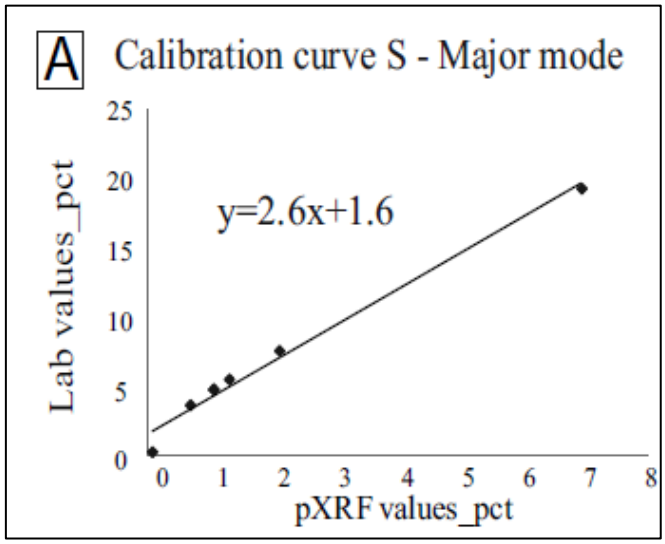

Figure 21. Yttrium/titanium versus zircon/titanium plot of pXRF results (Zhang and Lentz, 2016)

2.7 Using Copper/Nickel as PGE Pathfinders

Clark and Harper (2000) notes that there are many reasons to establish the presence and strength of a relationship between two variables citing three in particular:

- If one variable is cheaper to measure than the other, that variable can be measured and the other variable may be predicted from it

- To use predicted measurements as a source of information for stope cuts while awaiting assay results from the laboratory
- To determine which variables affect changes in productivity

Use of copper and nickel as PGE pathfinders falls within both the first and second categories above. It is cheaper to measure copper and nickel using the pXRF and the turn-around times for results are rapid.

Furthermore, pXRF machines cannot accurately measure PGEs and gold. Application in platinum mining in the Bushveld Complex must therefore be done using 'pathfinder elements' which have a 'genetic relationship' to the target element (Charnley and Lentz, 2016; Fisher *et al.,* 2014; Thermo Scientific, 2012; Zhang and Lentz, 2016).

An exercise was undertaken by Thermo Scientific (2012) using the portable Niton XL3t Series XRF machine on 63 Merensky Reef samples along a stratigraphic section. Pathfinder elements copper and nickel were used to target platinum group elements, platinum, palladium and gold. Positive correlations were found between pXRF measurements and laboratory ICP measurements as well as between pathfinder elements and target elements as shown in Figure 22 (Thermo Scientific, 2012).

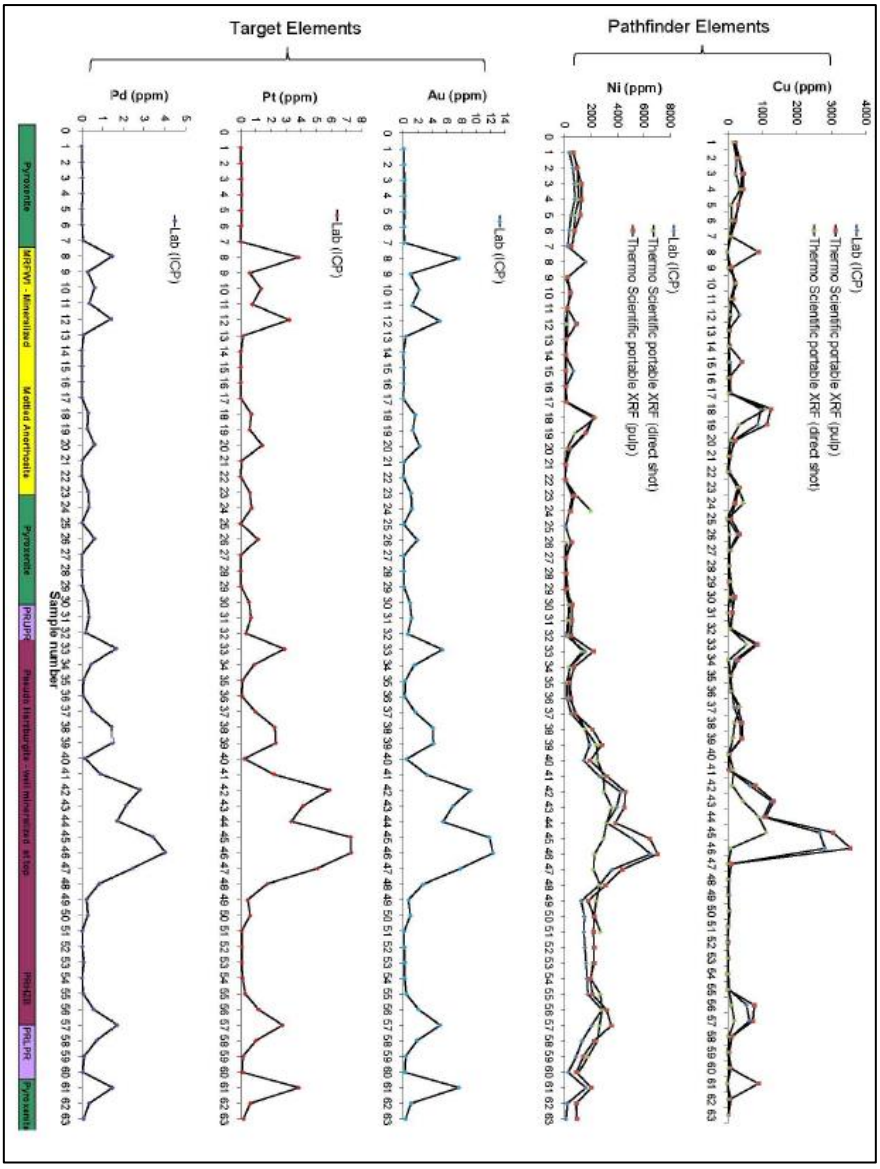

Figure 22. Thermo Scientific study on samples indicates positive correlations between pathfinder and target elements

To predict the PGE content from the copper/nickel results, a relationship must first be established. A scatter plot may be used as a tool to identify whether a relationship exists between two variables. It may provide an indication as to whether there is a direct or indirect relationship. A direct relationship is when each variable increases whereas an indirect relationship is when one variable increases and the other decreases. Plotting a straight line through the data points can assist determining the relationship. A perfect direct relationship produces a correlation coefficient (R) of +1 while a perfect indirect relationship produces a correlation coefficient of -1 (Clark and Harper, 2000; Coombes, 2008).

Data points will cluster around the straight line plotted on a scatterplot in a linear cigar shape if a strong relationship is found between variables. The difference between the actual data value and the

predicted value is called the residual (Figure 23). It is the vertical distance between the regression line and the actual sample value for each point (Clark and Harper, 2000). If relationship can be found between variables then further statistical analyses such as regressions may be undertaken. Coombes (2008) suggests that a correlation coefficient greater or equal to 0.6 is adequate for regression analyses in geostatistics. However, Clark and Harper (2000) cautions that data must be divided into single populations before any geostatistical analyses may be undertaken.

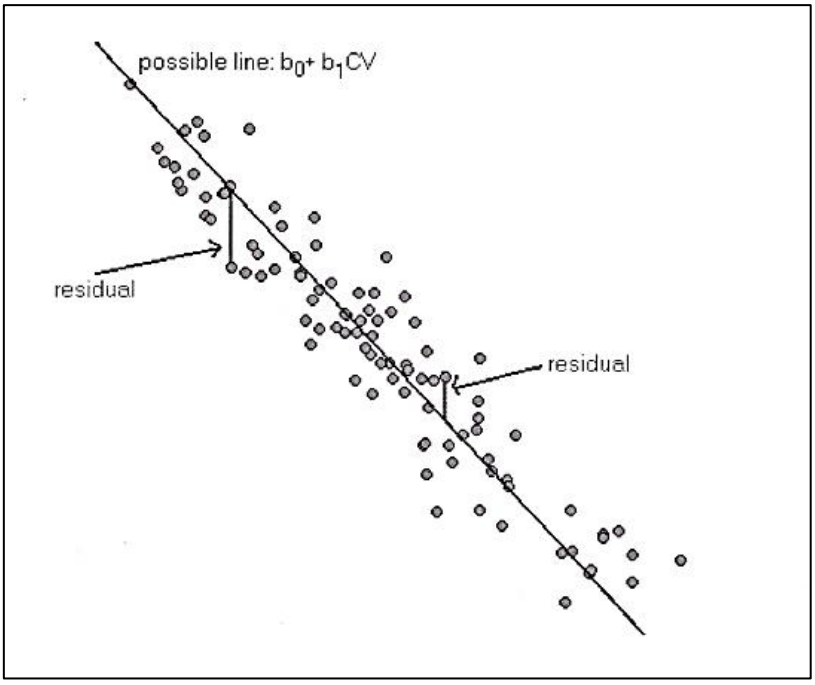

Figure 23. Scatter plot of an indirect relationship showing the residual (difference between the actual and predicted value) (Clark and Harper, 2000)

Chapter Three: Methodology

3.1 QAQC of Laboratory Data

All available sampled, quality checked drillholes which are not structurally disturbed and located in the study area were extracted from the RBPlat database for this study. This totalled 23 drillholes. Each drillhole was carefully logged and then split along its length to sample half of the core. The remaining half core has been retained at RBPlat for reference purposes. In the RBPlat geological drillhole database, the drillholes within the dataset used for this investigation have been coded as having reliable assay results. For the purpose of this study, the results have been re-analysed for accuracy and precision to verify the reliability of the data.

3.1.1 Laboratory Data Accuracy Analysis

Certified reference materials (CRMs) were inserted in the sample batch to assess accuracy and to identify contamination of samples during the laboratory analysis. The CRMs were divided into standards and blanks which were randomly inserted into the sample batch prior to sample dispatch. Each element is analysed separately per standard as each has a unique CRM certified value and standard deviation.

The samples submitted to the laboratory consisted of 85 % primary geological core samples (Merensky, UG2 and Pseudo-Reef) and 15 % control samples. The CRMs were split into 10 % standards and 5 % blanks (Table 2). The certificate for each CRM used for this investigation can be found in Appendix A. The results are discussed in Section 4.1.1. and presented graphically in Appendix B.

Table 2: Breakdown of sample types in the drillhole dataset

Sample Type	No. of Samples	Percentage Samples	Total Percentage
Primary	2251	85%	85%
CRM – Standards	277	10%	15%
CRM – Blanks	123	5%	
Total	2651	100%	100%

In cases where the primary sample was split into Leg 1 and Leg 2 for twinstream analysis, each leg was analysed separately in the accuracy analysis. Industry standard tolerance limits are used by RBPlat and were applied in analysing the CRM data. Standard tolerance limits are calculated per element by multiplying the certified standard deviation (σ) by three (Moodley, 2015). This value is added to the

certified value to produce the upper tolerance limit (Equation 1) and subtracted from the certified value to produce the lower tolerance limit (Equation 2) as shown below.

$$Standard\ Upper\ Limit = Certified\ Mean\ Value + 3\sigma$$ *……Equation 1*

$$Standard\ Lower\ Limit = Certified\ Mean\ Value - 3\sigma$$ *……Equation 2*

The upper tolerance limit for blanks is calculated by multiplying the element lower detection limit by 10 (Equation 3) (Moodley, 2015):

$$Blank\ Upper\ Limit = Element\ Lower\ Detection\ Limit \times 10$$ *……Equation 3*

3.1.2 Laboratory Data Precision Analysis

Twinstream analysis was undertaken on 50% of 4PGE analyses to assess precision. For cost-saving purposes, twinstream was undertaken on 25% of copper and nickel analyses to assess precision. The two separately analysed streams of the twinstream analysis are called Leg 1 and Leg 2. The Power Function Outlier Method was used to identify outliers. The samples have undergone lead collection fire assay analysis to determine the PGE and gold grade values. Copper and nickel were analysed by pressed pellet XRF. The sampling and QAQC procedure is illustrated in Figure 24.

The two separately analysed streams of the twinstream analysis are called Leg 1 and Leg 2. The percentage difference between the averages of each Leg should not exceed 5 % (Moodley, 2015) as depicted in Equation 4:

$$\%\ Diff\ Between\ Leg\ 1\ and\ Leg\ 2\ Datasets = \frac{Average_{Leg2} - Average_{Leg1}}{Average_{Leg1}} \times 100$$ *……Equation 4*

The accepted tolerance for the number of outliers is less than or equal to 5% of the total twinstream data analysed per element (Moodley, 2015). This is shown in Equation 5:

$$Total\ Outliers\ per\ Element \leq 5\%$$ *……Equation 5*

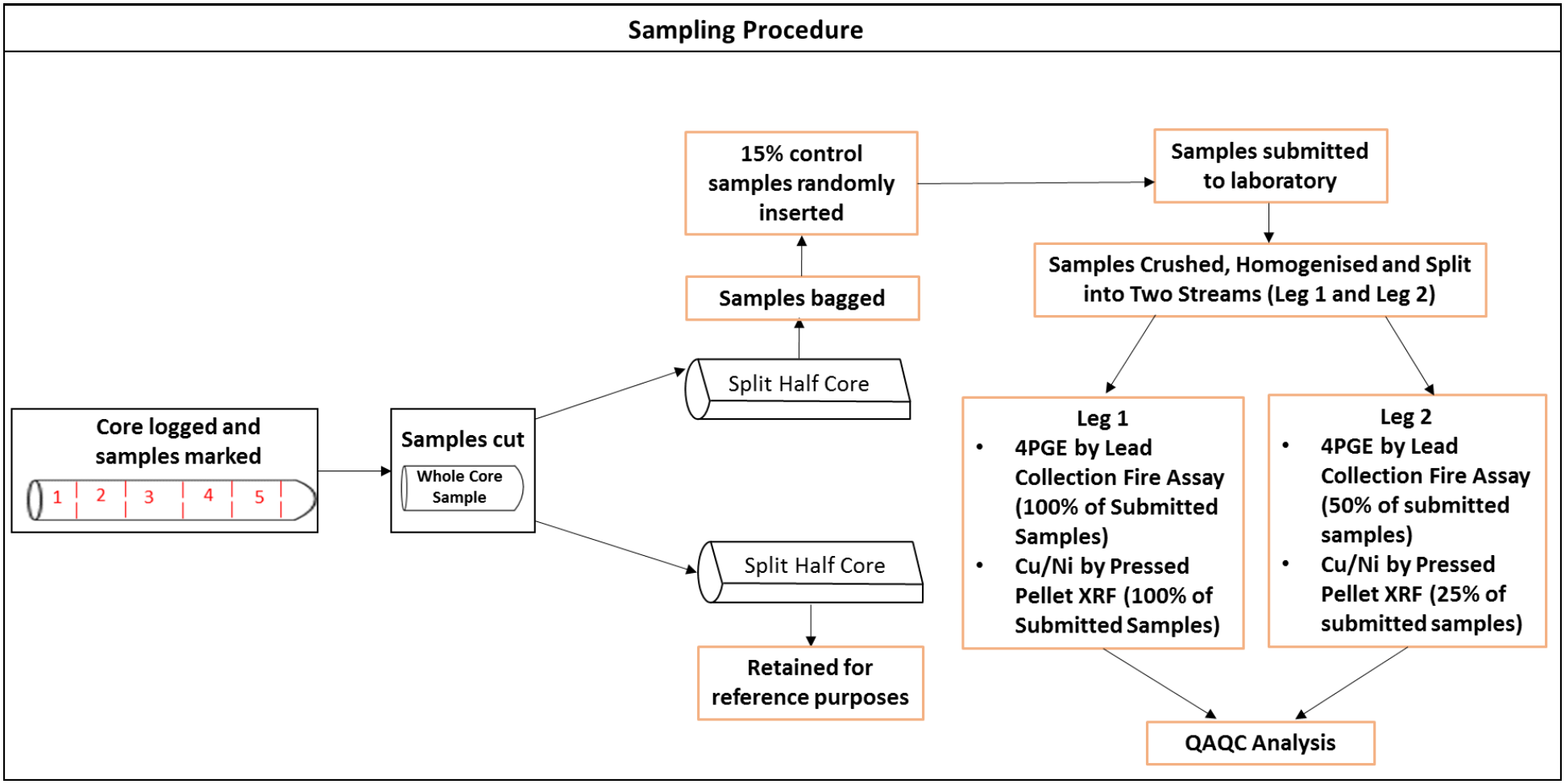

Figure 24. Drillhole sampling and QAQC procedure

3.2 pXRF Calibration

A Niton XL3t GOLDD analyser was used for the purpose of this study (Figure 25). Detailed product specifications of this model are available in Appendix C. For geological applications, the Niton XL3t GOLDD pXRF has two factory-installed calibrations called the mining and soil modes. The mining and soil modes have the same lower detection limits for copper and nickel. The detection limits are 30 ppm and 15 ppm for copper and nickel respectively (Thermo Scientific, 2010).

The mining mode can be calibrated for each element that is to be analysed. The calibration factors (a slope and intercept value per element) may be entered into the pXRF by the user. This investigation aims to produce pXRF results that are as accurate as possible therefore the mining mode was used for this study. This allows for calibration factors to be used during analysis to counter possible interference effects caused by the mineralogical matrix of the sample. A pXRF analysis reading time of 20 to 60 seconds is recommended to ensure adequate analysis length for an accurate result (Hall *et al*., 2013; Fisher *et al.,* 2014) therefore all readings during this study were taken for the maximum recommended reading time of 60 seconds.



Figure 25. Thermo Scientific Niton XL3T GOLDD pXRF analyser used for investigation

Calibration of the pXRF for this investigation was undertaken using 60 pressed pellet samples from the study area. Pressed pellets are sample discs made from crushed homogenised sample material for the purpose of laboratory pressed pellet XRF analysis (Figure 26). The pressed pellets used were randomly selected. Pressed pellets were used for the calibration as an accurate calibration requires site specific reference materials of known grade. The pressed pellets are therefore suitable for the calibration for the following reasons:

- The pressed pellet samples are from within the study area therefore it is the same mineralogical matrix of the rock samples to be analysed using the pXRF.
- The pressed pellet samples have been analysed at laboratory by XRF therefore the copper and nickel content is known.

The copper and nickel pXRF results were compared to the laboratory results using XY scatter plots. The regression line slope and intercept of each elements XY scatter plot were used as the calibration slope and intercept values.



Figure 26. Laboratory prepared homogenous pressed pellets used to test accuracy and precision of handheld XRF

3.3 Hypothesis One: pXRF Accuracy Test

Five sampled drillholes from within the study area were randomly chosen for the pXRF analysis. The pXRF analysis was undertaken on the split core that has been retained at RBPlat. The methodology used for Hypothesis One is outlined below and illustrated in Figure 29.

3.3.1 Sample Selection

The requirements for the five drillholes chosen for the accuracy test were:

- It occurs within the Styldrift I study area.
- There are no structural features (e.g. dykes, potholes) which may disturb the Merensky reef profile of the drillhole.

The Merensky intersection and the corresponding lithological log per analysed drillhole are illustrated in Appendix D.

3.3.2 Sample Preparation

The core sample must be cleaned of foreign particles and completely dried prior to analysis. This is because an incoming X-ray will interact with foreign particles or moisture within a sample resulting in interference which negatively affects the accuracy of the sample result (Brouwer, 2010; Hall *et al*., 2013). The half core was washed clean with a medium to high pressure hose pipe and a non-abrasive plastic hand brush to remove residual dust and debris (Figure 27). The core was then left to dry completely before proceeding with the pXRF analysis.



Figure 27. Core being cleaned with plastic brush to remove dust and foreign particles prior to handheld XRF analysis

3.3.3 Sample Analysis

Each geological sample ranges from 15 cm to 30 cm in length and is 25 cm on average. The disseminated nature of PGE-bearing sulphides presents a high likelihood of nugget effect during the pXRF analysis on the drillhole core as the pXRF may be placed directly on a sulphide grain which may produce a higher result than the overall grade of the sample. Alternatively, a low sample result will be produced if the pXRF is placed on a barren grain. A single pXRF reading for each geological sample is therefore inadequate as a representative result for the geological sample. The nugget effect cannot be totally eradicated when analysing a heterogeneous rock sample however readings were taken every 5cm and then averaged over the length of the geological sample to minimize the nugget effect and to try to achieve a more representative result (Figure 28).

The position of the Merensky bottom reef chromitite and the corresponding sample reading number was logged. The pXRF sampling results were compared to the laboratory results to determine if the pXRF results are reliable.

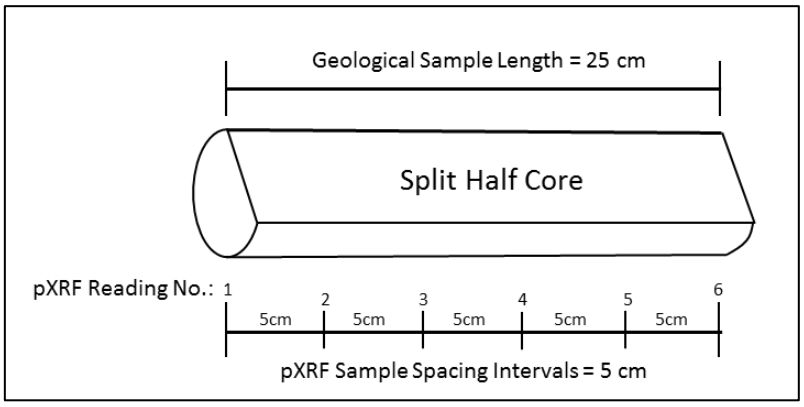

Figure 28. pXRF sample spacing intervals across a geological sample

3.3.4 Result Interpretation

The results from the pXRF were averaged across each geological sample to produce one result for every geological sample. Bar graphs were used to compare the laboratory and pXRF results. XY scatter plots were plotted to determine the correlation coefficient (R) to determine how closely the laboratory and pXRF results are related.

To determine if the laboratory and pXRF datasets display the same statistical properties and can be assumed to be from the population (i.e. no significant difference), F-Tests to analyse the variances between laboratory and pXRF datasets were run on each drillhole. This was undertaken as a precursor

to the undertaking of T Tests which were run on each drillhole to compare the pXRF and laboratory results. The F Test is required to determine if the variance between the two datasets are homogeneous or if they display different properties and indicate different population characteristics. Furthermore, this also dictated the T-Test type that is used to analyse the drillhole (i.e. assuming equal or unequal variances). The degrees of freedom used is the number of samples (n) minus one, i.e. 'n -1'. The tests were run on a 95% confidence level therefore the alpha value used was 0.05.

The value produced by comparing the pXRF and laboratory datasets is called T Stat. This value is compared to the T Critical value calculated for a specific alpha and degrees of freedom. When T Critical is lower than the T Stat, it is accepted that significant differences in the datasets exist and they do not belong to the same distribution or population. Alternatively, if the P statistic is ≤0.05, it is accepted that significant differences exist in the datasets. (Clark and Harper, 2000).

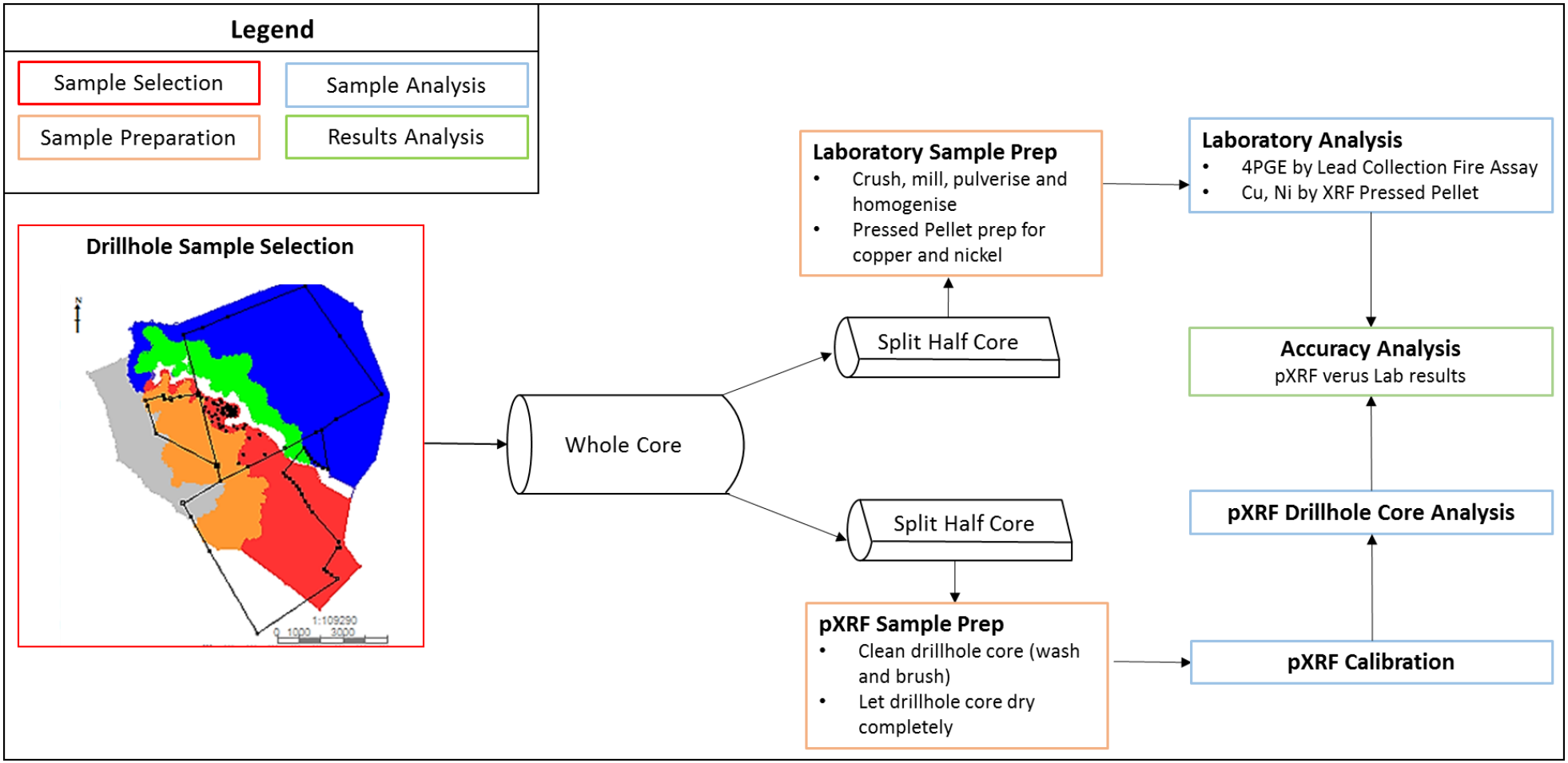

Figure 29. Methodology of Hypothesis One

3.4 Hypothesis Two: Copper and/or Nickel as a proxy for PGE content

3.4.1 Multivariate Data Analysis

A relationship or correlation must exist between variables if one is to be predicted by another. Multivariate data analyses must be undertaken per population (a dataset which shows consistent characteristics regarding the parameter under investigation) (Clark and Harper, 2000). Histograms of each variable were analysed to determine if the assay dataset belongs to the same mineralisation population. Pathfinder (copper and nickel) were analysed against the 3E grade content in scatter plots to isolate mineralisation populations. F Tests to assess the variance and T Tests to assess means were undertaken to verify the presence of different populations.

The following parameters were investigated to identify mineralisation domains/zones with unique copper/nickel to 3E content signatures (mineralisation populations):

i. Lateral analysis using spatial data (collar co-ordinates)

ii. Multivariate Data Analysis of 3E versus copper and nickel using the following parameters:

iii. Sample stratigraphy

iv. Sample grade

v. Sample lithology

Regression analyses were undertaken where distinct populations and trends were identified. The methodology used to investigate Hypothesis Two is illustrated in Figure 30.

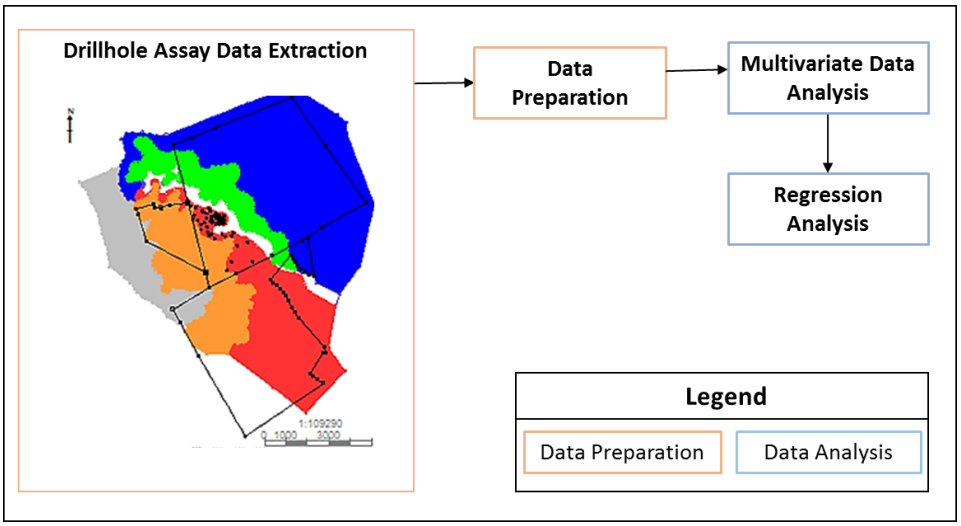

Figure 30. Methodology of Hypothesis No. 2 (Determining if a quantifiable relationship exists between copper and/or nickel and PGE)

3.5 Investigation into the Use of the pXRF in an Underground Environment

The pXRF was used to analyse five underground sections at Styldrift I Mine. Underground samples are 10 – 15 cm in length and are chipped from the rock face along reef development or stope faces using a diamond blade cutter. The sections were sampled and sent for geochemical laboratory analysis of 4PGE results by lead collection fire assay method.

The pXRF was calibrated as per the slope and intercept obtained from the pressed pellet calibration exercise. Sections where the readings were taken were washed with a hose pipe and brushed clean to ensure that no interference results from dust or foreign particles present on the rock surface during the pXRF analysis. Sections were left to dry prior to analysis. pXRF readings were taken every 5cm and averaged across each sample for a more representative sample than a single reading per sample.

The pXRF copper and nickel results were evaluated by comparing it to the laboratory 3E result (sum of platinum, palladium and gold) per sample. 3E results were used instead of 4PGE for consistency as rhodium was selectively sampled when 3E is greater than 1.5g/t. The methodology applied for the underground trial is depicted in Figure 31**.**

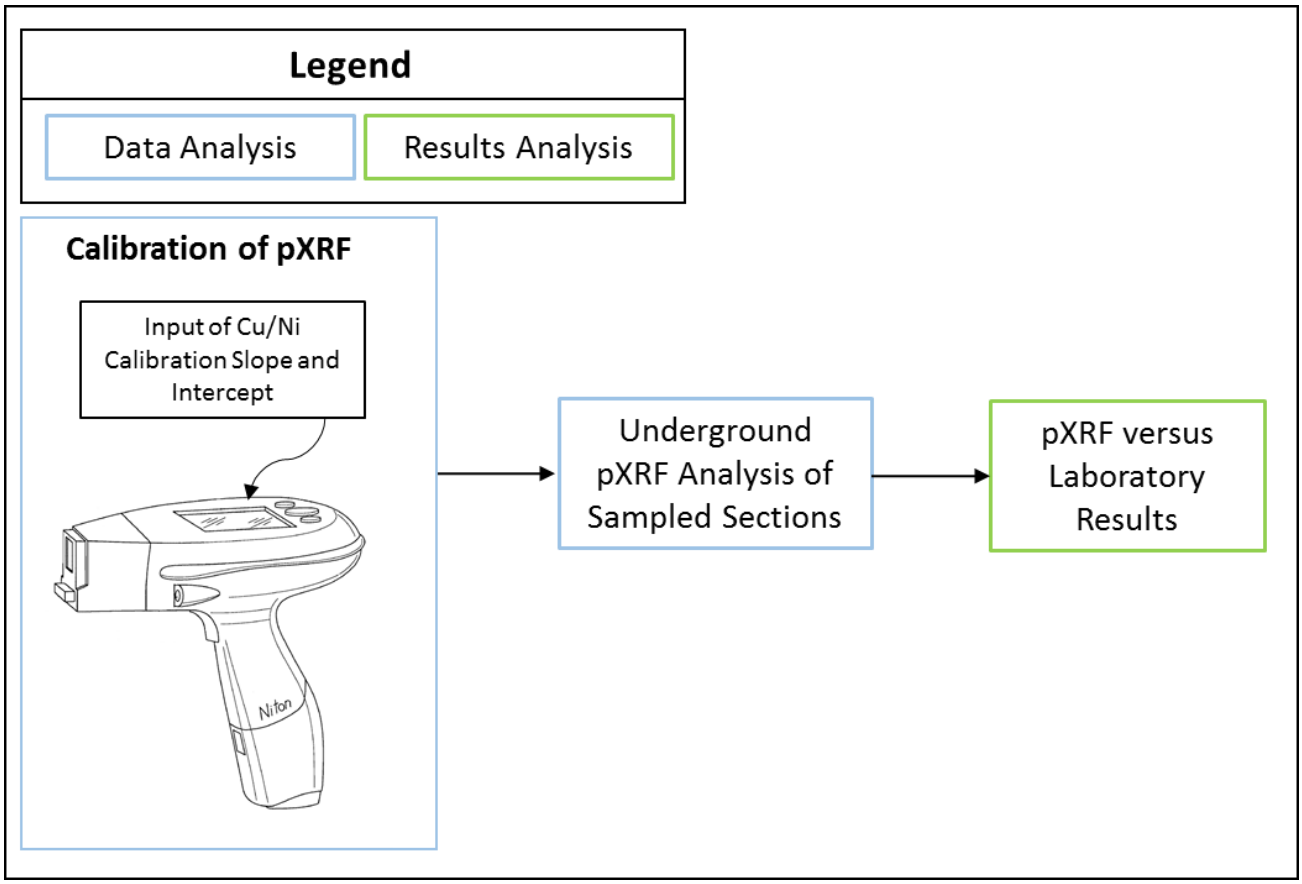

Figure 31. Methodology of pXRF underground trial

Chapter Four: Results

4.1 QAQC of Laboratory Data

4.1.1 Accuracy of Laboratory Data

The graphs in Appendix B depict the results of the inserted CRMs in the dataset. Upper and lower tolerance/confidence limits are depicted in red on the graphs as 'UCL' and 'LCL' respectively. The standard mean is indicated in green. Table 3 lists the percentage bias per standard and element analysed. The cells highlighted in dark grey are not certified for the specific element and therefore have not been analysed for that element. The cell in red has been excluded from calculations of the average percentage bias for that element (gold) as the percentage bias of 166.67% is not representative of the gold data (see analysis below).

Table 3: Percentage Bias per Standard and Element Analysed

Standard	Pt	Pd	Au	Cu	Ni
AMIS0151	4.36	3.41	2.78	-7.32	8.41
G1	0.00	0.86			-1.45
G10	-7.72	-3.57			
G13	-3.03	-3.32	3.50	8.83	1.42
G2	-0.56	-0.06	-3.57	-13.20	-15.50
G21	-3.49	1.92		-9.91	
G24	18.07	7.35	166.67		-2.59
G25	1.27	1.00			-9.32
G3	3.15	6.25	0.28	5.78	4.67
G4	8.00	4.42		52.62	-10.87
G6	1.93	-2.99		25.03	-3.70
G8	-1.03	-0.36	0.61	-14.16	-15.09
G9	1.50	3.89	-10.87	3.22	-8.86
Average	1.73	1.45	-1.21	5.65	-4.81

The analysis of the CRMs indicates the following:

- All standard results fall within the defined tolerance limits (Appendix B).
- Large biases are seen in element G24 however this is because the absolute values of G24 are very low resulting in large percentage biases. All G24 sample results are within the tolerance limits (Appendix B). A very large percentage bias of 166.67% was seen in the gold results of G24 however this is due to the fact that the certified value is 0.05 however the detection limit

is 0.1 resulting in many of the samples reported at the 0.1 which is the lowest possible result using the choice of analysis and laboratory. The absolute difference is negligible (approximately 0.05) and it is impossible to achieve the actual certified value as this is below the laboratory detection limit for this element. Therefore, this data has been accepted. The G24 percentage bias was not used to calculate the average percentage bias for gold as the high percentage bias result in an average percentage bias that is not representative of the gold data.

- The results of the blanks are acceptable with all the blanks results falling below the upper tolerance limit.
- Nickel results show a general trend of a bias as majority of the results fall below the certified value resulting in most standards with negative percentage biases. It can therefore be accepted that nickel results are slightly low or conservative by an average of 4.81% (Table 3).
- The results of the remaining elements fall both above and below the standard mean therefore the data is spread randomly around the standard mean. This indicates that there is no consistent bias.

Based on these findings, the data is of acceptable and adequate accuracy as per the defined tolerance limits of the standards however nickel results are conservative. No detectable contamination occurred during the laboratory analysis of the drillholes within the dataset. The dataset has been verified as accurate for use in the investigation however the laboratory nickel results which are conservative is to be borne in mind.

4.1.2 Precision of Laboratory Data

The results of twinstream Leg 1 versus Leg 2 are depicted in scatter plot diagrams from Figure 32 to Figure 36. Accepted twinstream samples are depicted in blue and outliers are depicted in red. The correlation coefficient (R) is displayed in the left-hand corner of each scatter plot.

Table 4 lists the precision statistics for each element.

Table 4: Precision statistics for drillhole dataset used for investigation

Element	N	Average Leg 1	Average Leg 2	Leg 1 vs Leg 2 %Diff	R	Outliers	% Outliers
Pt	1231	1.127	1.156	2.549	0.99	7	0.57
Pd	1231	0.517	0.541	4.425	0.99	5	0.41
Au	1231	0.05	0.052	3.846	0.98	14	1.14
Cu	615	0.025	0.025	0.109	0.99	0	0.00
Ni	615	0.086	0.086	0.417	0.99	1	0.16

The results indicate that Leg 1 and Leg 2 of all elements analysed are well correlated with coefficients (R) of at least 0.97 (Table 4). Percentage differences between Leg 1 and Leg 2 datasets for all elements are less than 5% and is therefore acceptable. Outliers are within the tolerance limit of less than 5% for all the elements analysed.

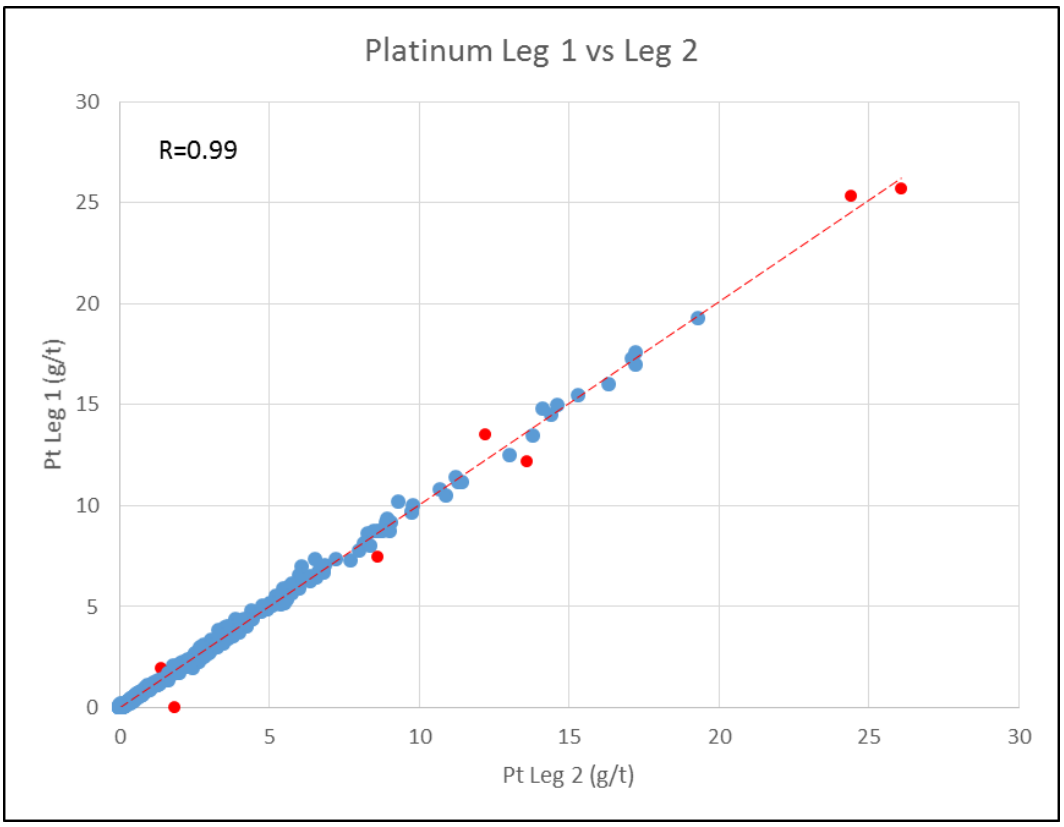

Figure 32. Platinum Twinstream Results (Leg 1 versus Leg 2); outliers indicated in red

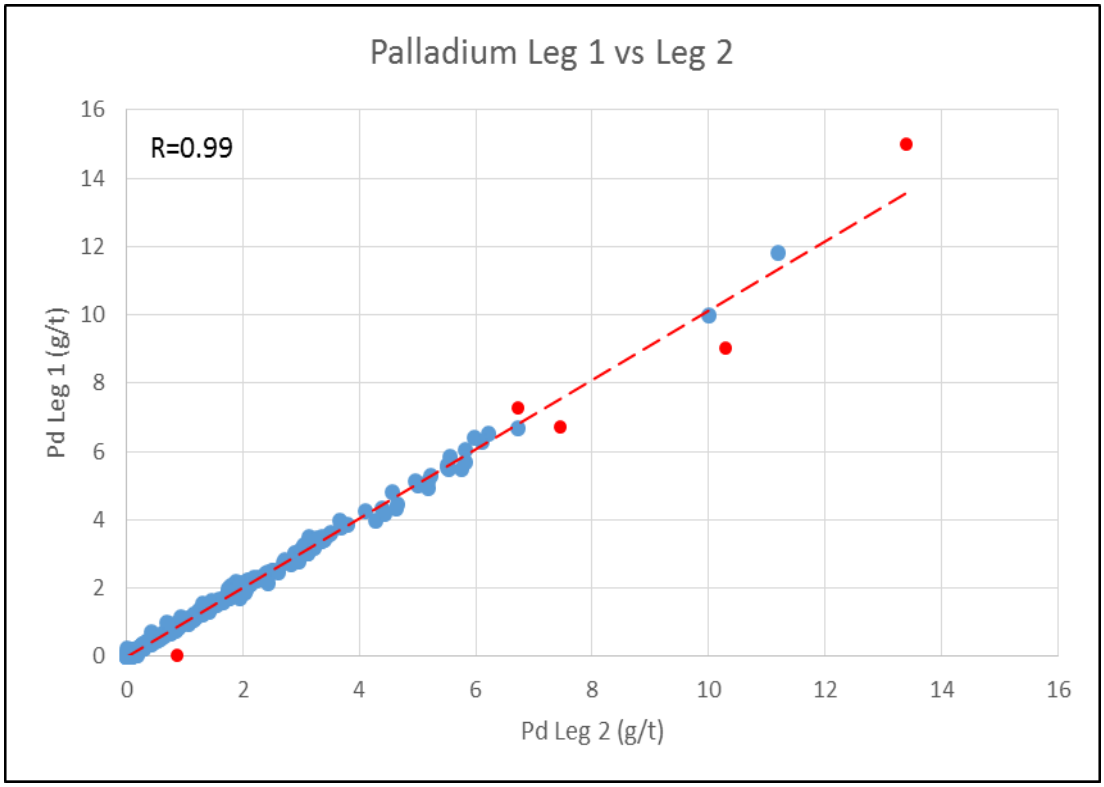

Figure 33. Palladium Twinstream Results (Leg 1 versus Leg 2); outliers indicated in red

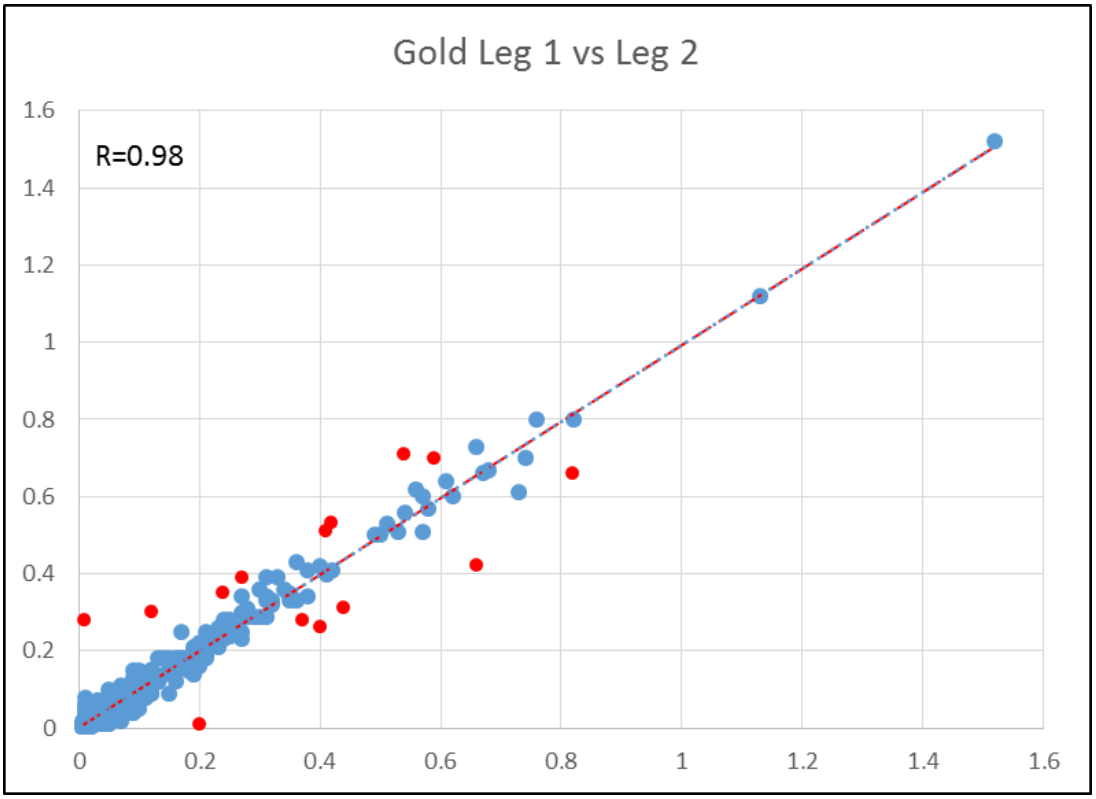

Figure 34. Gold Twinstream Results (Leg 1 versus Leg 2); outliers indicated in red

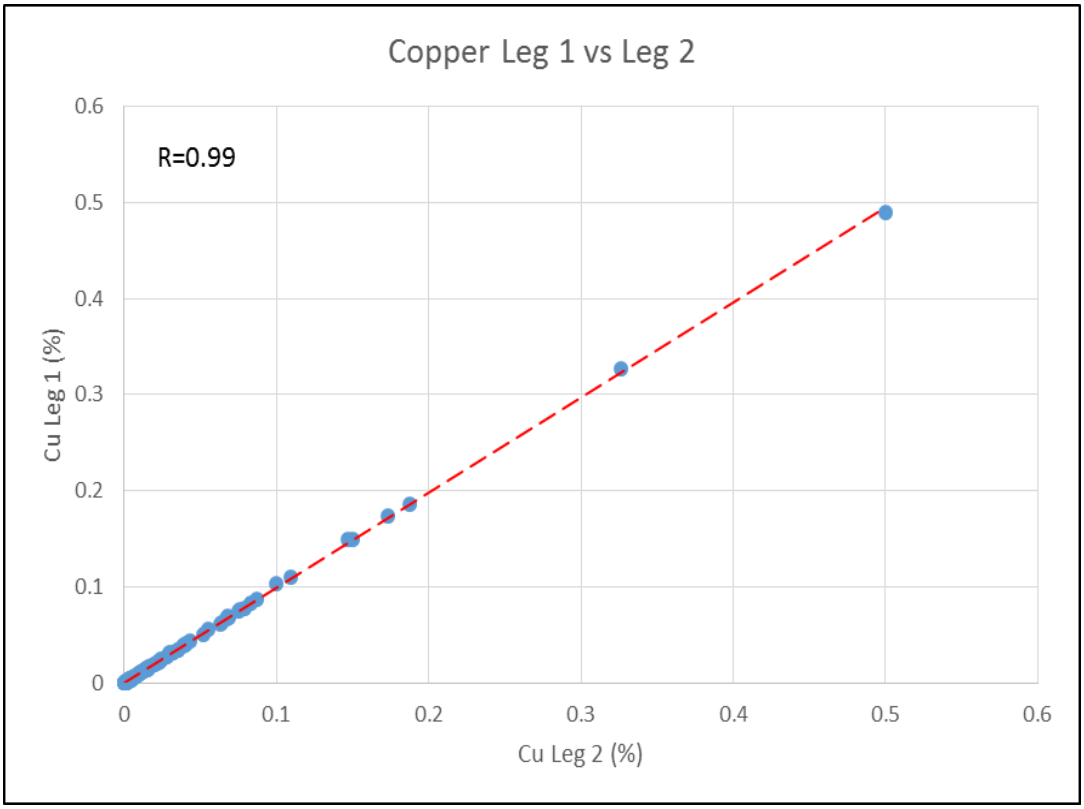

Figure 35. Copper Twinstream Results (Leg 1 versus Leg 2)

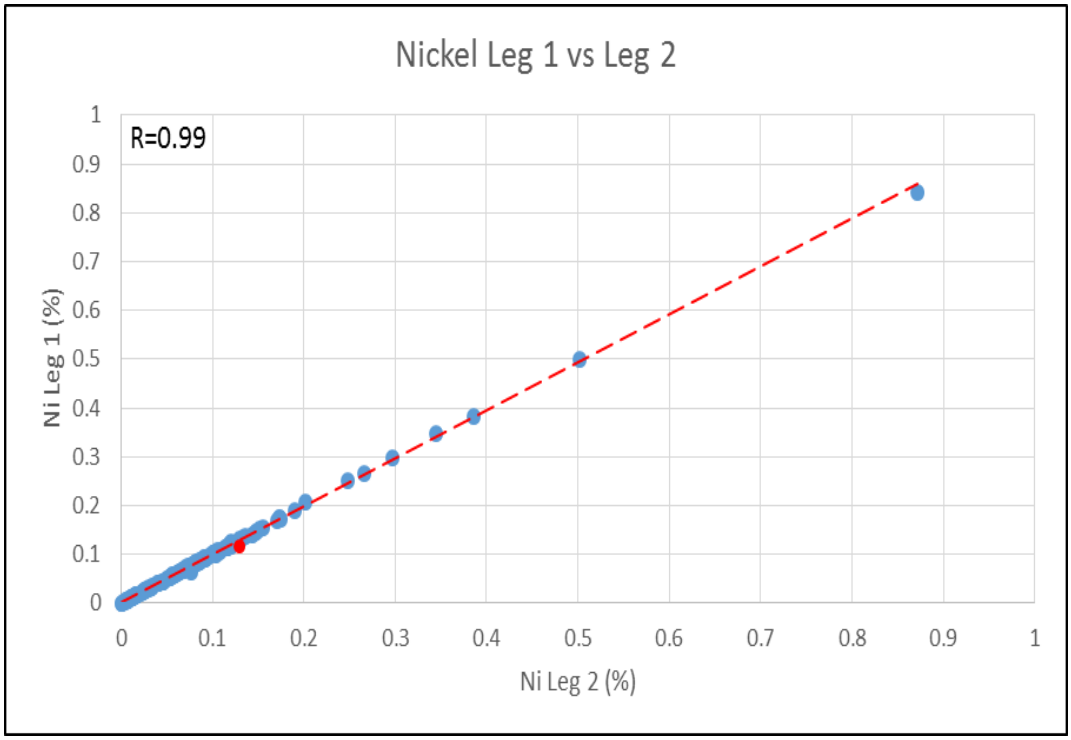

Figure 36. Nickel Twinstream Results (Leg 1 versus Leg 2); outliers indicated in red

4.1.3 Data Validation

A data export of the twenty-three quality checked drillholes was taken from the RBPlat geological drillhole database. The Merensky Unit assay data and associated information such as sample name, sample width, sample lithology and drillhole collar co-ordinates of each drillhole was exported. From the 23 drillholes, there were 547 primary Merensky Unit sample records in total. Grade results of elements extracted include the 3E results (platinum, palladium and gold), copper and nickel. Rhodium has been analysed only when the sum of platinum, palladium and gold is greater than 1.5 g/t. This has been undertaken as a cost saving measure. Approximately 50% of sample records do not have a rhodium analysis. Rhodium has therefore not been used for the study to avoid data skews where some sample records have a rhodium result and others do not. The following quality checks were performed on each sample record:

- Assay results required for the analysis are present (platinum, palladium, gold, copper and nickel)
- Sample lithology type has been logged and recorded
- Sample stratigraphic zone has been logged and recorded
- Valid collar co-ordinates

44 out of the 547 (8%) extracted sample records were found to have insufficient or missing data for analysis (missing lithologies/stratigraphic zone). The remaining 503 sample records (the 'dataset') were validated for use in the multivariate data analysis (Hypothesis Two).

4.2 pXRF Calibration

The 60 pressed pellet samples which were retrieved from the laboratory were analysed using the pXRF analyser for 60 seconds per reading. The pXRF results were compared to laboratory results in scatter plots (Figure 37 and Figure 38) and bar graphs (Figure 39 and Figure 40). The red 45° line in each scatter plot depicts the relationship expected if perfect correlation exists between the datasets. The bar graphs were plotted with the laboratory results and pXRF results.

The findings are:

- The reported results show an excellent correlation between the datasets with correlation coefficients in excess of 0.99 for both copper and nickel as indicated in Figure 37 and Figure 38.
- There is a visible bias of pXRF analyses with results consistently lower than the laboratory results. This can be seen by the regression slopes of Figure 37 and Figure 38 which is below

the red 45° line. The pXRF results are visibly lower than the laboratory results as illustrated in Figure 39 and Figure 40.

The slope and intercept of the copper/nickel scatter plots allows for the calibration of the pXRF to best overcome the bias seen in the pXRF results. The machine was therefore calibrated by applying the slope and intercept values as analysed during the pressed pellet exercise. Figure 37 and Figure 38 indicates slopes of 0.76 and 0.77 for copper and nickel respectively. The intercepts for copper and nickel used are 0.0002 and 0.0018 respectively.

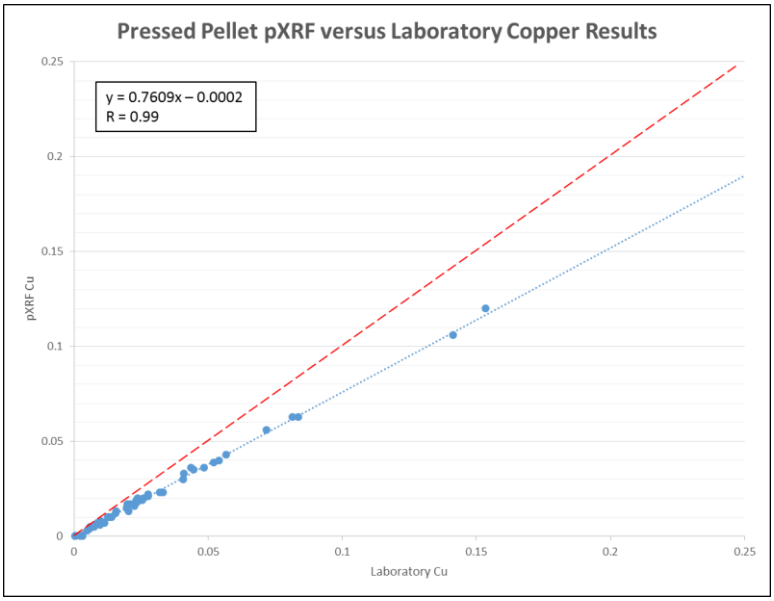

Figure 37. Pressed pellet pXRF copper results versus laboratory results

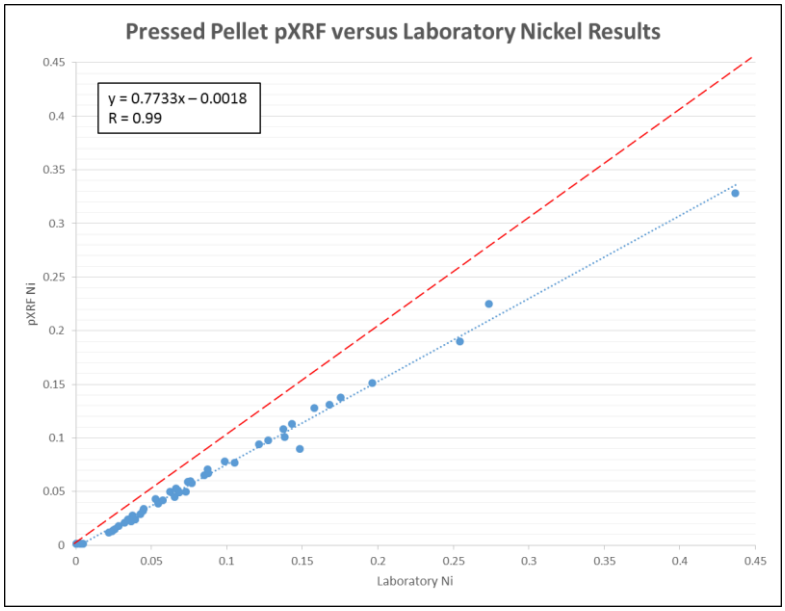

Figure 38. Pressed pellet pXRF nickel results versus laboratory results

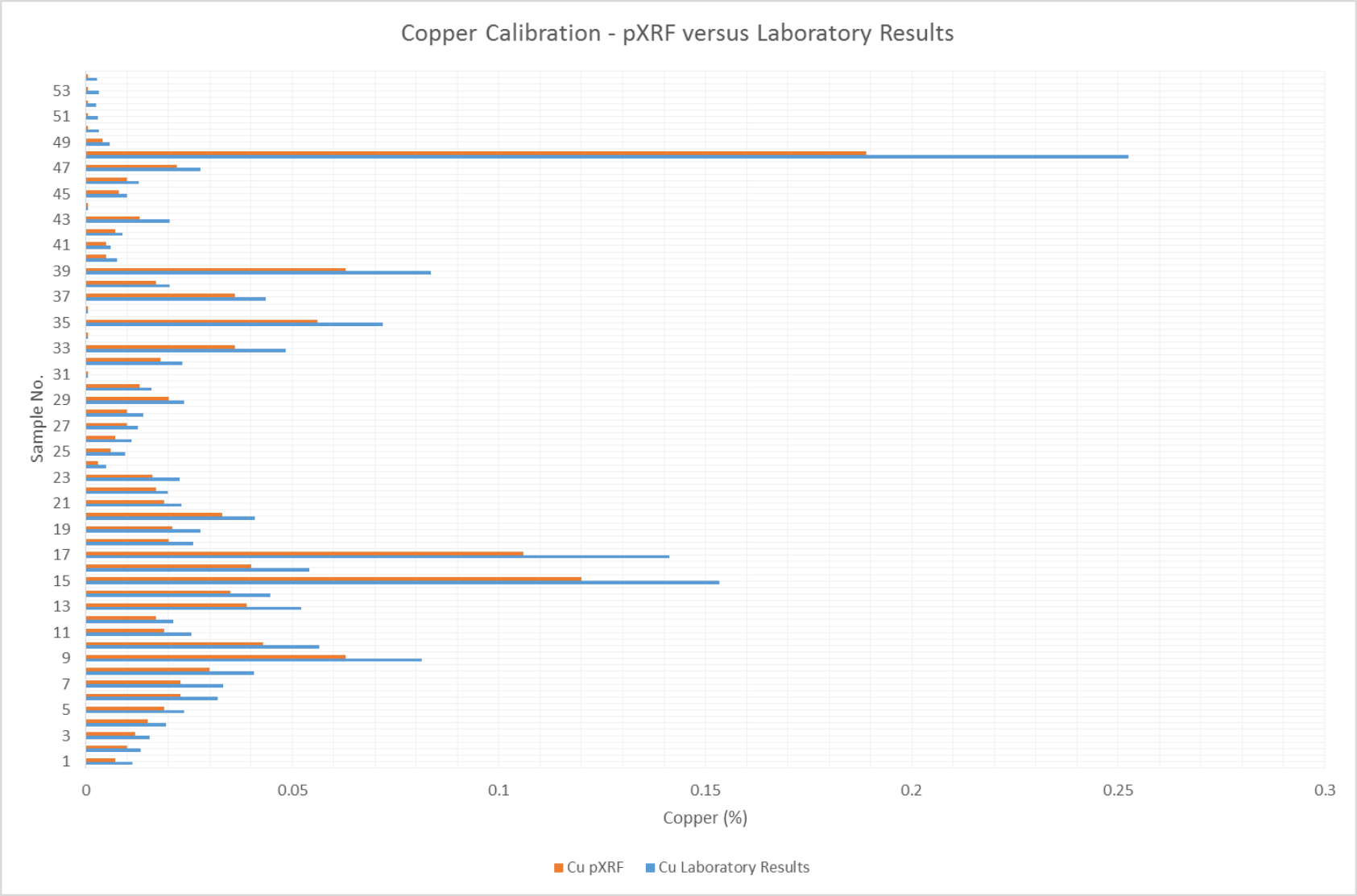

Figure 39. Pressed pellet pXRF copper versus laboratory results per pressed pellet sample analysed

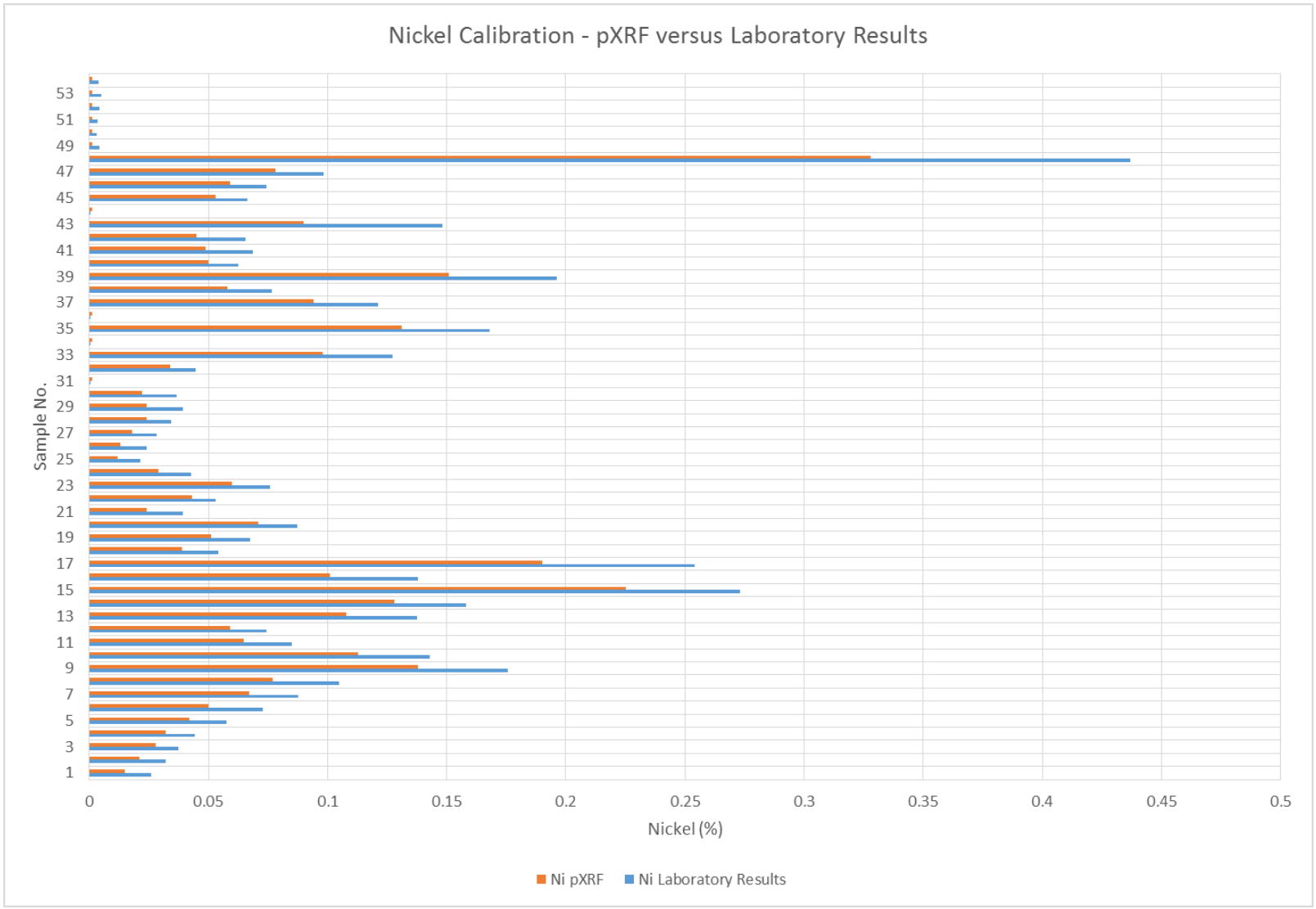

Figure 40. Pressed pellet pXRF nickel versus laboratory results per pressed pellet sample analysed

4.3 Hypothesis One: pXRF Accuracy Test

The pXRF copper and nickel results from the core analysis of five drillholes were compared to determine how similar the pXRF results are to the laboratory results. The results for each drillhole are depicted from Figure 41 to Figure 45. Each drillhole result diagram contains a simplified stratigraphic column to reference the results back to the sample number in the drillhole. Detailed stratigraphic columns are depicted in Appendix D.

The results of the F Test and T Tests and analysis of the differences between the datasets is provided in Table 6 and Table 7.

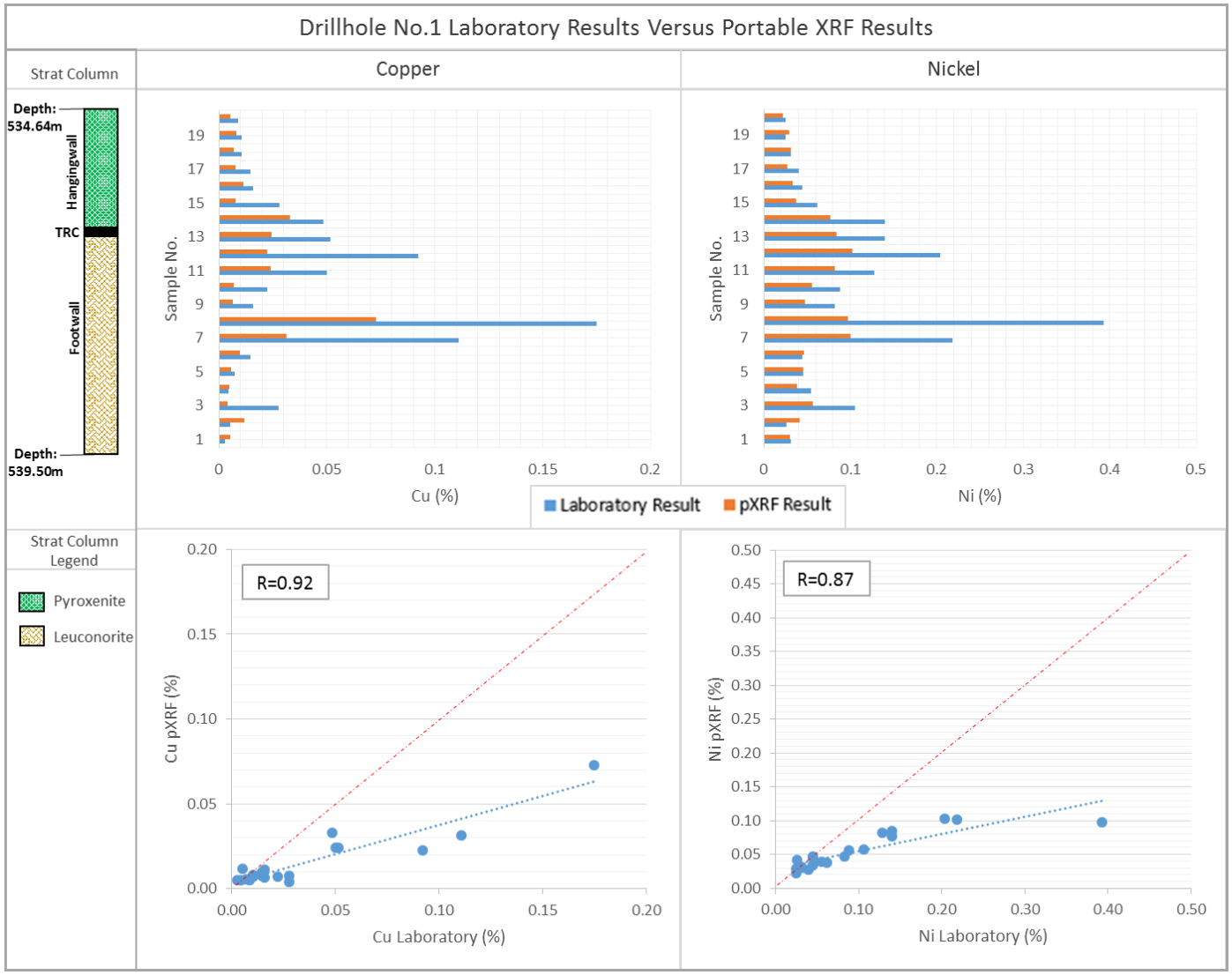

Figure 41. Drillhole No.1 pXRF Results versus Laboratory XRF Results

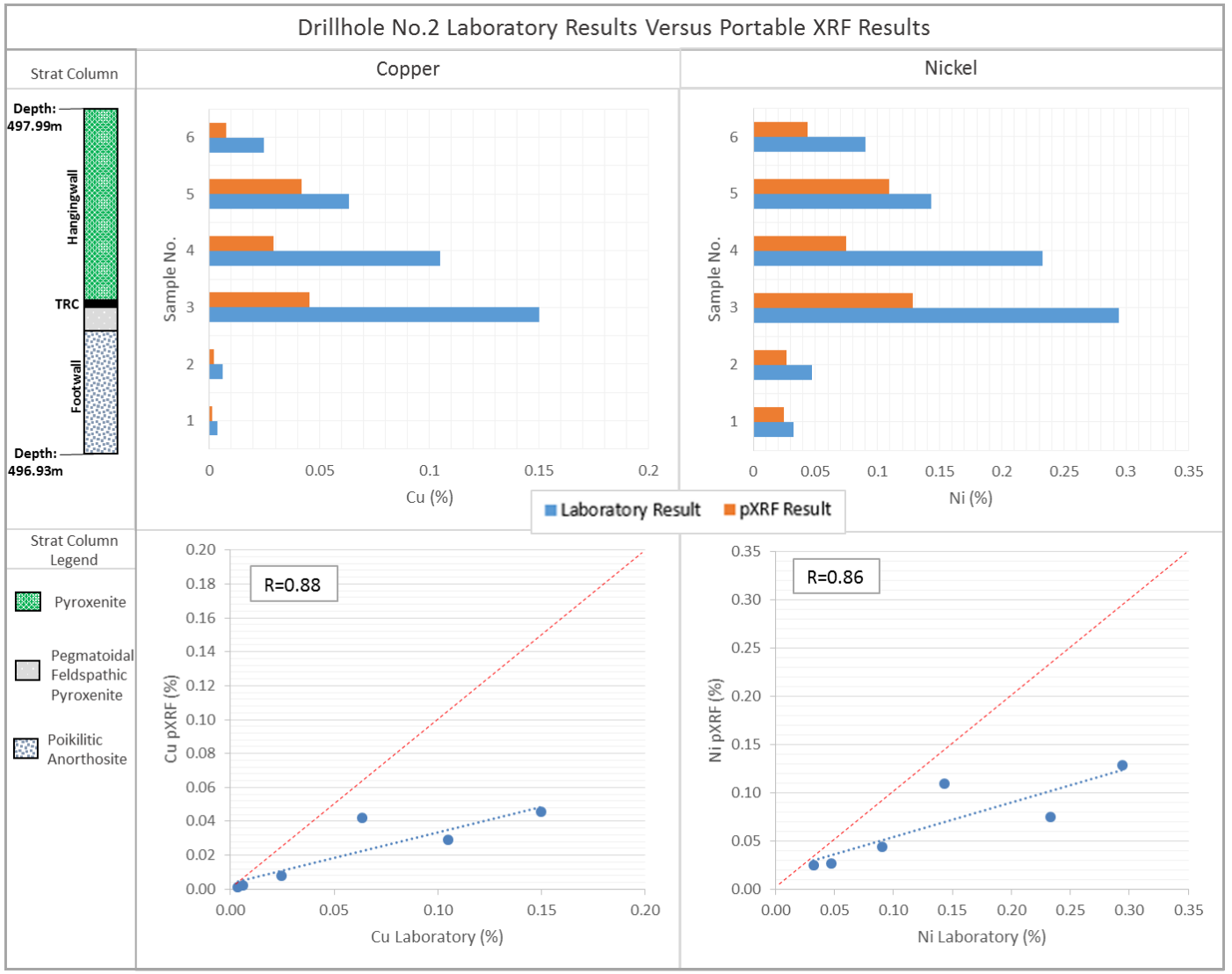

Figure 42. Drillhole No.2 pXRF Results versus Laboratory XRF Results

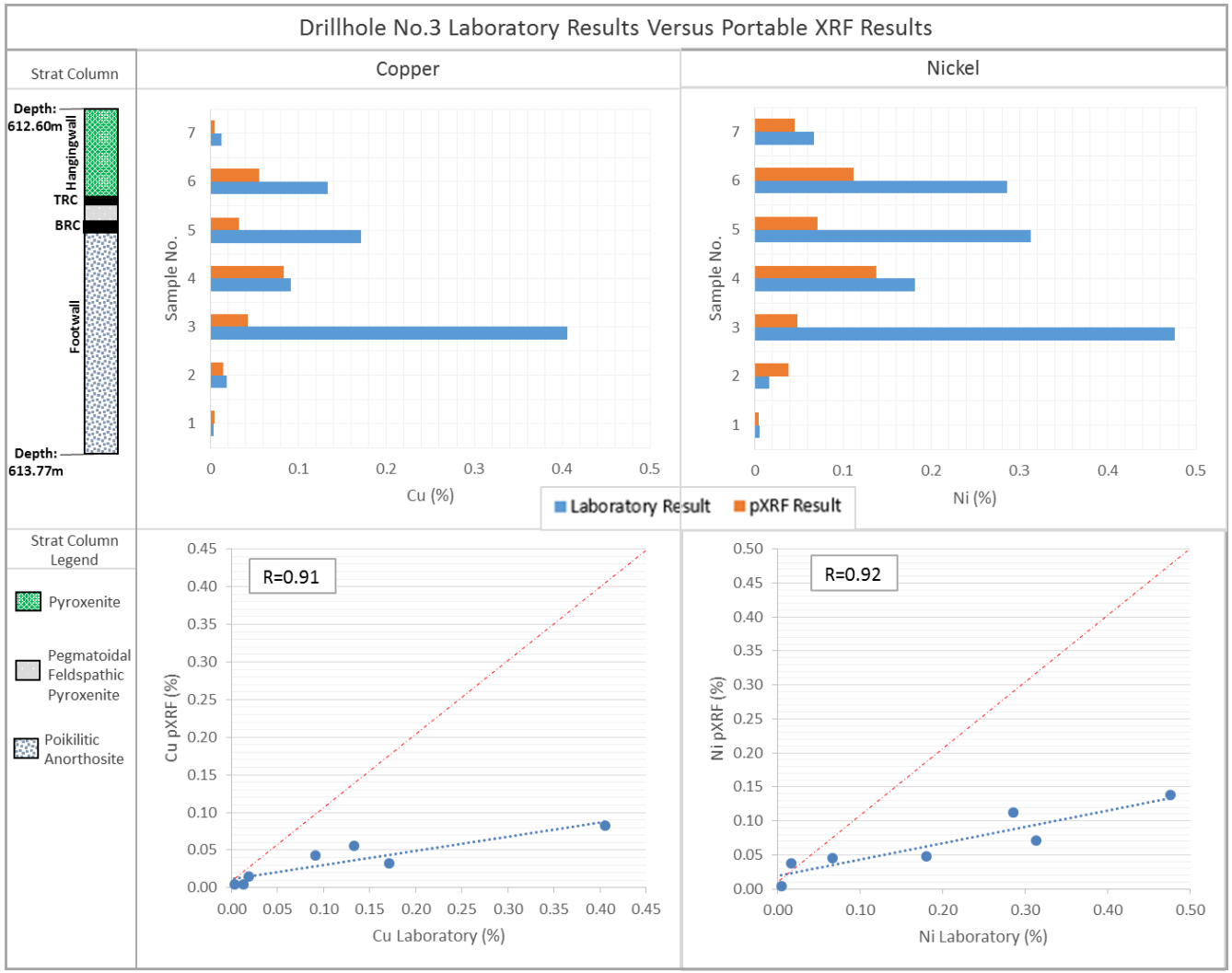

Figure 43. Drillhole No.3 pXRF Results versus Laboratory XRF Results

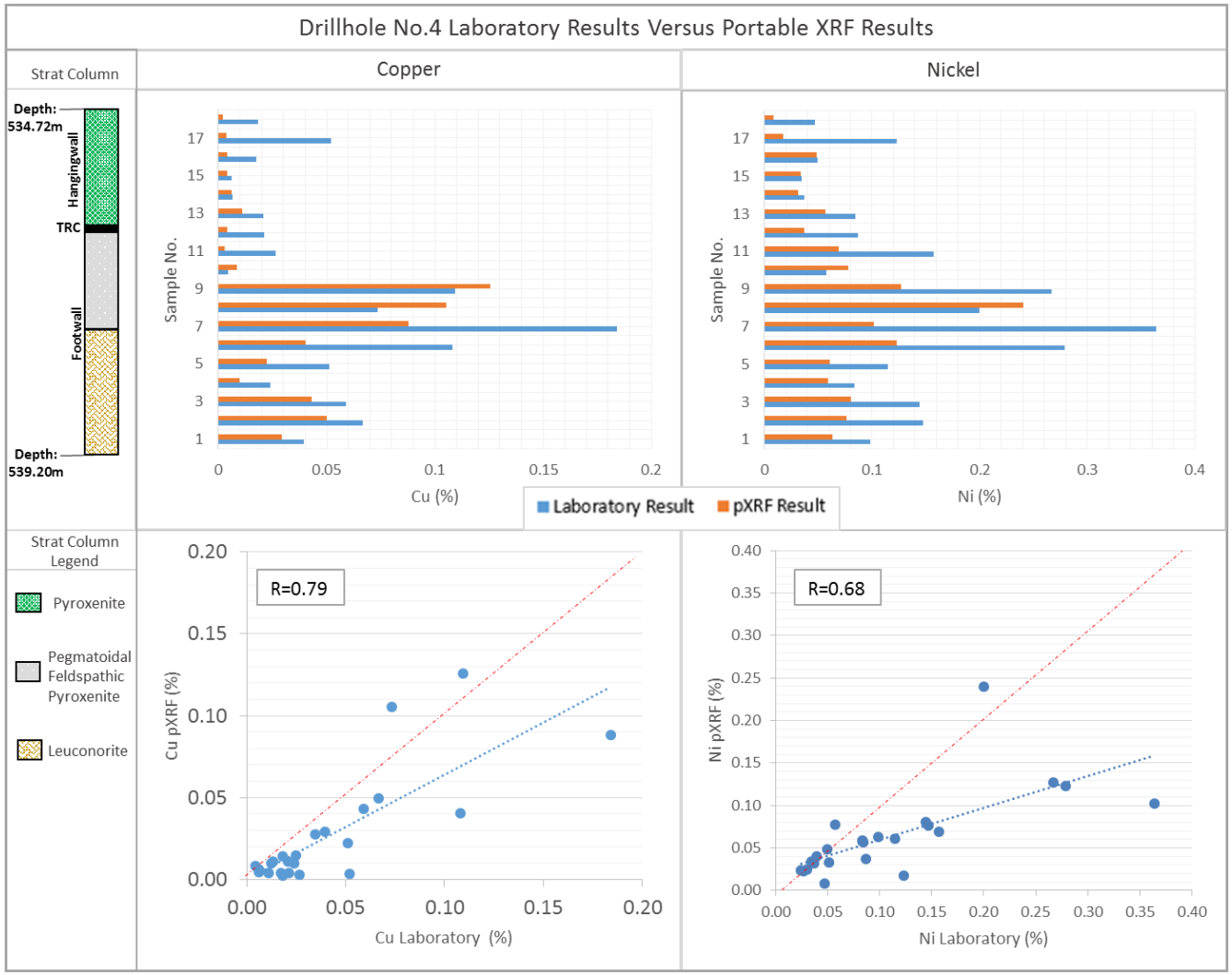

Figure 44. Drillhole No.4 pXRF Results versus Laboratory XRF Results

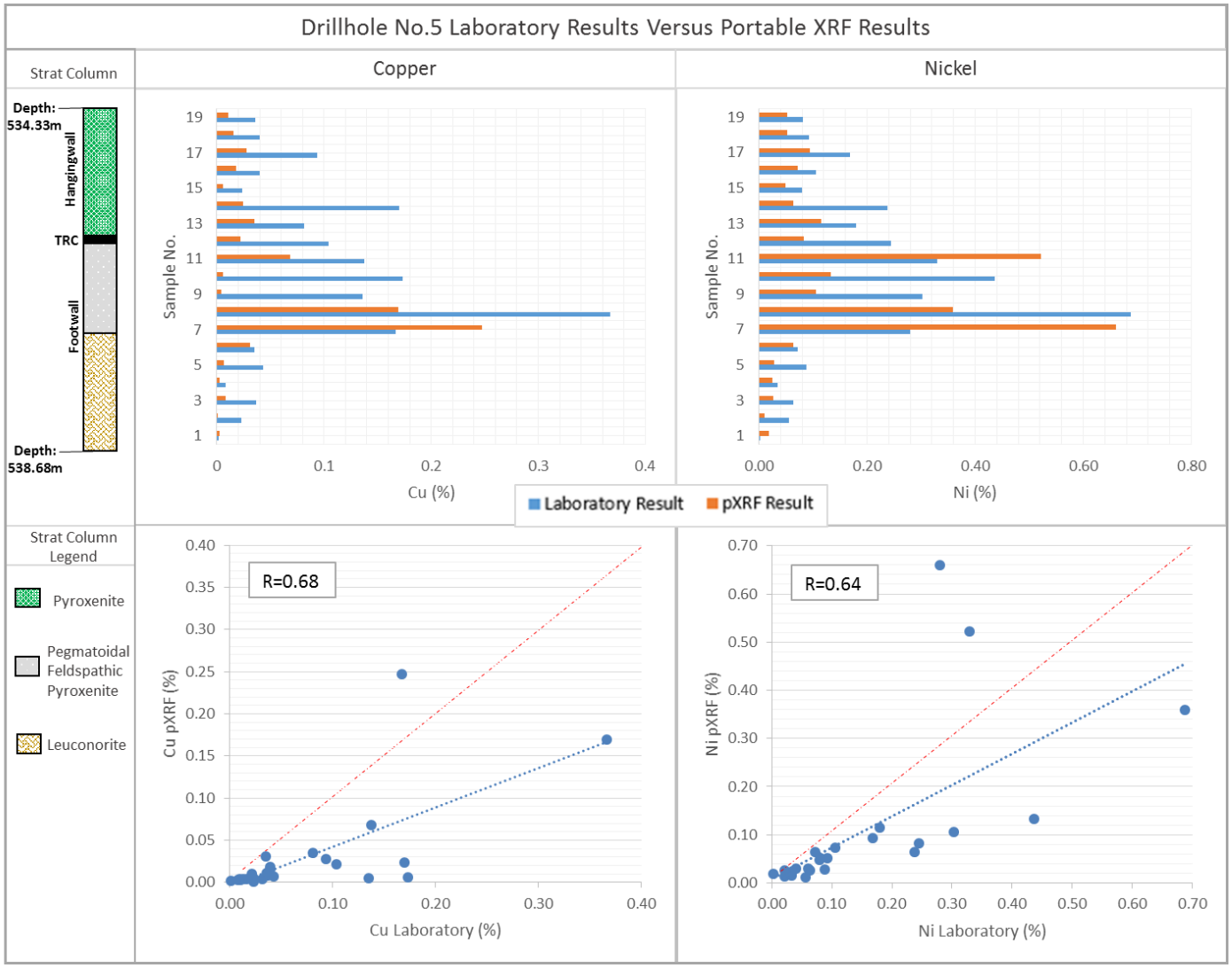

Figure 45. Drillhole No.5 pXRF Results versus Laboratory XRF Results

Table 5: Sample occurrences where pXRF result is greater than laboratory result

Drillhole No.	Total Samples	Samples pXRF > Lab	% Samples pXRF > Lab
1	20	2	10%
2	6	0	0%
3	7	2	29%
4	18	3	17%
5	19	3	16%
Total	70	10	14%

Table 6: F Test Statistics and Variance Comparisons between pXRF and laboratory datasets per drillhole (unequal variance highlighted in red)

Drillhole No.	Degrees of Freedom	Copper			Nickel		
		P	Lab Variance	pXRF Variance	P	Lab Variance	pXRF Variance
1	19	0.00004	0.002	0.0002	0	0.008	0.0007
2	5	0.017	0.003	0.0004	0.017	0.003	0.0004
3	6	0.0006	0.02	0.0008	0.002	0.03	0.002
4	17	0.2	0.002	0.001	0.01	0.008	0.002
5	18	0.09	0.008	0.004	0.39	0.02	0.03

Table 7: T Test Statistics and Mean Comparisons of pXRF Versus Laboratory Results (population differences highlighted in red)

Copper								Nickel							
T Stat	T Critical	P	pXRF Mean	Lab Mean	Mean %Diff	Min %Diff	Max %Diff	T Stat	T Critical	P	pXRF Mean	Lab Mean	Mean %Diff	Min %Diff	Max %Diff
2.06	1.94	0.04	0.02	0.03	50.00	14.54	124.13	2.07	1.99	0.04	0.05	0.10	50.00	0.17	75.15
1.47	2.44	0.19	0.02	0.06	66.67	33.96	72.28	1.55	2.36	0.16	0.07	0.14	50.00	23.35	67.88
1.56	2.36	0.16	0.03	0.12	75.00	21.72	31.93	1.84	2.36	0.11	0.07	0.19	63.16	25.71	130.61
1.29	2.11	0.21	0.03	0.05	40.00	3.64	93.04	2.35	2.05	0.02	0.07	0.13	46.15	1.43	86.00
2.13	2.10	0.04	0.03	0.09	66.67	13.15	97.76	0.93	2.10	0.35	0.13	0.19	31.58	10.63	568.37

The XY scatter plots of the pXRF versus the laboratory results of both copper and nickel reveal good to excellent correlations with the correlation coefficient (R) ranging from 0.68 to 0.91 and from 0.64 to 0.92 for copper and nickel respectively.

However, a visible bias can be seen where pXRF results are lower than laboratory results. Majority of the pXRF results (85% of the samples) are lower than the laboratory result. This indicates a trend or bias of pXRF results which are generally lower than the laboratory result. This is evident by the regression line of each scatter plot lying below the red 45° line. However, it was shown in Section 4.1.1. that the nickel laboratory results are lower than the true nickel value of the pressed pellet sample (laboratory nickel results show a consistent bias of lower results). This implies that the bias is larger than the current difference observed between pXRF and laboratory results as the laboratory result should be approximately 4% higher as indicated by the QAQC analyses in Section 4.1.1. There are a total of ten occurrences where the pXRF copper or nickel result is higher than the laboratory result (Table 5). These occurrences represent 10 out of 70 samples (15%).

The F Tests indicate that the variance between the laboratory and pXRF results are generally not equal (highlighted in red) with 70% of the data with $P < 0.05$. The results of the T Test shows that six out of the ten datasets are comparable as T Critical is greater than T Stat (highlighted in green). Where T Critical is less than T Stat (highlighted in red) or when $P < 0.05$, a significant difference in the dataset exists. This indicates that the datasets are not from the same population or distribution and are therefore not comparable (Clark and Harper, 2000). This is true for almost half of the datasets (four out of ten). The average differences between the pXRF and laboratory results are wide in range with differences between the datasets of 40% to 75% (Table 7). There is a large range of percentage differences between the individual pXRF and laboratory readings as well. The copper results show differences from 3.64% to 124.13%. Nickel results show negligible differences of 0.17% to extremely large differences of 568%. These may be interpreted as percentage error in the pXRF results as it is compared to the accepted laboratory result.

Due to the bias, the large range of error of the pXRF results and that almost half of the datasets are shown to not belong to the same population, the pXRF results cannot be used with confidence. While the bias is generally consistent in that it is lower than the laboratory results, the large range of error of individual direct core sample measurements indicates that further calibration or correction will not be adequate to address the bias. The results are therefore of inadequate accuracy to apply the pXRF with confidence for copper and nickel analysis. Pulverising the samples prior to analysis may decrease the error range as indicated in Figure 37 and Figure 38. However, based on the inaccuracy of the results on direct core, and for the purpose of this study, the null hypothesis of the Hypothesis One Test ($H1_0$)

'The pXRF produces accurate copper/nickel results' is rejected in favour of the alternate hypothesis ($H1_1$) which states 'The pXRF does not produce accurate copper/nickel results'.

4.4 Hypothesis Two: Copper and/or Nickel as a proxy for PGE content

4.4.1 Multivariate Data Analysis

XY scatter plots of copper and nickel versus 3E content were produced (Figure 46 and Figure 47) to determine trends or relationships between the variables. Data trends are difficult to identify from the scatter plots due to the varying concentrations and units of measurement of the variables under analysis. All variables occur in trace values however copper and nickel are lower in range and are reported in percent. Copper results range from 0.0017% to 0.49% and nickel ranges from 0.0055% to 0.86%. 3E values are higher and are reported in grams per ton. 3E values are higher with range of 0.045g/t up to 35.42g/t. The data range and distribution of the variables being compared results in scatter plots of data points which are largely condensed.

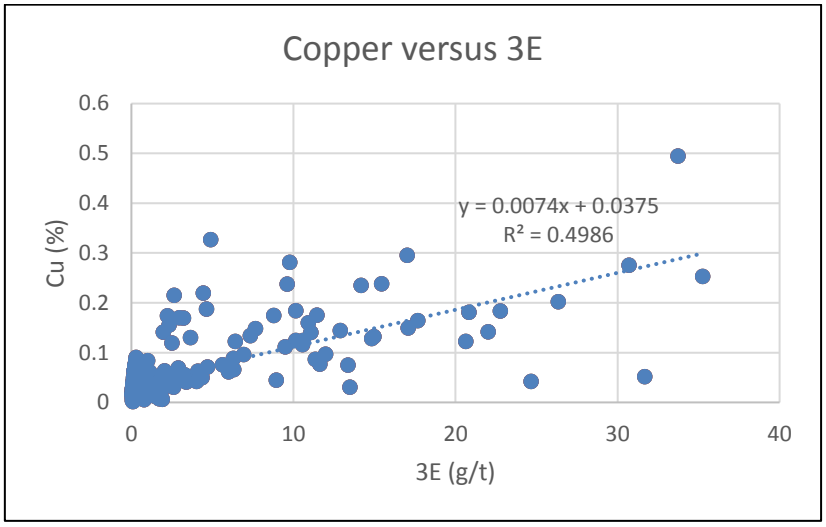

Figure 46. Copper Versus Laboratory 3E Grade Content

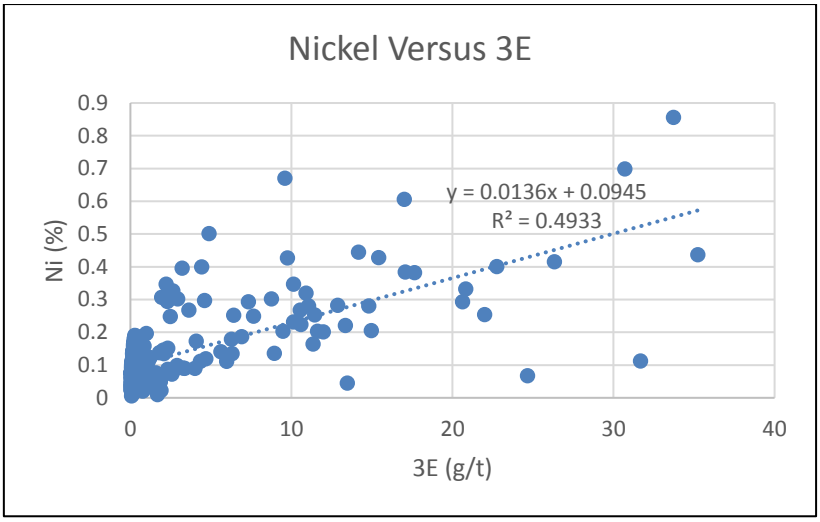

Figure 47. Nickel Versus Laboratory 3E Grade Content

Logarithmic values and constants may be applied to sample records to magnify the data for potential relationships prior to conducting conclusive statistical analyses (Clark and Harper, 2000). The logarithm and a constant of +3 was added to each 3E, copper and nickel sample record to magnify the data on the XY scatter plot as per Equation 6, 7 and 8. Each variable was calculated to ensure that all data was treated in the same manner for the purpose of magnifying the data to reliably identify trends only (not to quantify or to regress grade values). The result of this is depicted in Figure 48 with data points, trends and potential data populations more clearly visible

$$log_{10}(3E) + 3 \quad \text{.....Equation 6}$$

$$log_{10}(Cu) + 3 \quad \text{.....Equation 7}$$

$$log_{10}(Ni) + 3 \quad \text{.....Equation 8}$$

The magnified data indicates that at least two major data populations exist with regard to 3E to copper/nickel assay data (Figure 48). A dense cluster of points occurs to the left of the scatter plot ('Population One') and a scattered cloud of points occurs to the right ('Population Two'). Each of these populations display a visibly different 3E to Cu/Ni content trend or signature and may be considered unique mineralisation populations.

The frequency distributions (histograms) of each of the variables (3E, copper and nickel) displays a positive skew or lognormal distribution with a high frequency of low grade values and a decreasing number of high grade values. The histograms of each variable are a further indication that there are at least two to three populations within each variable. The populations are visible by two to three

prominent peaks or data averages in the frequency distributions. The most notable data averages of the various populations are depicted in blue and green (Figure 49 to Figure 51).

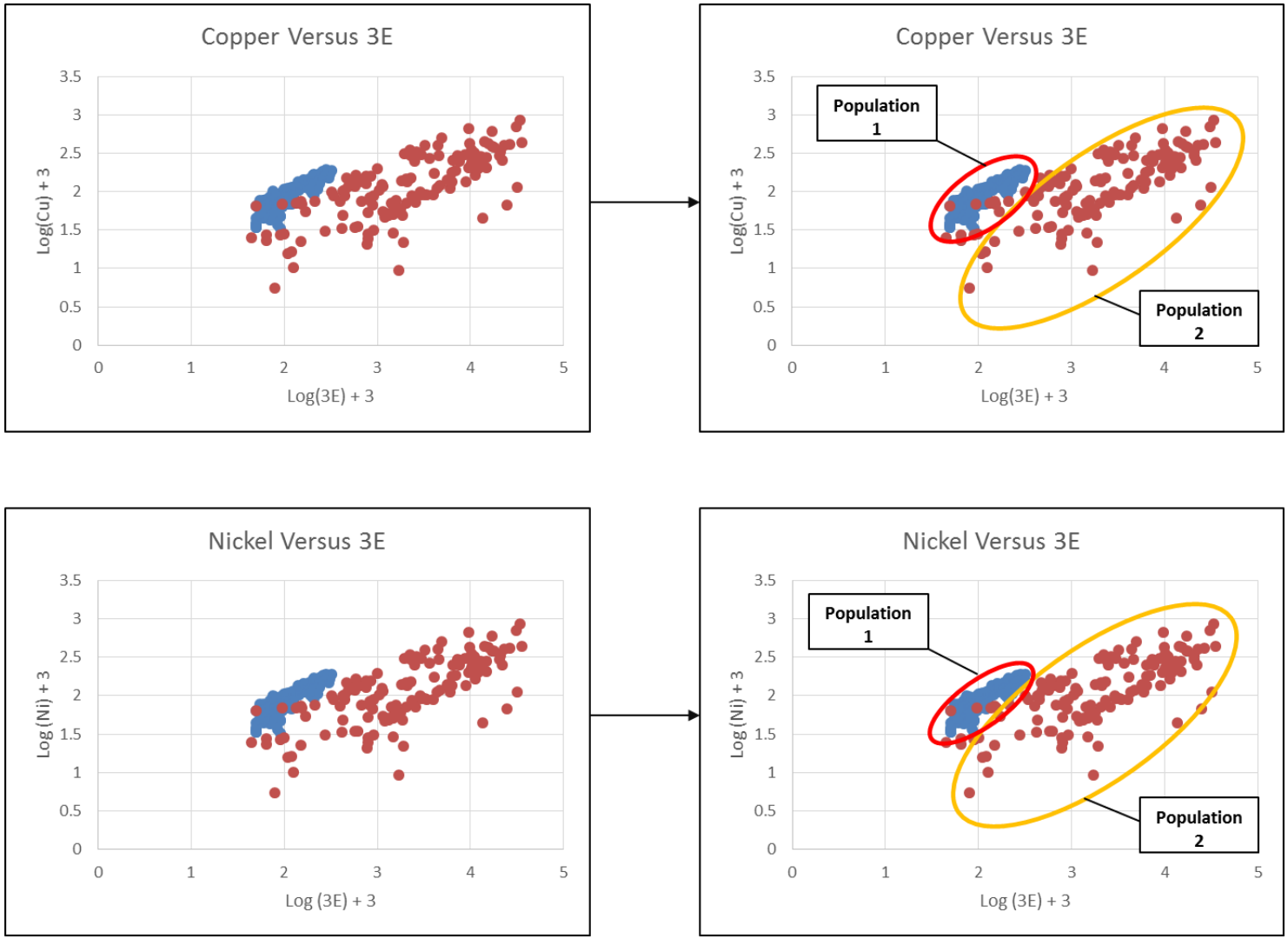

Figure 48. Magnified data (log transformed and +3 constant) – copper/nickel versus 3E (left) indicating at least two data populations (right)

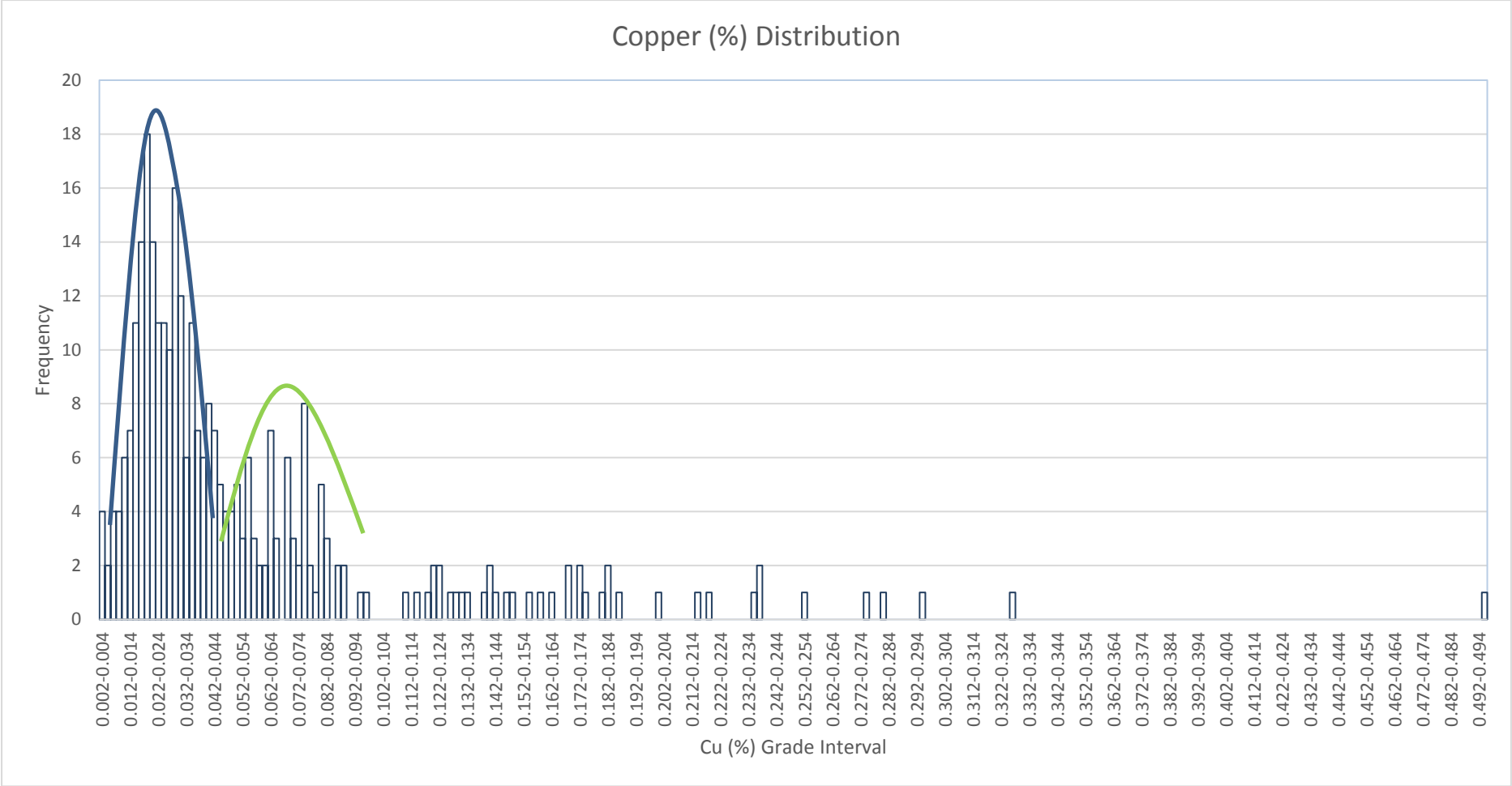

Figure 49. Copper grade frequency distribution within Styldrift I; Central Reef Facies

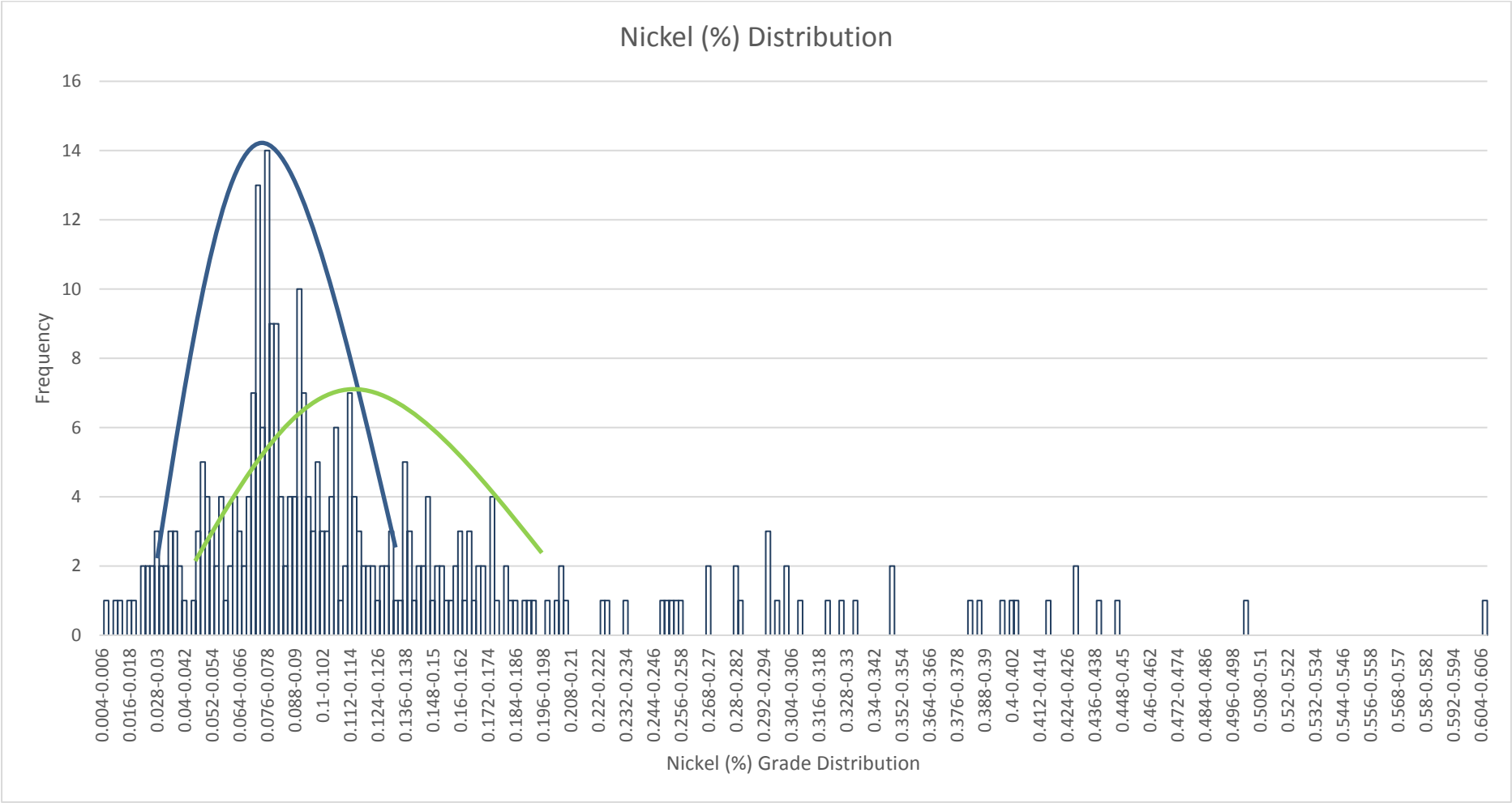

Figure 50. Nickel grade frequency distribution within Styldrift I; Central Reef Facies

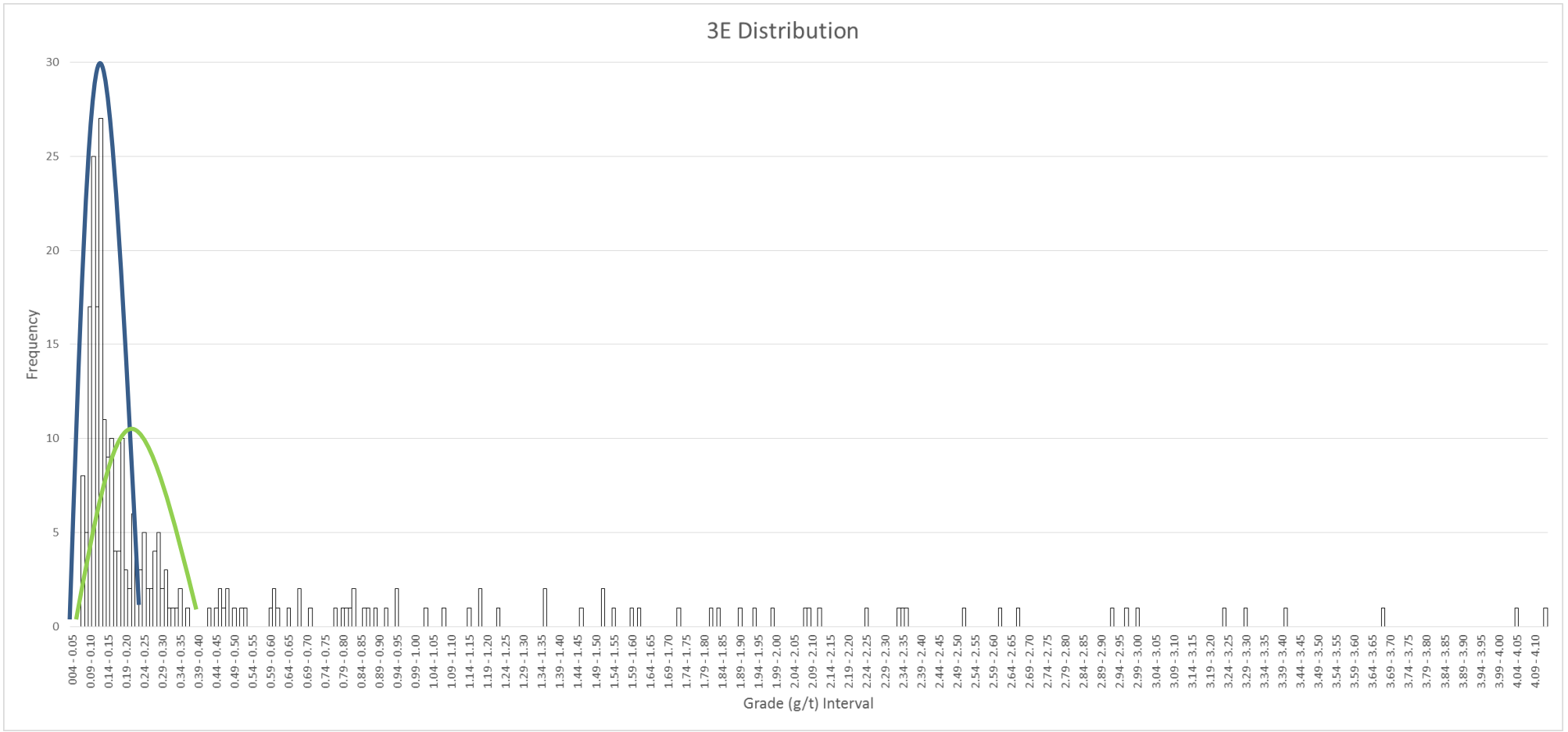

Figure 51. 3E grade frequency distribution within Styldrift I; Central Reef Facies

Table 8: F Test Statistics of Population 1 and Population 2

Element	P	Variance	
		Population 1	Population 2
3E	0.00	0.002	58.09
Copper	0.00	0.0003	0.0059
Nickel	0.00	0.0011	0.0207

Table 9: T Test Statistics of Population 1 and Population 2

Element	T Stat	T Critical	P	Mean	
				Population 1	Population 2
3E	-9.39	1.97	0.00	0.110	5.539
Copper	-9.78	1.96	0.00	0.030	0.088
Nickel	-8.855	1.97	0.00	0.001	0.020

The P values are very low. As the result is up to seventeen decimal places, Table 8 and Table 9 report P values of 0.00 (as it is reported to two decimal places). The F Test undertaken on 3E, copper and nickel indicate that the variance between Population 1 and Population 2 are significantly different. The T Test also indicates significant differences between each population. It can therefore be accepted that these datasets belong to two separate populations as indicated in the scatter plots (Figure 48).

The various populations that exist in the dataset must be isolated to find a consistent relationship between the variables (3E, copper and nickel) to perform statistical analyses such as a regression (Clark and Harper, 2000). The following parameters have been investigated to determine if these are controls resulting in the populations observed:

i. Lateral Zones – XY collar co-ordinates of the sample drillhole to assess if the populations emanate from distinct spatial lateral zones

ii. Lithology – Distinct populations based on the lithology of the sample

iii. Stratigraphic Zone – Vertical zones based on the stratigraphic zone of the samples

iv. Grade – Distinct populations based on grade values

i. Lateral Zone Analysis

The 23 drillholes which exist in each population were plotted spatially using XY collar co-ordinates (Figure 52). This was done to determine if distinct lateral spatial zones could be determined as a control of the populations observed in the data analyses. However, Population One and Population Two both contain the same drillholes. This can be seen by the green (Population One) and red dot (Population Two) overlapping at every collar position (Figure 52). Lateral zones are therefore not the control or the differentiating factor between Population One and Population Two.

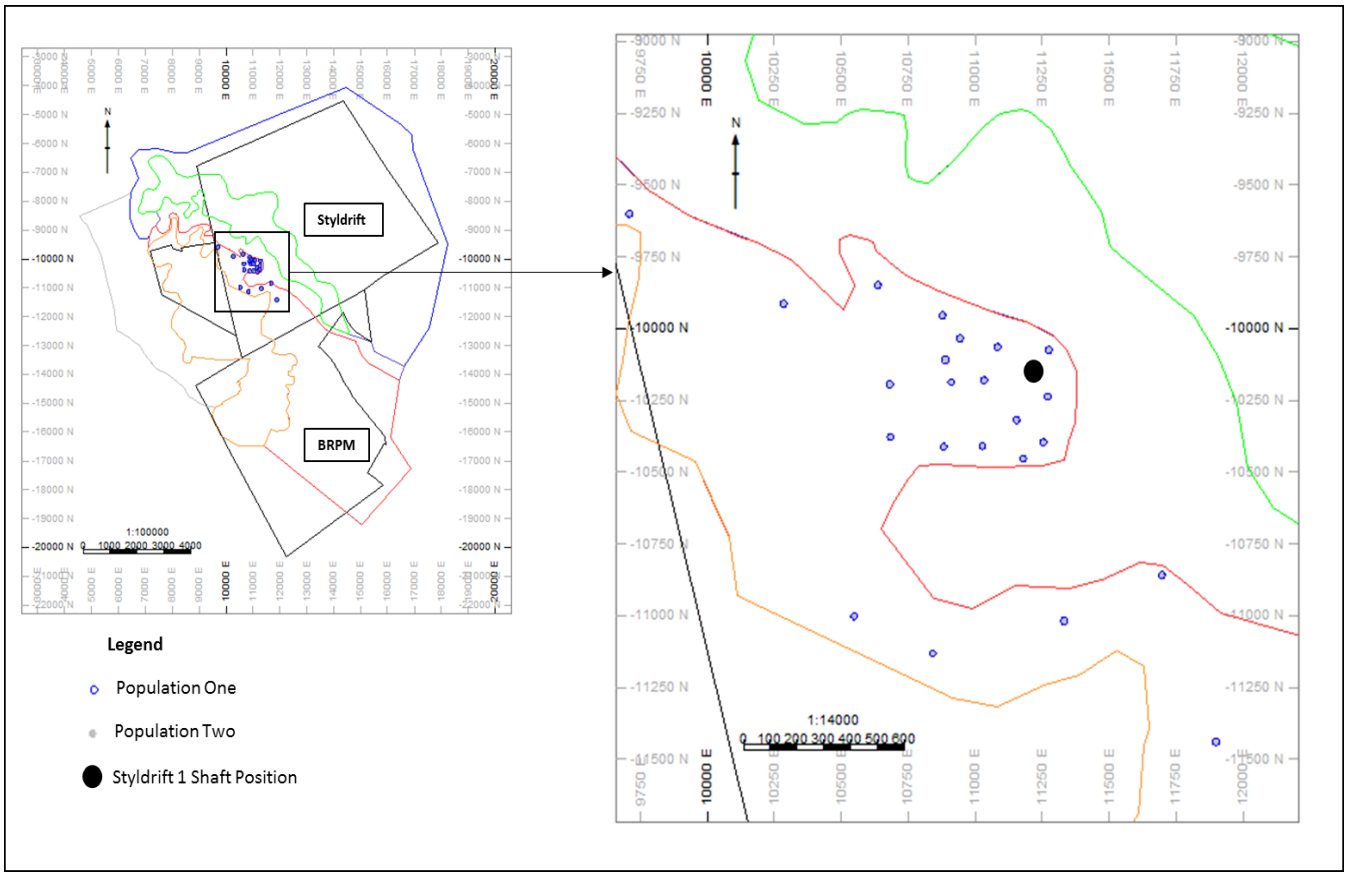

Figure 52. Spatial plotting of Population One and Population Two Boreholes

ii. Lithology Analysis

The lithology of each sample was coded on the XY scatter plots of 3E versus copper and 3E versus nickel content (Figure 53 and Figure 55) to determine if the lithology type is a control of the populations. Both Population One and Population Two indicate the emergence of two sub-populations (Figure 54 and Figure 56). The sub-populations and dominant lithologies are listed in Table 10.

Table 10: Data populations and associated lithologies

Major Population	Sub-Population	Dominant Lithologies
Population 1	1.1	Anorthosite/Norite
	1.2	Feldspathic Pyroxenite
Population 2	2.1	Anorthosite/Norite
	2.2	Feldspathic Pyroxenite

The sub-populations 1.1 and 2.1 consist primarily of anorthosite and norite with minor occurrences of feldspathic pyroxenite (Figure 54 and Figure 56). The primary lithologies of sub-population 1.1 and 1.2 are typically Merensky Footwall lithologies. The sub-populations 1.2 and 2.2 consist primarily of feldspathic pyroxenite with minor to moderate occurrences of anorthosite/norite. Feldspathic pyroxenite is a Merensky Reef and Merensky Hangingwall lithology. There is an overlap in the grade range of sub-populations 1.1 and 1.2.

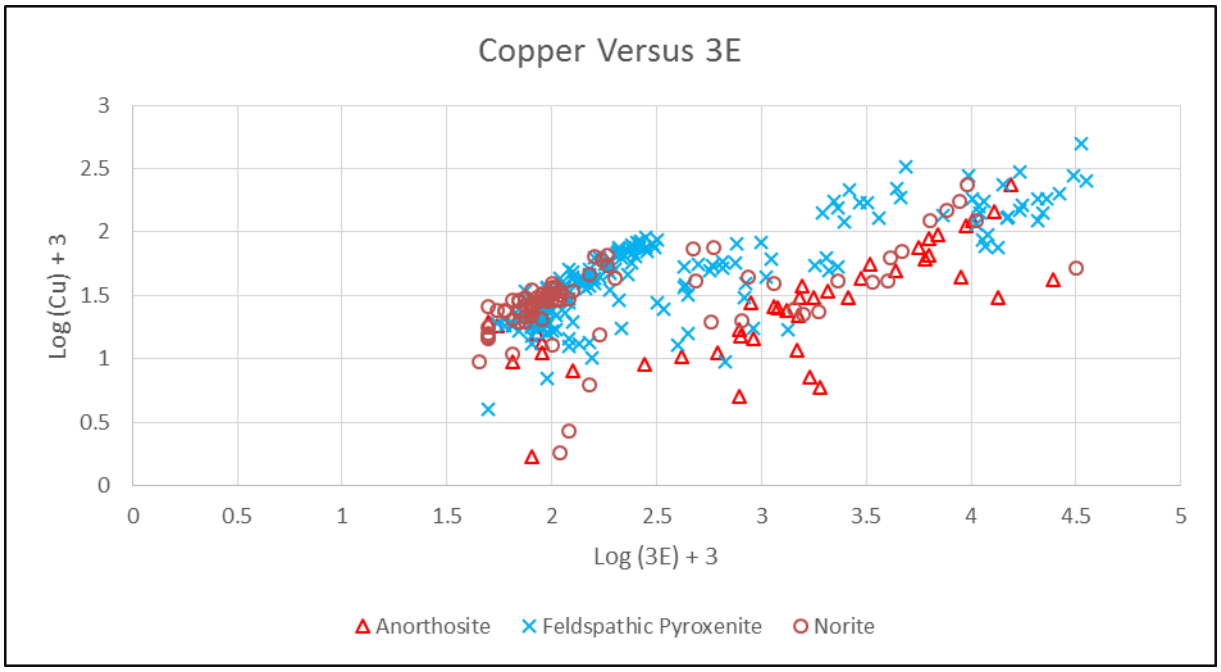

Figure 53. Copper Versus 3E grade content coded by lithological type

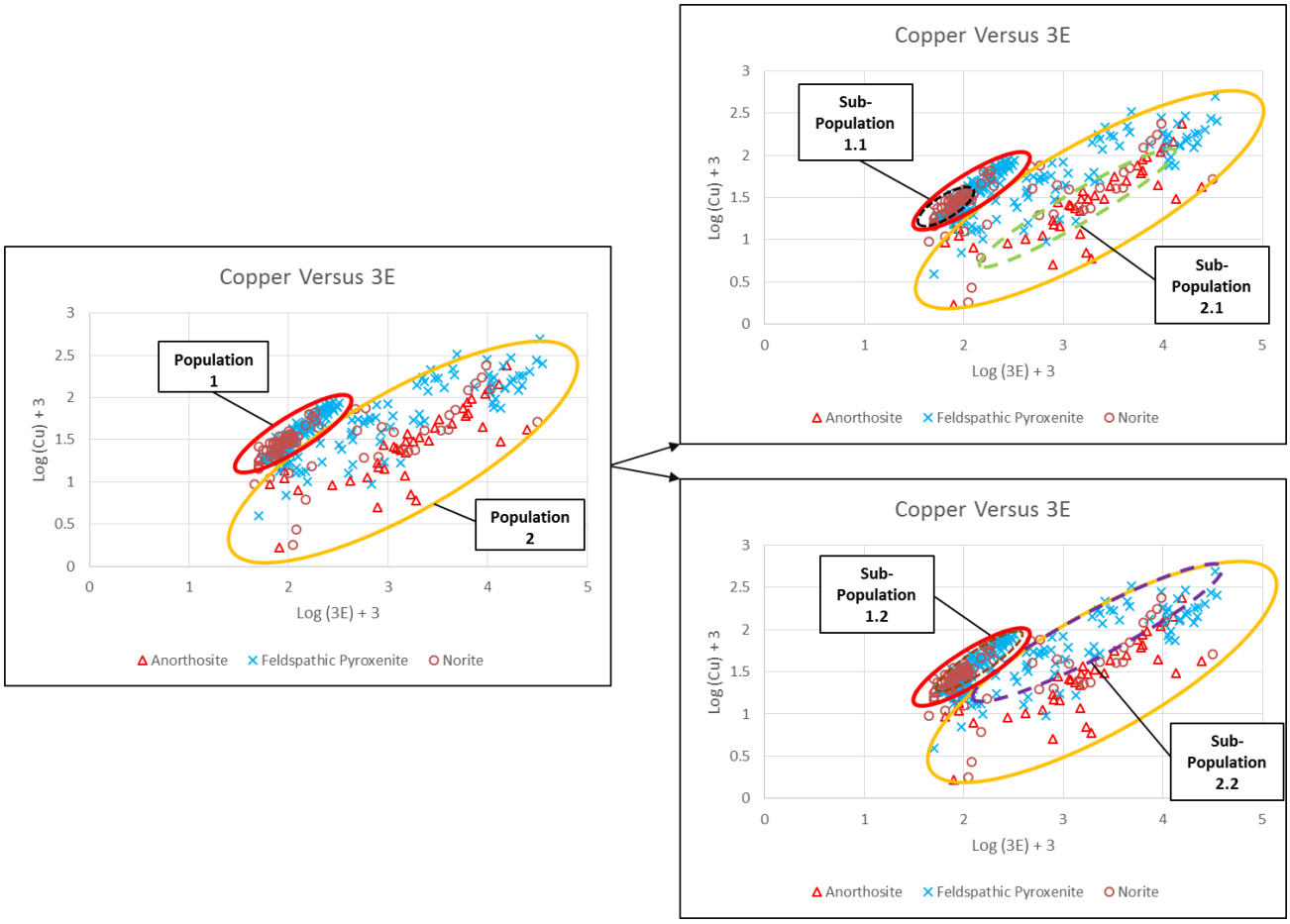

Figure 54. Lithological sub-populations within the Copper versus 3E mineralisation populations

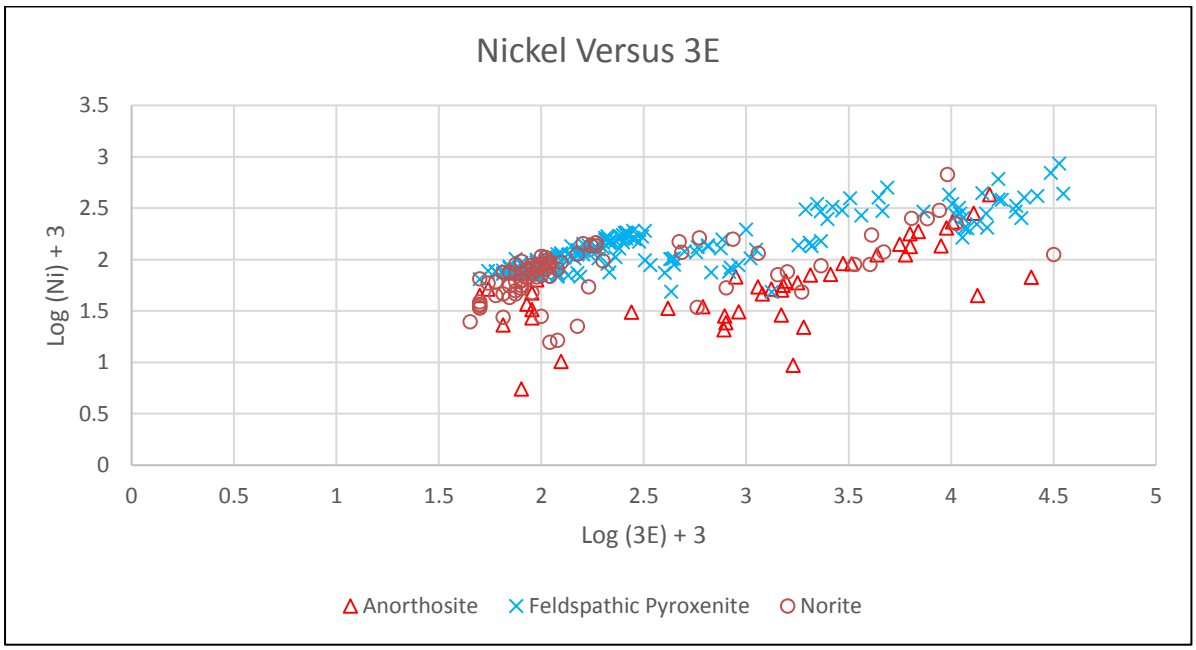

Figure 55. Nickel Versus 3E grade content coded by lithology of the sample

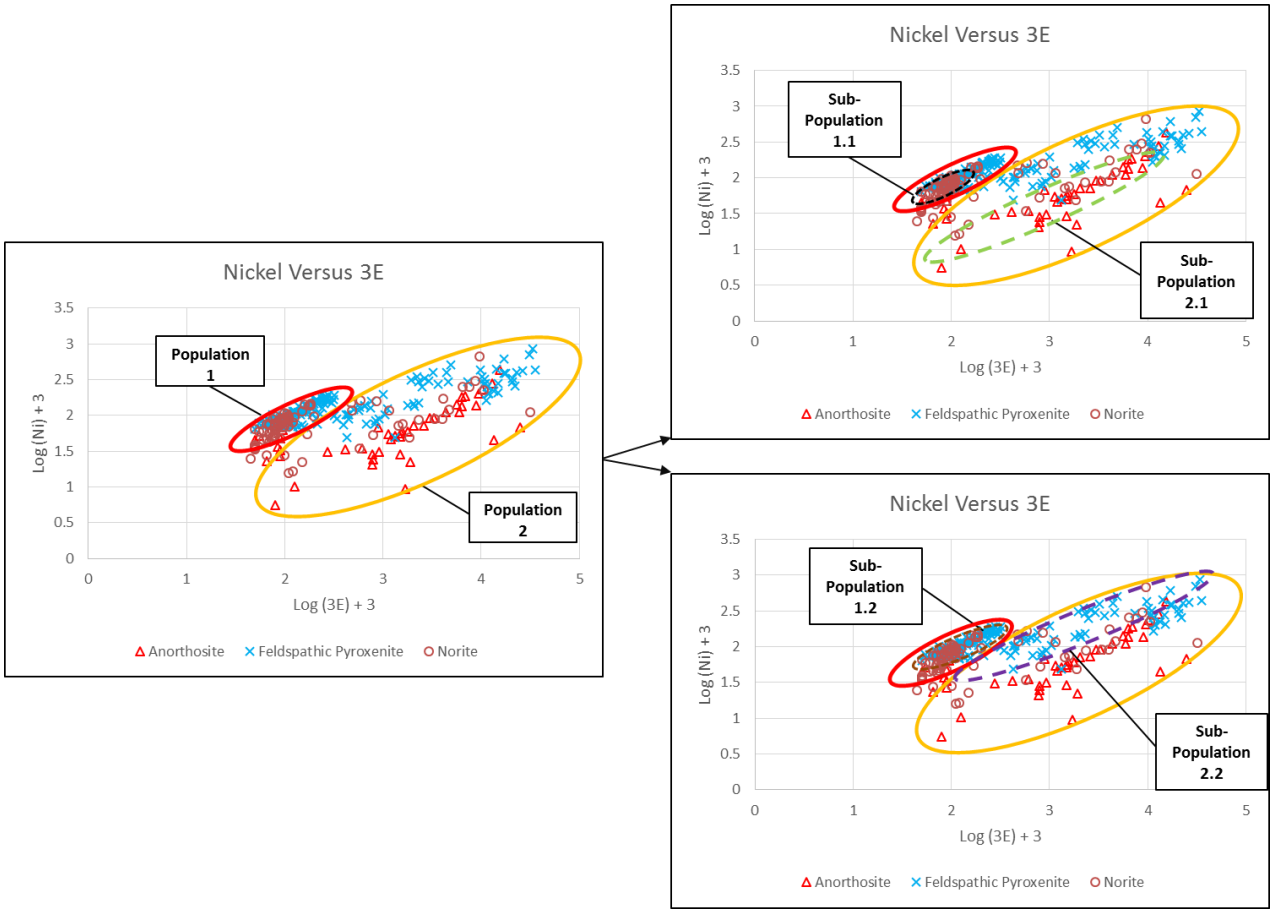

Figure 56. Lithological sub-populations within the Copper versus 3E mineralisation populations

iii. Stratigraphic Analysis

The stratigraphic zone in which each sample occurs (Merensky Footwall/Merensky Reef/Merensky Hangingwall) was coded on the XY scatter plots of 3E versus copper and 3E versus nickel content (Figure 57). This was done to determine if the 3E to Cu/Ni data populations are a function of the sample stratigraphic zone.

Figure 57 reveals that the Merensky Footwall displays a distinct population trend that can be isolated. This trend is in line with sub-population 2.1 identified in the lithological analysis (Figure 54 and Figure 56). The Merensky Hangingwall and Merensky Reef cannot be isolated as the data points are intermingled displaying no distinct population trends.

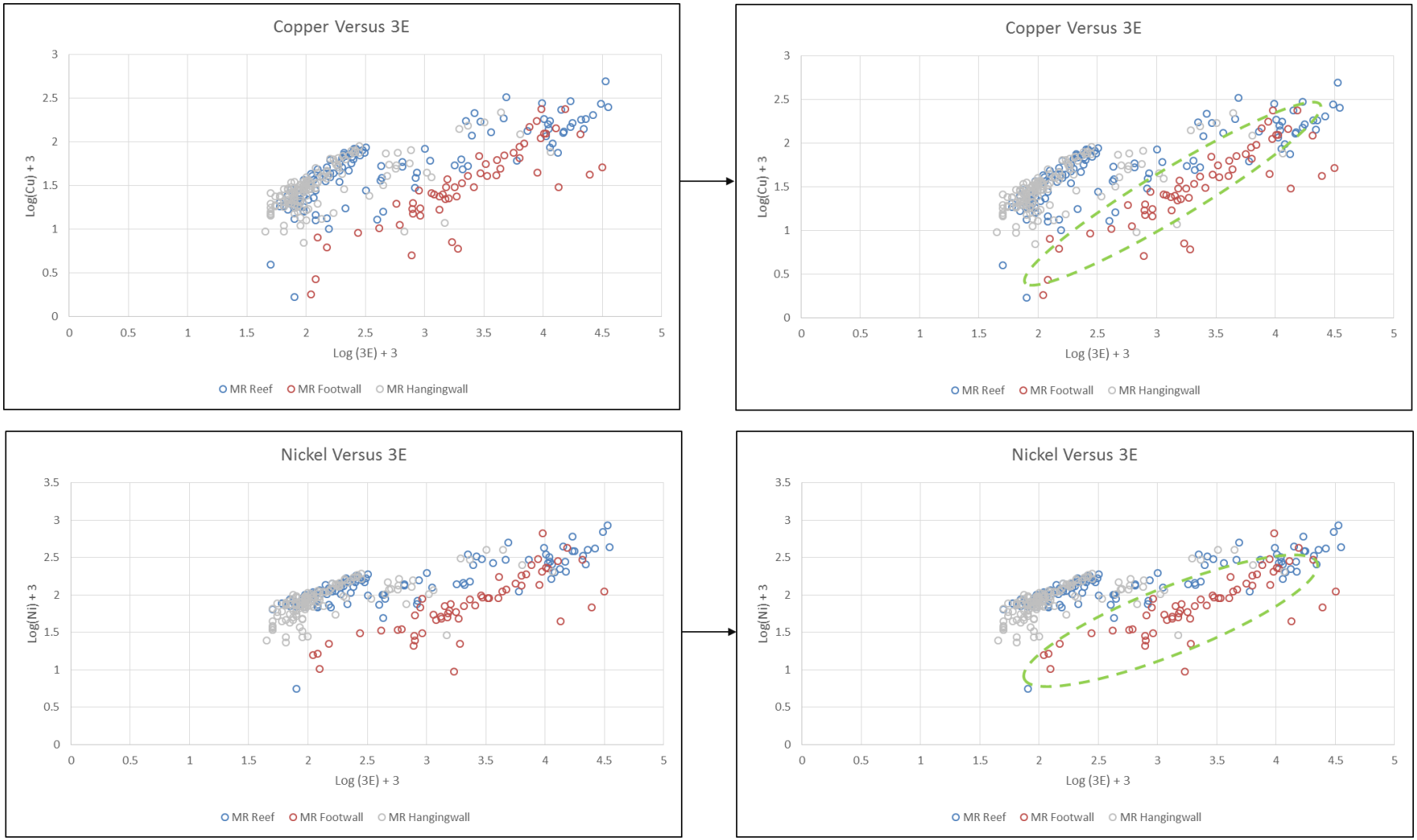

Figure 57. 3E Versus Copper/Nickel (left) and resulting footwall trends (right)

iv. 3E Grade Analysis

The 3E grade range of Population One and Population Two was determined by sorting the 3E assay data in ascending order. Distinct grade populations exist with all samples from Population One at a grade range of <0.3 g/t. Majority (90%) of the samples from the Population Two dataset has a grade range that is >0.3 g/t. Stratigraphic zones have been coded in the grade analysis to further assist in the identification of the data populations (Figure 58). The Merensky Footwall samples create a distinct population that can be isolated. Merensky Reef and Merensky Hangingwall sample data is intermingled revealing no distinct trends or characteristics which separate these two stratigraphic zones unlike the Merensky Footwall which can be isolated as a distinct population on its own.

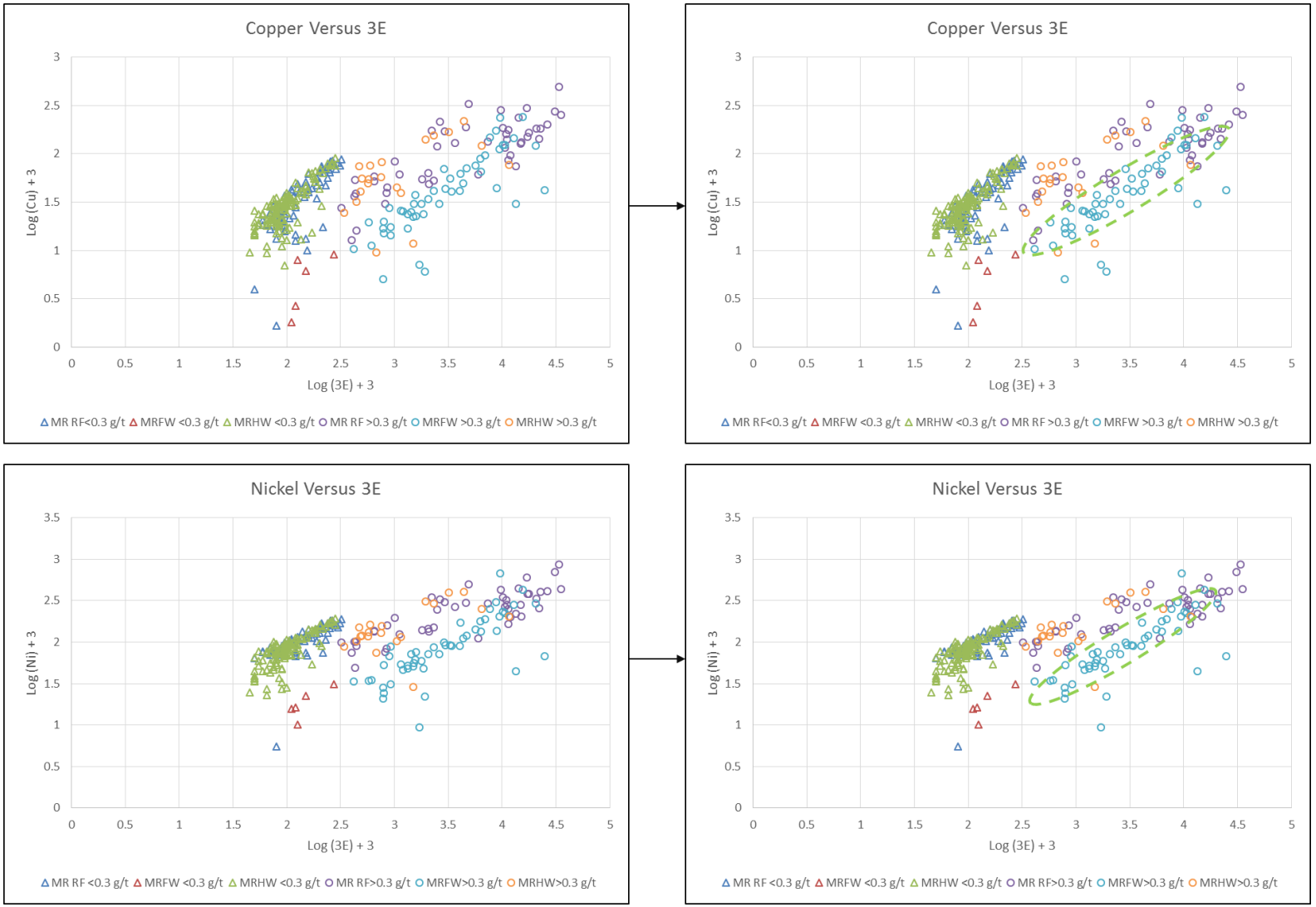

Figure 58. 3E Versus Copper/Nickel (left) and resulting grade trends (right)

4.4.2 Regression of the Merensky Footwall

Each multivariate data analysis has indicated that the Merensky Footwall can be isolated as a population which displays a distinctive unique copper/nickel to 3E mineralisation trend or signature. Further statistical analyses such as a regression may therefore be undertaken on the Merensky Footwall data.

XY scatter plots of the Merensky Footwall data were produced to assess if a regression between 3E and copper/nickel is possible (Figure 59 and Figure 60). There is a moderate direct correlation (Coombes, 2008) between the 3E and copper/nickel content indicated by correlation coefficients of 0.66 and 0.59 respectively. Outliers are those samples with a 3E to copper/nickel ratio outside of the majority of sample ratio of 3E and copper/nickel. The outliers therefore do not fit on the regression line. This is due to mineralisation signature rather than the type which has a 3E to copper/nickel correlation, it is not due to any laboratory error in the sampling as only quality checked hole that have passed accuracy tests have been used for any analyses in this study. Outliers have been identified by any data point that has a residual error (difference between actual value and estimated value of the regression line) that is greater than 25%. This results in 16% of the data points as outliers in the 3E to copper regression analysis while 21% of the data points are regarded as outliers in the 3E to nickel regression analysis.

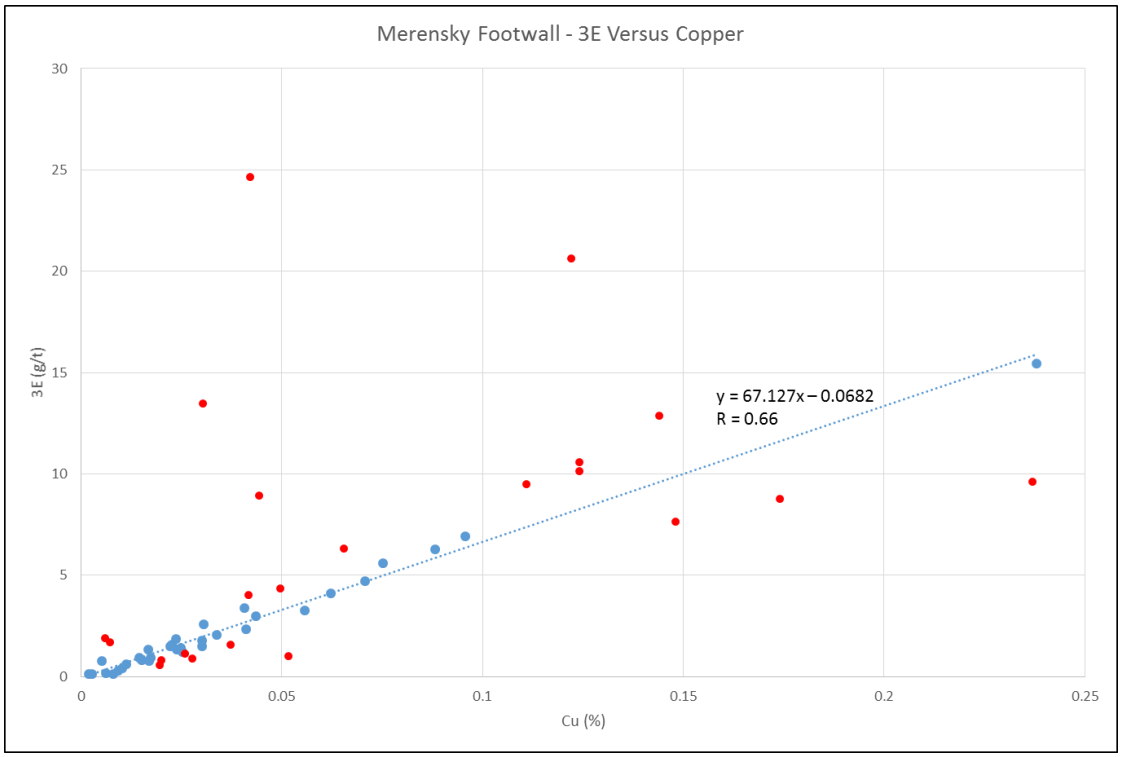

Figure 59. Merensky Footwall 3E versus Cu regression with outliers indicated in red

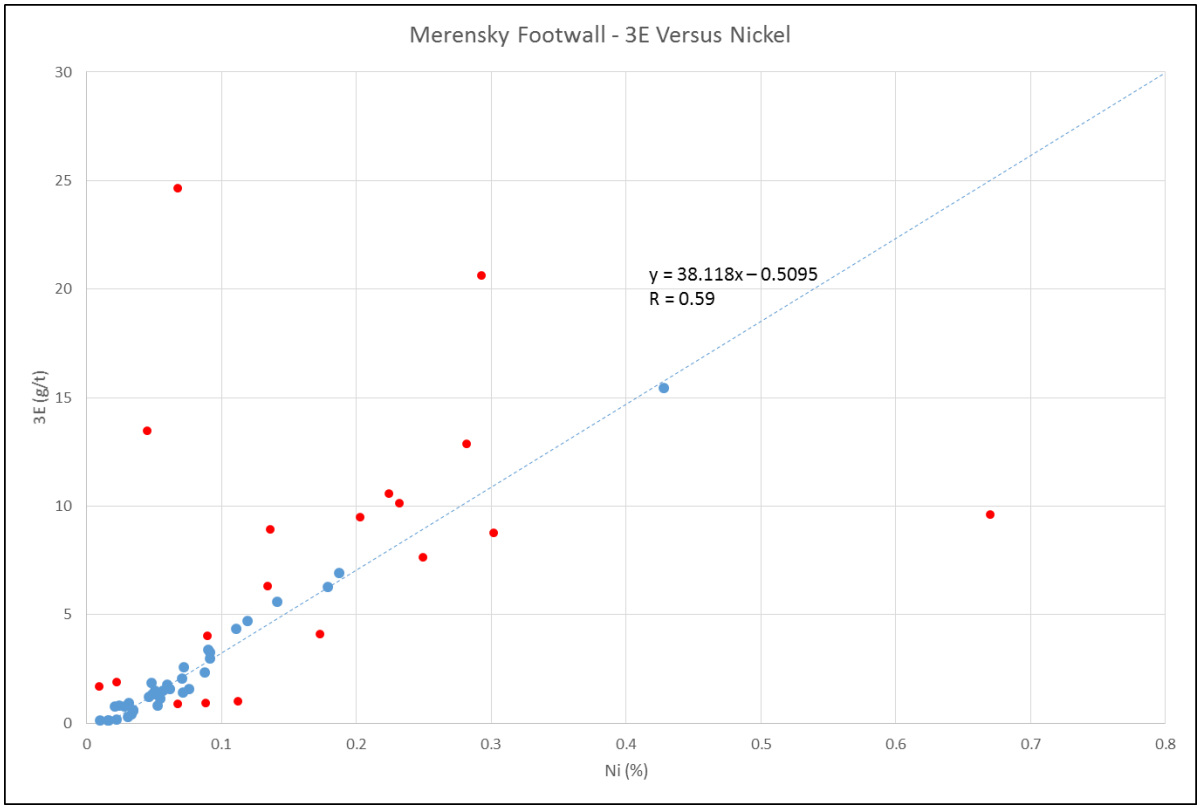

Figure 60. Merensky Footwall 3E versus Ni regression with outliers indicated in red

The regression from copper/nickel to PGE content is not possible due to the following:

- The Merensky Reef and Merensky Hangingwall cannot be isolated as populations based on the available data therefore these stratigraphic units cannot be regressed.
- The Merensky Footwall which can be isolated as a data population may be regressed however there are outliers which do not fit the regression line. The regression is therefore not representative of all possible sample results.

The null hypothesis of the Hypothesis Two test ($H2_0$), 'Copper and/or nickel can be used to predict 3E content' can therefore be rejected in favour of the alternate hypothesis ($H2_1$) which states 'Copper and/or nickel cannot be used to determine 3E content'.

4.5 Investigation into the Use of the pXRF in an Underground Environment

The major practical challenge experienced underground was the risk of introducing interference to the X-ray produced by the pXRF which negatively affects the accuracy of the result (Brouwer, 2010). The pXRF analysis requires a clean dry surface to ensure there is no interference between the pXRF X-ray and the moisture or dust on the rock surface (Brouwer, 2010; Hall *et al.,* 2011). To clean the rock surface so that it is free of dust, the sampler must hose down the rock surface that is to be analysed.

However, hosing down the rock surface results in a wet surface that does not dry rapidly underground due to the lack of both sunlight and wind. Alternatively, the sampler may brush the rock surface to attempt to clean the face however this can leave behind fine dust material. The rock surface is also jagged from blasting unlike the smooth half drillhole core surface. Taking two readings at an exact 5 cm spacing is sometimes not possible as the rock surface is too jagged to place the lens of the pXRF. The reading spacing may therefore become irregular to cater for the jagged rock surface.

A further interference risk was due to the sidewall of a development end of an underground which is painted following blasting as per standard practice. In areas where the development is on-reef, the lead based paint layer will cause interference with the incoming X-ray (Brouwer, 2010). To avoid interference the sampler must take pXRF readings prior to any paint being applied on the rock surface. This may introduce logistical challenges in the work schedule of the sampler as he/she would be required to analyse the planned area prior to paint application. This is not always possible due to the operational cycle. For this investigation, two planned sample sections were changed to analyse in an unpainted area to avoid possible interference.

The copper and nickel readings obtained using the pXRF have been plotted against the laboratory 3E result in a bar chart per section analysed (Figure 61 to Figure 65). Copper and nickel are plotted in percent (upper scale) and 3E is plotted in grams per ton (lower scale). The corresponding stratigraphy of each section is depicted to the left of the bar chart with the position of the Merensky Bottom Reef Chromitite labelled as 'BRC'. The trend line of the 3E results is depicted in a black dashed line.

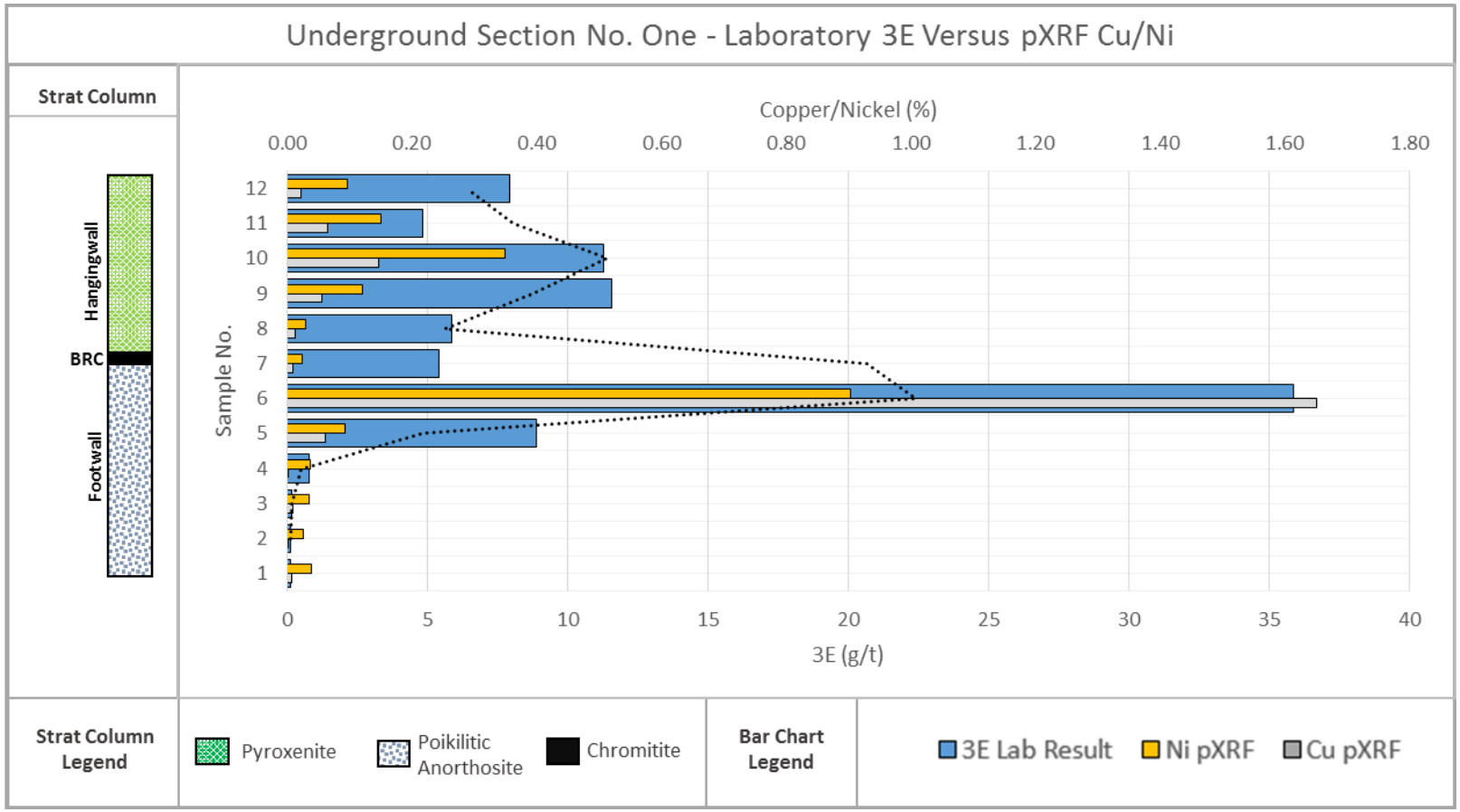

Figure 61. Section No. 1 Copper and Nickel pXRF Results versus Laboratory 3E Results

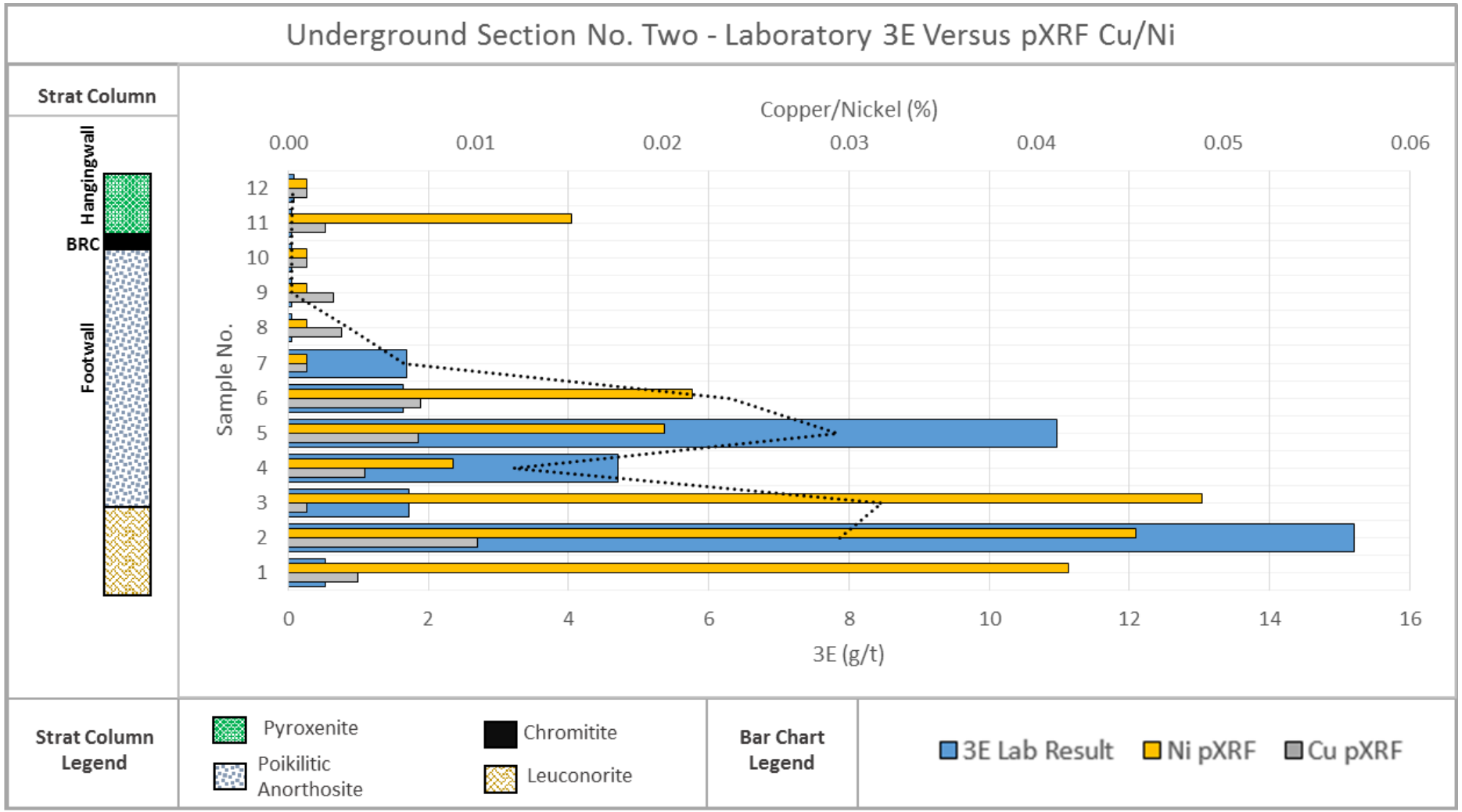

Figure 62. Section No. 2 Copper and Nickel pXRF Results versus Laboratory 3E Results

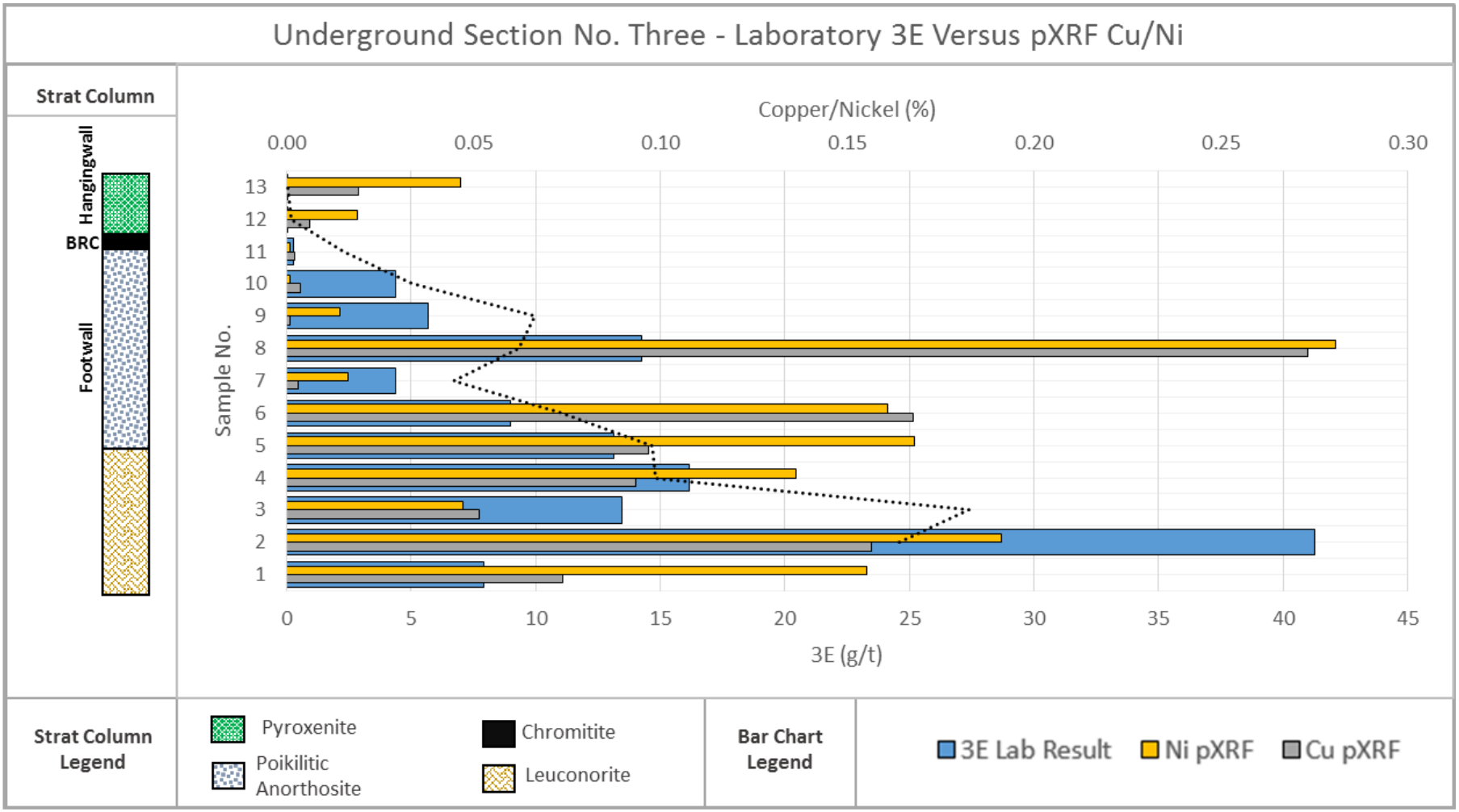

Figure 63. Section No. 3 Copper and Nickel pXRF Results versus Laboratory 3E Results

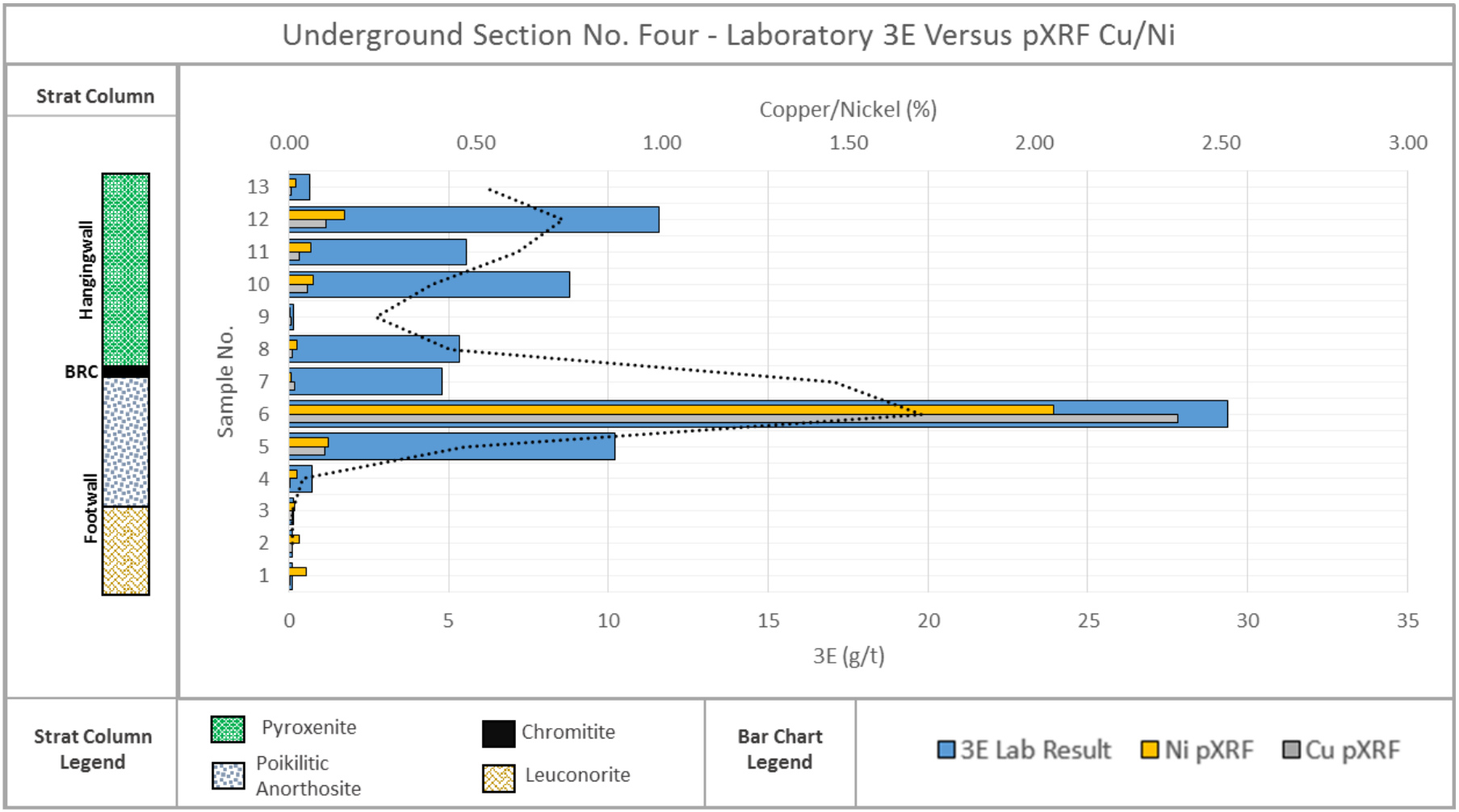

Figure 64. Section No. 4 Copper and Nickel pXRF Results versus Laboratory 3E Results

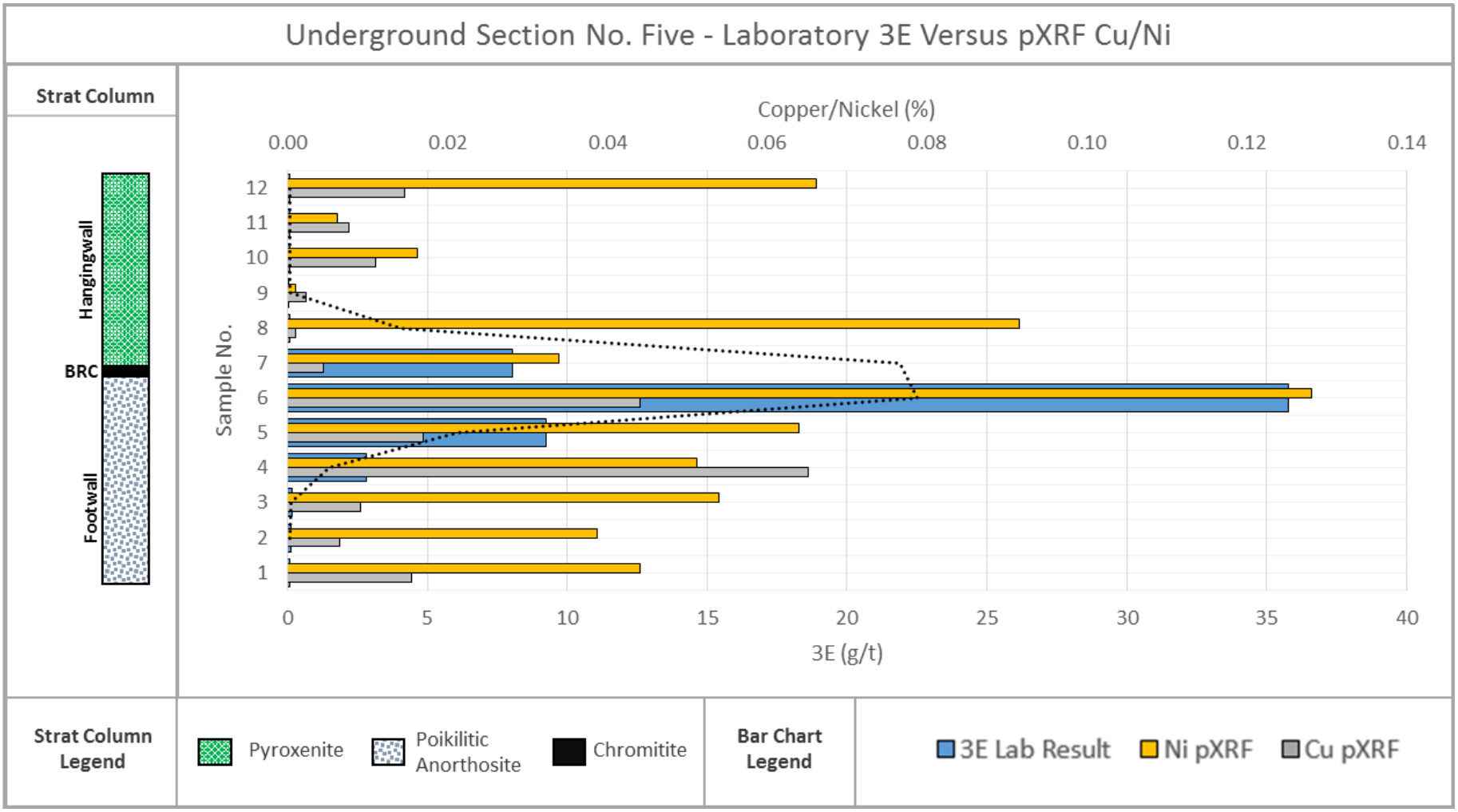

Figure 65. Section No. 5 Copper and Nickel pXRF Results versus Laboratory 3E Results

By tracing the 3E result trend (black dashed line), it can be seen that the pXRF copper and nickel results follow the general trend of the 3E results. pXRF copper and nickel peaks in the footwall which are not visible to the naked eye are well-correlated to 3E content especially in the footwall of Underground Sections 2 and 3. However marked exceptions to the correlation of 3E and copper/nickel occur such as:

- Section No.2

Sample 1 and 11 display peaks in pXRF nickel results however there is no corresponding peak in the 3E result.

- Section No.3

Samples 12 and 13 display peaks in pXRF measured copper and nickel however there is no corresponding peaks in 3E results.

Sample 8 has the highest pXRF copper and nickel results within this section resulting in a marked peak on the bar graph however the 3E result does not display the same trend of being the highest 3E result within the section.

- Section No.4

Most samples within this section do not display significant peaks in the copper and nickel content even when 3E mineralisation peaks are visible. Samples 1 to 5 and 7 to 13 have high 3E results and low pXRF results. Only Sample 6 has a significantly high copper and nickel pXRF result which coincides well with the 3E result.

- Section No.5

3E and copper/nickel in the footwall and hangingwall of this section do not correlate. Samples 1 to 3 and 8 to 11 display peaks in pXRF copper and nickel results with especially prominent nickel peaks in Samples 8 and 12. However there is no corresponding 3E mineralisation in these samples.

The samples listed in Table 11 are outliers where the copper/nickel results show no correlation with PGE results. These outliers are consistent with the outliers identified in the regression analysis of the Merensky Footwall.

XY scatter plots were undertaken on the 3E and copper/nickel results to determine the correlation between these results in the underground trial. As the copper/nickel and 3E results vary in content, the same equations as applied in the testing of Hypothesis Two to magnify the data on the scatter plots, have been applied to the result values to assess the relationship between the variables. The equations are:

$$log_{10}(3E) + 3 \quad \text{.....Equation 6}$$

$$log_{10}(Cu) + 3 \quad \text{.....Equation 7}$$

$$log_{10}(Ni) + 3 \quad \text{.....Equation 8}$$

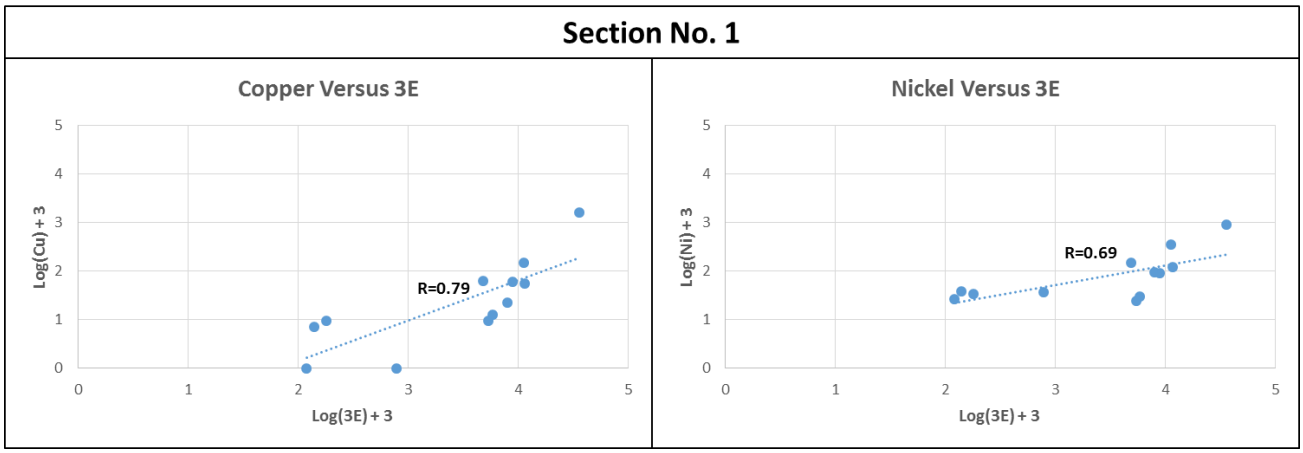

Figure 66. Section No.1 Laboratory 3E versus pXRF Copper (left) and Nickel (right)

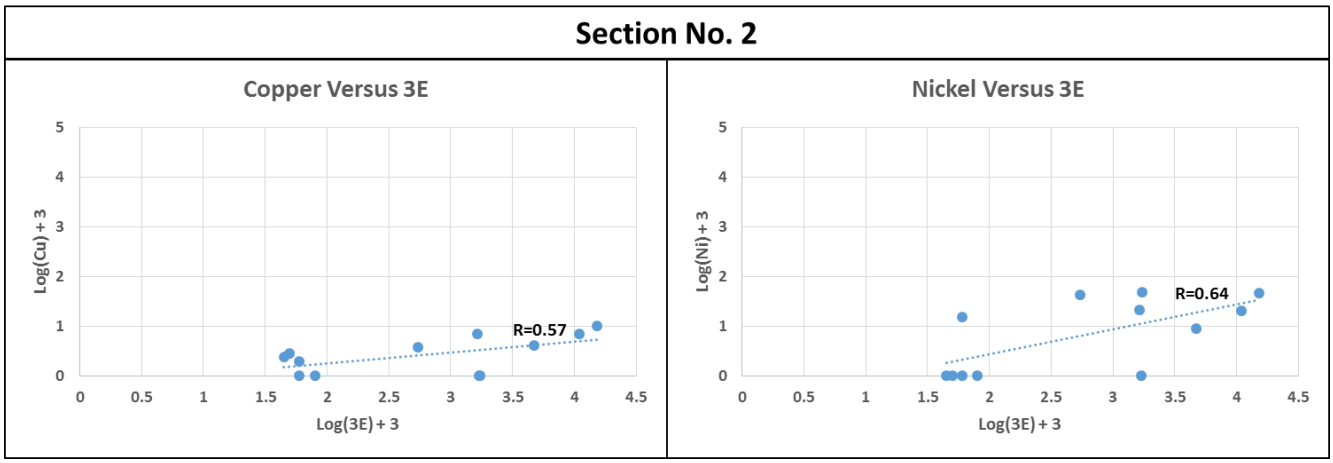

Figure 67. Section No.2 Laboratory 3E versus pXRF Copper (left) and Nickel (right)

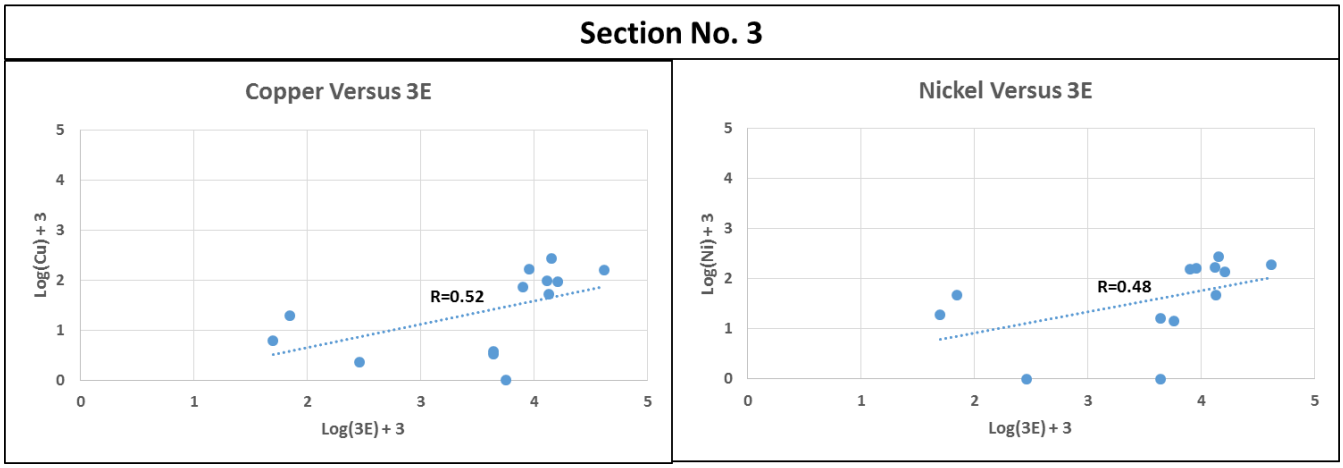

Figure 68. Section No.3 Laboratory 3E versus pXRF Copper (left) and Nickel (right)

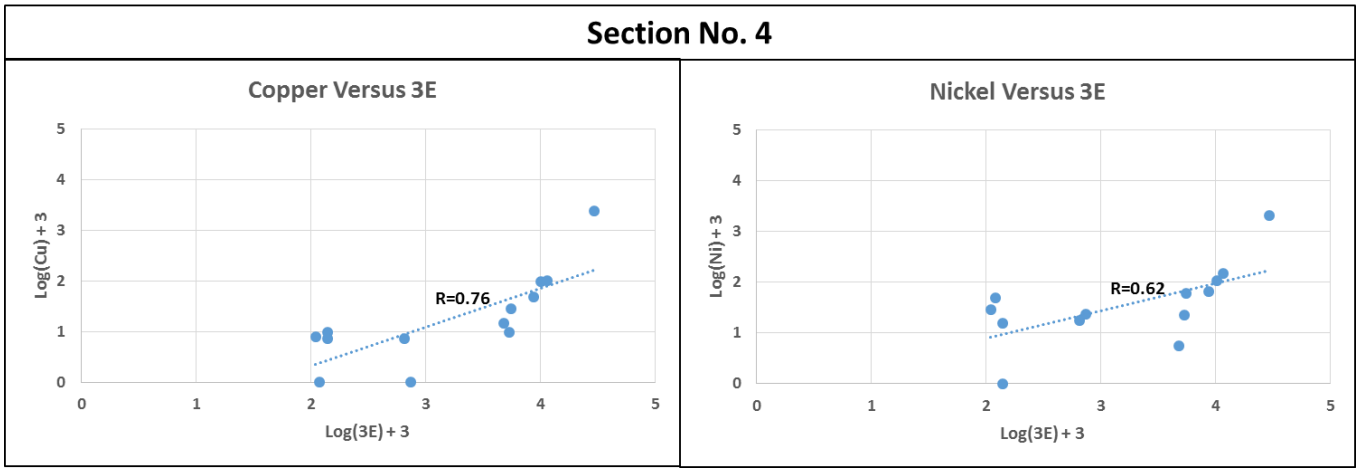

Figure 69. Section No.4 Laboratory 3E versus pXRF Copper (left) and Nickel (right)

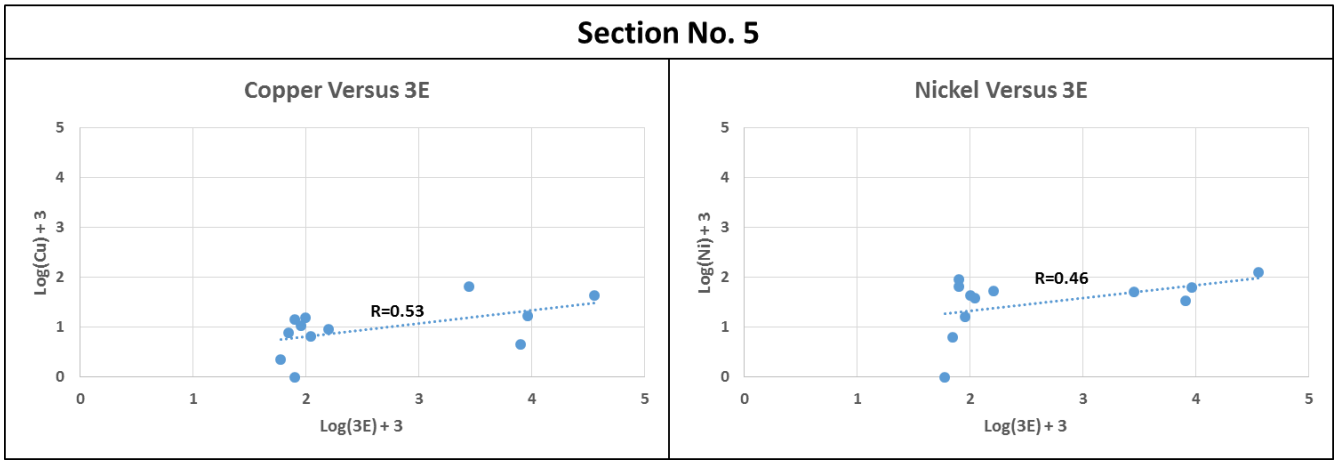

Figure 70. Section No.5 Laboratory 3E versus pXRF Copper (left) and Nickel (right)

Table 11: Sample occurrences where pXRF result is greater than laboratory result

Section No.	Total Samples	Samples Without 3E to Cu/Ni Correlation	% Samples Without 3E to Cu/Ni Correlation	3E to Cu Correlation (R)	3E to Ni Correlation (R)
1	12	0	0%	0.79	0.69
2	12	3	25%	0.57	0.64
3	13	4	31%	0.52	0.48
4	13	9	69%	0.76	0.62
5	12	8	67%	0.53	0.46

The results reveal moderate to good correlations between laboratory 3E results and pXRF copper/nickel however as noted, exceptions to the correlation exist. Furthermore, the data points on the XY scatter plot do not plot in the expected continuous line across the plotted regression line of the XY scatter plots.

Chapter Five: Discussion

It has been difficult to measure the reliability (accuracy and precision) of pXRF data since its use has grown in the mining and minerals industry. The factors that contribute to this difficulty include a lack of quality control measures when obtaining the pXRF data as well as insufficient records regarding if and how calibration procedures were undertaken (Hall *et al.,* 2011; Hall *et al.,* 2013; Fisher *et al.,* 2014). This study therefore applied recommended QAQC measures to allow for a reliable unbiased analysis of pXRF performance at Styldrift I Mine. The testing of two hypotheses and an underground investigation were undertaken to determine if the pXRF could be used to predict 4PGE content from copper/nickel content at Styldrift I Mine:

i. Hypothesis One (H1)

   $H1_0$: The pXRF produces accurate copper/nickel results

   $H1_1$: The pXRF does not produce accurate copper/nickel results

ii. Hypothesis Two (H2)

   $H2_0$: Copper and/or nickel can be used to determine 3E content

   $H2_1$: Copper and/or nickel cannot be used to determine 3E content

iii. Underground pXRF Trial

The analyses undertaken in Hypothesis One and Hypothesis Two include the use of laboratory assay data. A comparison of pXRF and laboratory assay data was carried out in the testing of Hypothesis One while multivariate data analyses using assay data was undertaken in testing of Hypothesis Two. The analysis of laboratory data was essential to reliably assess the performance of the pXRF. As noted by Fisher *et al.* (2014), inadequate QAQC measures are often taken when analysing pXRF data making it difficult to assess the reliability of the pXRF. It was therefore necessary to first determine the reliability of the laboratory assay data to determine the confidence of the findings from Hypothesis One and Hypothesis Two.

The accuracy of laboratory data was tested by the insertion of certified reference materials divided into 10% standards and 5% blanks. Accuracy was found to be acceptable and within the prescribed tolerance limits. No detectable contamination occurred during the laboratory analysis of the drillholes within the dataset. Precision was tested by twinstream analysis of 50% of the data. The data was found to be within the prescribed tolerance limits for outliers as well as percentage difference between the

Leg 1 and Leg 2 averages. Very strong correlations were produced by the comparison of Leg 1 and Leg 2 for each element analysed. 44 out of the 547 (8%) extracted sample records were found to have insufficient or missing data for analysis (missing lithologies/stratigraphic zone). The remaining 503 sample records (the 'dataset') were validated for use in the multivariate data analysis (Hypothesis Two). The laboratory data was therefore found to be of acceptable accuracy and precision to be of use in this study.

Calibration of the pXRF analyser is strongly recommended to enhance the accuracy of results. The calibration must be undertaken on samples with the same mineralogical matrix as the samples that are to be analysed (Hall *et al.,* 2011; Hall *et al., 2013;* Fisher *et al.,* 2014; Le Vailant *et al.,* 2014; Charnley and Lentz, 2016) therefore pressed pellets from the study area were used to calibrate the pXRF. The pXRF was calibrated with unique slopes and intercepts for copper and nickel analysis as per the calibration exercise. The maximum recommended pXRF reading time of sixty seconds (Fisher *et al.,* 2014) was used for all analyses throughout this study to ensure the best possible accuracy of results.

A general bias of the pXRF producing lower copper and nickel results than that found at the laboratory was detected in the calibration exercise. The QAQC analyses revealed that the laboratory nickel results are biased low therefore the difference between the pXRF and laboratory results are in fact higher than observed in the results. The laboratory results are approximately 4% higher than reported (Section 4.1.1.)

Following the application of the calibration parameters, the split drillhole core was analysed using the pXRF. Majority of the pXRF results from the core analysis (85% of the samples) are lower than the laboratory result therefore the bias still exists even when the calibration parameters are applied. The calibration was not adequate to eradicate the bias of consistently lower pXRF results than laboratory results.

The heterogenous nature of the unprepared core sample may introduce nugget effect. Readings were taken every 5 cm and averaged over the length of a sample to produce a more representative result than a single pXRF reading. The heterogenous nature of the sample or the nugget effect can be ruled out as factor towards the bias because the bias has also been detected in the calibration exercise which used homogenous pressed pellet samples.

The bias may be attributed to detection limit constraints of the pXRF. The copper and nickel in the mineralised zone of the Merensky Unit has grades that are largely close to but greater than the lower detection limit of copper and nickel (15 ppm). However according to Hall *et al.* (2011) a widespread problem encountered when using pXRF technology is that the advertised detection limits are not

always accurate. The detection limit may even differ from one ore body to another. A calibration exercise was undertaken to enhance the accuracy of the pXRF however this was inadequate to produce results of adequate accuracy.

The T Test undertaken on the pXRF and the laboratory results reveal that the pXRF and laboratory datasets are not consistently comparable with 4 out of 10 of the datasets compared showing differences that indicate the results are from different populations. Furthermore, analysis of the mean of each dataset yielded a large percentage differences between the datasets ranging from 40% to 75% for copper and 32% to 63% for nickel. These differences are too large for a reliable analysis of copper and nickel as well as regression of such biased values to determine PGE content.

The null hypothesis of Hypothesis One is 'the pXRF does not produce accurate copper/nickel results' and can therefore be accepted. The pXRF cannot be used as a tool to reliably measure copper and nickel content in its naturally occurring form within the study area.

Analysis of the 3E, copper and nickel assay data revealed that various populations exist within the dataset. This has been verified by T Tests which confirm that different populations exist within the dataset. Each population displays a unique 3E to copper/nickel mineralisation profile or signature which can be seen in the data histograms and scatter plots of 3E, copper and nickel. Characteristics of the sample populations were investigated to determine the cause of the various populations observed. A spatial analysis, lithology, stratigraphic zone and grade were analysed to isolate the cause of the populations. The findings of each analysed parameter are summarised below:

i. Lateral Zones

All the boreholes used for the analysis occur in both Population and Population Two. Lateral zones can therefore be ruled out as the factor leading to different 3E to Cu/Ni populations.

ii. Lithology

Based on the lithology of the sample, Population One and Population Two show the emergence of sub-populations 1.1 and 2.1 consisting primarily of anorthosite and norite which are typically Merensky Footwall lithologies. Population One and Two also show the emergence of sub-populations 1.2 and 2.2 consisting primarily of feldspathic pyroxenite which can occur in the Merensky Reef and Merensky Hangingwall Horizons. However, there are minor to moderate occurrences of alternative lithologies in each of the sub-populations. This indicates that lithology may be correlated to the function resulting in the data populations while not the actual cause. This is further evident by the overlap of sub-population 1.1 and 1.2 which indicates that lithology alone does not differentiate the 3E to Cu/Ni assay data.

iii. Stratigraphic Zone

The identification of stratigraphic zones within the dataset results in the isolation of the Merensky Footwall as a distinct population. This population is in line with the sub-population 2.1 identified in the lithological analysis which comprises mainly anorthosite and norite which are Merensky Footwall lithologies. The Merensky Hangingwall and Merensky Reef cannot be isolated as the sample points are intermingled displaying no distinct population trends.

iv. Grade

Population One comprises lower grade 3E samples of less than 0.3 g/t whereas majority of the Population Two samples are higher grade of greater than 0.3 g/t. Further coding the grade scatter plot by the stratigraphic zone of each sample reveals that the Merensky Footwall creates a distinct population.

The multivariate analyses revealed that the Merensky Footwall creates a population with its own distinct 3E to Cu/Ni signature. This is in line with findings from the study conducted by Smith (2014) on drillholes on the neighbouring mine (BRPM) within the same facies (Central Reef Facies) as the area of this investigation. Smith (2014) notes that the Merensky Footwall is mineralised largely by PGE bearing base metal sulphides (BMS) with a minor amount of other PGE bearing minerals such as PGE alteration minerals and PGE tellurides. The Merensky Footwall can therefore be isolated as a data population due to the predominance of base metal sulphides as the PGE – bearing mineral as well as the fact that BMS have a close correlation to both copper and nickel. The populations are therefore based on mineralisation types which is the control of the various 3E to copper/nickel populations.

The Merensky Hangingwall and Merensky Reef cannot be isolated as distinct populations as the data from these horizons is intermingled using physical and grade properties of the samples. PGE tellurides and alteration minerals become increasingly abundant upwards into the Merensky Reef and Merensky Hangingwall horizons resulting in BMS no longer being the main PGE bearing mineral (Smith, 2014). Instead there is a variety of PGE bearing minerals present (Smith, 2014), some of which have no correlation to copper or nickel (Schouwstra *et al.* 2000). Due to the co-occurrence of these minerals at the Merensky Reef and Merensky Hangingwall horizons, it is not possible to separate the populations by the tested parameters such as lithology, stratigraphic zone or grade. The populations are a control of mineralisation type. The mineralisation populations cannot be differentiated visually as the mineralisation type cannot be identified. The parameters used in the multivariate data analysis (lithology, stratigraphic zone and grade) which indicated an emergence of the data populations are functions of the mineralisation type which is the actual cause of the various data populations or 3E to Cu/Ni signatures observed. The populations cannot be isolated without a trace mineral study with

both assay and mineralogical results therefore the Merensky Reef and Merensky Hangingwall could not be regressed.

The Merensky Footwall could be isolated as a separate unique population with regard to 3E and copper/nickel mineralisation therefore a regression from copper/nickel to 3E was undertaken. The regression produced moderate correlations however outliers which did not fit the regression were detected. 16% and 21% of the Merensky Footwall data were identified as outliers which did not fit the regression for copper and nickel respectively.

Two types of outliers were observed in the regression analysis of the Merensky Footwall:

- High 3E content and low copper/nickel

  These occur above the regression line of the Merensky Footwall XY scatterplots. This type of outlier will result in a false low 3E result using the regression estimation. This means that the estimation will falsely indicate that there is negligible 3E content because the copper/nickel content is low. This outlier type is due to PGE barren base metal sulphides. Strong associations have been shown to exist between PGEs and copper/nickel within base metal sulphides within and adjacent to the study area however there are rare exceptions when sulphides such as pentlandite, pyrrhotite, chalcopyrite, pyrite occur without PGE mineralisation (Schouwstra *et al.* 2000; Smith, 2014; Ramlall, 2015).

- Low 3E content and high copper/nickel content

  This outlier type occurs below the regression line of the Merensky Footwall XY scatterplots. This type of outlier will result in a false high 3E result using the regression estimation as the high copper/nickel will be used as a positive indicator of high 3E content. This type of outlier is attributed to non-sulphide PGE mineralisation. A recent detailed study within the same facies type of the study area (Smith, 2014) indicates that PGE mineralisation within the Merensky Footwall is predominantly composed of base metal sulphides however minor amounts of minerals outside the BMS phases are present. These are minerals such as PGE tellurides, arsenides, alloys and alteration minerals. Early investigations into the mineralogy of the BRPM JV area (Kinloch, 1982) indicated that only 29.4% of Merensky PGEs occur in sulphides. Unlike bulk of the BMS, the alternative PGE minerals do not typically co-occur with copper and nickel therefore these minerals often have a high 3E result and a low copper/nickel content.

There are occurrences of primary silicates and base metal sulphides which have formed and are later altered to secondary silicates such as epidote and actinolite (Smith, 2014). Due to the alteration of the mineral, it does not retain the correlation with copper and nickel but may retain the PGE content.

Copper and nickel cannot be used as proxies for 3E content within the study area due to the possibility of false or incorrect estimations based on the regression which assumes a direct positive correlation between the 3E content and copper/nickel content. The outliers indicate that this correlation does not always exist due to the presence of other minerals within the sample. The regression outliers are true values (as only quality checked drillholes were used for the analysis). The outliers are therefore mineralised differently compared to most of the data population. Such outliers make it unsuitable to use the pXRF as a tool to measure PGE values as some occurrences may not produce accurate results. Smith (2014) cautions against the use of copper, nickel or sulphur as proxies for PGEs due to the fact that PGEs occur in a variety of different minerals in which copper, nickel and sulphur do not occur. Hypothesis Two null statement 'copper and/or nickel cannot be used to determine 3E content' can therefore be accepted.

The results from the underground trial confirm the findings from testing of Hypotheses One and Two. Moderate to good correlations exist between laboratory 3E and copper/nickel results however several outliers exist. The outliers are due to the mineralisation of PGEs where some minerals contain PGE content and not copper/nickel and vice versa as explained. The pXRF can only be used a low confidence tool to identify potential PGE mineralisation. The analysis of underground sections show varying levels of correlation between the 3E and copper/nickel content. Sections Four and Five show poor correlation with 69% and 67% of the samples where 3E and copper/nickel mineralisation do not coincide. These samples are the outlier types such as those identified in Hypothesis Two where 3E and copper/nickel are not correlated.

Chapter Six: Recommendations and Conclusion

6.1 Recommendations

Based on the findings the following is recommended for the study area:

- As conducted on BRPM, a trace mineral study detailing both the assay and mineralogical results of the study area can be undertaken to allow for a better understanding of the PGE mineralogy within the various stratigraphic zones of the study area.
- The Merensky Unit PGE modes of occurrence within the study area are variable due to the fact that PGEs occur in many types of minerals such as sulphides, tellurides, alteration minerals (Kinloch, 1982; Schouwstra *et al.,* 2000; Smith, 2014). Therefore, any element, as demonstrated by the testing of copper and nickel, will have an inconsistent relationship with PGEs resulting in no element that is suitable as a reliable pathfinder. Furthermore, current pXRF technology cannot accurately measure PGEs directly (Hall *et al*., 2011; Hall *et al*., 2013; Smith, 2014). The pXRF is therefore currently unsuitable for the measurement of PGE grade content within the Merensky Reef. Advances in the detection limit of the pXRF for PGEs may result in successful application of the technology in the future to directly measure PGE content. Currently the pXRF may be used as a low confidence tool to indicate potential areas of PGE mineralisation however the user must be aware that there is a possibility of PGE mineralisation that occurs which is not correlated with copper/nickel content.
- While the pXRF cannot reliably measure PGE content through pathfinder elements due to PGE mode of occurrence, the accuracy and precision of the pXRF instruments can vary (Hall *et al.,* 2011) therefore other instruments can be tested to improve accuracy of copper and nickel results.

The following is recommended for use of the pXRF in the mining industry in general:

- pXRF machines are marketed to the mining and minerals industry however results have often been inconsistent with manufacturer claims (Hall *et al.,* 2011; Hall *et al.,* 2013) therefore trial analyses should be undertaken before purchase of a pXRF. The trial should test the effectiveness of the pXRF analyser per site as the geological, mineralogical and grade characteristics of each orebody varies. These factors may have an influence on pXRF performance (Hall *et al.,* 2011; Hall *et al.,* 2013; Gazley *et al.,* 2014; Fisher *et al.,* 2014). The

trial should test various aspects such as calibration of the pXRF to the mine site and reliability of the pXRF readings.

- Manufacturers provide support to assist to set up calibrations for specific areas to enhance accuracy of readings. Such support and assistance should be optimised to enhance the reliability of pXRF data.
- In cases where pathfinder elements are used as proxies for target elements, such as this study, it is recommended that mineralogical studies such as a trace element or bulk modal analysis be undertaken to understand the exact relationship between the elements. Furthermore, the pathfinder and target elements are required to have consistent known relationships, at least in local areas, in order to regress pathfinder element values back to the target element.
- The handheld XRF analyser should ideally be applied to analyse elements directly. This minimizes the possible errors in regression analyses. Furthermore, the element being analysed must be in concentrations that are above the detection limit allowing for reliable results with less noise data.

6.2 Conclusion

The objective of this study was to investigate a more cost effective, rapid method to current geochemical assaying for quantifying PGE grade within the Central Reef Facies of Styldrift I Mine. To this end, pXRF analysis was investigated as a potential alternative method to geochemical assay. Precious elements such as PGEs and gold cannot be accurately measured using pXRF technology (Hall *et al*., 2011; Thermo Scientific, 2012; Hall *et al*., 2013; Fisher *et al*., 2014) therefore copper and nickel were tested as potential pathfinder elements to target PGEs.

The pXRF cannot fulfil the conditions required for accurate measurement of PGEs as it cannot directly measure PGE content. The study has shown that pathfinder elements, such as copper and nickel, cannot be used to measure PGE content as PGE modes of occurrence is inconsistent. The technology is suitable only to be used as an indicator for PGE mineralisation trends on Styldrift Mine along the Merensky Reef horizon. Currently geochemical assay is the most reliable method to determine PGE grades and should not be replaced with pXRF technology. The tool can be useful to detect potential PGE mineralisation peaks. Upon detecting grade peaks, samples should be taken and dispatched to the laboratory for geochemical assay analysis.

The project has highlighted that the success of the application of the pXRF on a mine is dependent on factors such as the mineralogy of the reef and the concentrations of the elements of interest. This varies between orebodies therefore testing of the pXRF is essential prior to use. The pXRF may be most useful in a mine with high grades of base metals as these can be directly analysed using the pXRF.

References

Arne, D., Jeffress, G., Sergeev, N. and Margerson, A., 2014. What Reporting Portable XRF Data to 2012 JORC Code Guidelines Means. In *Australian Institute of Geoscientists Quarterly Newsletter, No. 115, February 2014.*

Brouwer, P., 2010. Theory of XRF, getting acquainted with the principles. *PANalytical B.V.*

Cawthorn, R.G. 1999. Platinum Group Element Mineralisation in the Bushveld Complex – a critical reassessment of geochemical models. *South African Journal of Geology*, 102(3): 268 – 281.

Cawthorn, R.G., 2010. Geological Interpretations from the PGE distributions in the Bushveld Merensky and UG2 Chromitite reefs. *The 4th International Platinum Conference, Platinum in transition 'Boom or Bust'*, The Southern African Institute of Mining and Metallurgy, 2010.

Cawthorn, R.G., Eales, H.V., Walraven, F., Uken, R. and Watkeys, M.K., 2006. The Bushveld Complex. In: Johnson, M.R., Anhausser, C.R. and Thomas, R.J. (Eds), *The Geology of South Africa, Geological Society of South Africa/The Council for Geoscience*, Johannesburg, 261 – 281.

Cawthorn, R.G., Merkle, R.K.W., and Viljoen, M.J., 2002. Platinum-group element deposits in the Bushveld Complex, South Africa, Cabri, L.J., (ed.). *The Geology, Geochemistry, Mineralogy and Beneficiation of Platinum-Group Elements.* Canadian Institute of Mining, Metallurgy and Petroleum, Spec. vol. 54, 2002, pp. 389-430.

Charnley, B.E. and Lentz D.R., 2016. Petrogeochemical Assessment of the Various Felsic Volcanic and Subvolcanic Igneous Rocks Associated with Sn-Cu-Zn and W-Mo-Bi Mineralisation in the North Zone, Mount Pleasant, New Brunswick: A pXRF Study. *New Nouveau Brunswick, Energy and Mines.*

Clark, I and Harper, W.V., 2000. Practical Geostatistics 2000. *Ecosse North America Llc Publishers.*

Coombes, J., 2008. The Art and Science of Resource Estimation: A Practical Guide for Geologists and Engineers. *Coombes Capabilities.*

Fisher, L., Gazley, M.F., Baensch, A., Barnes, S.J., Cleverley, J. and Duclaux, G, 2014. Resolution of geochemical and lithostratigraphic complexity: a workflow for application of portable X-ray fluorescence to mineral exploration. *Geochemistry: Exploration, Environment, Analysis.* The Geological Society of London (Pg 149 – 159).

Gazley, M.F., Tutt, C.M., Latham, A.R., Duclaux, G., Taylor, M.D. and de Beer, S.J., 2014. Objective geological logging using portable XRF geochemical multi-element data at Plutonic Gold Mine, Maymia Inlier, Western Australia. *Journal of Geochemical Exploration* (143; Pg 74 – 83).

Glacken, I.M. and Snowden, D.V., 2001. Mineral Resource Estimation. Mineral Resource and Ore Reserve Estimation – *The AusIMM Guide to Good Practice*; The Australian Institute of Mining and Metallurgy.

Hall, G., Buchar, A. and Bonham-Carter, G. 2011. Quality Control Assessment of Portable XRF Analysers: Development of Standard Operating Procedures, Performance on Variable Media and Recommended Uses; Phase 1. *Canadian Mining Industry Research Organization (CAMIRO) Exploration Division.*

Hall, G., Page, L. Bonham-Carter, G.F. 2013. Quality Control Assessment of Portable XRF Analysers: Development of Standard Operating Procedures, Performance on Variable Media and Recommended Uses; Phase 2. *Canadian Mining Industry Research Organization (CAMIRO) Exploration Division.*

Kinloch, E.D., 1982. Regional trends in the platinum group mineralogy of the Critical Zone of the Bushveld Complex, South Africa, *Economic Geology Journal*, 1982, 77, 1328.

Kinnaird, J.A., 2016. The Bushveld Large Igneous Province. www.largeigneousprovinces.org/LOM.html [May 2005].

Lee, C.A. 1996. A review of mineralisation in the Bushveld Complex and some other layered intrusions, In: Cawthorn, R.G. (Ed.), *Layered Intrusions, Elsevier*, Amsterdam.

Leeb du Toit, A., 1986. The impala platinum mines. In: Anhaeusser, C.R., Maske, S. (Eds.), Mineral Deposits of Southern Africa. *Geological Society of South Africa*, Johannesburg, pp. 1091–1106.

Le Vailant, M., Barnes, S.J., Fisher, L., Fiorentini, M.L. and Caruso, S., 2014. Use and calibration of portable X-ray fluorescence analysers: application to lithogeochemical exploration for komatiite-hosted nickel sulphide deposits. *Geochemistry: Exploration, Environment, Analysis*. The Geological Society of London.

Lionnet, M.D. and Lomberg, K.G. 2006. The application of facies classification in evaluating the Merensky Reef at Bafokeng Rasimone Platinum Mine, South Africa. *International Platinum Conference 'Platinum Surges Ahead,'* The South African Institute of Mining and Metallurgy.

Lomberg, K., 2014. Best practice sampling methods, assay techniques and quality control with reference to platinum group elements (PGEs). *The Journal of The Southern African Institute of Mining and Metallurgy,* 114.

Mostert, A.B., Hofmeyr, P.K. and Potgieter, G.A., 1982. The Platinum-Group Mineralogy of the Merensky Reef at Impala Platinum Mines, Bophuphatswana. *Economic Geology*, 77, 1385-1394.

Moodley, P. 2008. Facies variation in the Merensky Reef at Bafokeng Rasimone Platinum mine. *Third International Platinum Conference 'Platinum in Transformation,'* The South African Institute of Mining and Metallurgy.

Moodley, Y., 2015. RBPlat Annual QAQC Report. Unpublished Internal Report.

Padiachy, P., 2015. RBPlat Annual MR Model Report. Unpublished Internal Report.

Prichard, H.M., Barnes, S.J., Maier, W.D. and Fisher, P.C., 2004. Variations in the Nature of the Platinum Group Minerals in a Cross Section through the Merensky Reef at Impala Platinum: Implications for the Mode of Formation of the Reef. *The Canadian Mineralogist*, 42, 423-437.

Ramlall, N. 2015. A Brief Geometallurgical Study on XLP and Conventional Samples from the Royal Bafokeng Platinum Styldrift Two deposit. Internal Report (unpublished).

RBPlat, 2010. Annual Integrated Report. Royal Bafokeng Platinum.

RBPlat, 2016. Retrieved from http://www.bafokengplatinum.co.za/bus-man-rasimone-venture.php; cited 15/06/2016.

Schouwstra, R.P., Kinloch, E.D. and Lee, C.A., 2000. A Short Geological Review of the Bushveld Complex. *Platinum Metals Review*, 44, 33-39.

Schwellnus, J.S.I., Hiemstra, S.A. and Gasparrini, E., 1976. The Merensky Reef at Atok Platinum Mine and its Environs. *Economic Geology*, 71, 249 – 260.

Smith, A.J.B., 2014. The Geometallurgical Characterization of the Merensky Reef at Bafokeng Rasimone Platinum Mine, South Africa. *University of Johannesburg*.

Smith, A.J.B., Viljoen, K.S., Schouwstra, R., Roberts, J., Schalkwyk, C. and Gutzmer, J. 2013. Geological variations in the Merensky Reef at Bafokeng Rasimone Platinum Mine and its influence on flotation performance. Minerals Engineering, 52, 155 – 168.

Smith, D.S., Basson, I.J. and Reid, D.L., 2004. Normal Reef Subfacies of the Merensky Reef at Northam Platinum Mine, Zwartklip Facies, Western Bushveld Complex, South Africa. *Canadian Mineralogist*, 42, 243 -260.

Thermo Scientific. 2012. Application of the Thermo Scientific Portable XRF Analyzer in PGE Exploration. *Thermo Scientific Inc.*

Thermo Scientific. 2015. Retrieved from https://www.thermoscientific.com/en/about-us/general-landing-page/xrf-technology.html. Cited 20/11/2015.

Thermo Scientific. 2017. Retrieved from https://www.atecorp.com/ATECorp/media/pdfs/data-sheets/Niton-XL3t-GOLDD_Datasheet.pdf. Cited 13/04/201.

United States Patent, 2011. Retrieved from https://docs.google.com/viewer?url=patentimages.storage.googleapis.com/pdfs/US7916834.pdf; cited 4/07/2016.

Vermeulen, J. 2010. Merensky Reef Facies Delineation on the Farms Boschkoppie and Styldrift in the Western Bushveld Complex. Internal Report (unpublished).

Viljoen, M.J., 1994. A review of the regional variations in facies and grade distribution of the Merensky Reef, western Bushveld Complex, with some mining implications, *Proceedings of the 15th CMMI Congress*, The South African Institute of Mining and Metallurgy.

Viljoen, M.J. 1999. The nature and origin of the Merensky Reef of the Western Bushveld Complex based on geological facies and geological data. *South African Journal of Geology*. Sep99, Vol. 102 Issue3, p221.

Wagner, P.A. 1929. The Platinum Deposits and Mined of South Africa. *Oliver and Boyd*, Edingburgh.

Zhang, W. and Lentz, D., 2016. Application of portable X-ray fluorescence analyses to discriminate rock units in the Fire Tower Zone, Mount Pleasant Deposit, *New Brunswick. New Nouveau Brunswick, Energy and Mines.*

Appendix

7.1 Appendix A: CRM Certificates

CERTIFICATE OF ANALYSIS

G1 at a 95% confidence limit
Merensky F/W Anorthosite Ore

Certified Values

Lead Collection Fire Assay			
Element	Mean ± standard error	Standard Deviation	%RSD
Au (g/t)	0.249 ± 0.037	0.018	7.0
Pt (g/t)	2.98 ± 0.18	0.065	2.2
Pd (g/t)	1.85 ± 0.04	0.019	1.0
Rh (g/t)	0.158 ± 0.021	0.018	11.2
Nickel Sulfide Collection Fire Assay			
Element	Mean ± standard error	Standard Deviation	%RSD
Au (g/t)	0.277 ± 0.048	0.047	17.0
Pt (g/t)	3.04 ± 1.54	0.136	4.5
Pd (g/t)	1.87 ± 0.2	0.022	1.2
Rh (g/t)	0.172 ± 0.039	0.026	15.2
Totals			
Element	Mean ± standard error	Standard Deviation	%RSD
Cu %	0.092 ± 0.003	0.002	2.5
Ni %	0.173 ± 0.004	0.005	2.7

CERTIFICATE OF ANALYSIS

G2 at a 95% confidence limit
Merensky H/W Pyroxenite Ore

Certified Values

Lead Collection Fire Assay			
Element	Mean ± standard error	Standard Deviation	%RSD
Au (g/t)	0.194 ± 0.021	0.017	8.7
Pt (g/t)	1.87 ± 0.08	0.074	4.0
Pd (g/t)	0.82 ± 0.04	0.029	3.5
Rh (g/t)	0.107 ± 0.016	0.007	6.7
Nickel Sulfide Collection Fire Assay			
Element	Mean ± standard error	Standard Deviation	%RSD
Au (g/t)	0.206 ± 0.02	0.015	7.1
Pt (g/t)	1.92 ± 0.13	0.083	4.3
Pd (g/t)	0.84 ± 0.03	0.026	3.1
Rh (g/t)	0.119 ± 0.008	0.005	4.2
Totals			
Element	Mean ± standard error	Standard Deviation	%RSD
Cu %	0.117 ± 0.004	0.004	3.1
Ni %	0.238 ± 0.009	0.008	3.5

CERTIFICATE OF ANALYSIS

G3 at a 95% confidence limit
Merensky Reef (LM5) Ore

Certified Values

Lead Collection Fire Assay			
Element	Mean ± standard error	Standard Deviation	%RSD
Au (g/t)	0.626 ± 0.141	0.060	9.6
Pt (g/t)	8.76 ± 2.11	0.441	5.0
Pd (g/t)	2.88 ± 0.43	0.101	3.5
Rh (g/t)	0.428 ± 0.455	0.085	19.9
Nickel Sulfide Collection Fire Assay			
Element	Mean ± standard error	Standard Deviation	%RSD
Au (g/t)	0.633 ± 0.093	0.080	12.6
Pt (g/t)	8.94 ± 0.65	0.434	4.9
Pd (g/t)	3.07 ± 0.15	0.129	4.2
Rh (g/t)	0.535 ± 0.201	0.022	4.1
Totals			
Element	Mean ± standard error	Standard Deviation	%RSD
Cu %	0.16 ± 0.008	0.019	12.1
Ni %	0.348 ± 0.004	0.009	2.5
SG g/ml	3.28 ± 0.05	0.039	1.2

Figure 71. Standard Certificates G1, G2 and G3

CERTIFICATE OF ANALYSIS

G4 at a 95% confidence limit

UG2 F/W Pegmatoid Ore

Certified Values

Lead Collection Fire Assay			
Element	Mean ± standard error	Standard Deviation	%RSD
Pt (g/t)	0.2 ± 0.02	0.017	8.4
Pd (g/t)	0.14 ± 0.01	0.007	4.8
Rh (g/t)	0.07 ± 0.07	0.024	34.9
Nickel Sulfide Collection Fire Assay			
Element	Mean ± standard error	Standard Deviation	%RSD
Pt (g/t)	0.22 ± 0.03	0.015	6.7
Pd (g/t)	0.13 ± 0.03	0.013	9.7
Rh (g/t)	0.06 ± 0.012	0.008	13.1
Totals			
Element	Mean ± standard error	Standard Deviation	%RSD
Cu %	0.003 ± 0.004	0.001	36.9
Ni %	0.077 ± 0.005	0.004	5.7
Cr %	0.75 ± 0.024	0.026	3.5
SG g/ml	3.3 ± 0.02	0.132	4.0

CERTIFICATE OF ANALYSIS

G6 at a 95% confidence limit

UG2 Chromitite Ore

Certified Values

Lead Collection Fire Assay			
Element	Mean ± standard error	Standard Deviation	%RSD
Pt (g/t)	3.03 ± 0.7	0.408	13.4
Pd (g/t)	2.18 ± 0.19	0.119	5.4
Rh (g/t)	0.66 ± 0.32	0.112	17.1
Nickel Sulfide Collection Fire Assay			
Element	Mean ± standard error	Standard Deviation	%RSD
Pt (g/t)	3.57 ± 0.21	0.178	5.0
Pd (g/t)	2.27 ± 0.11	0.090	4.0
Rh (g/t)	0.7 ± 0.09	0.054	7.7
Totals			
Element	Mean ± standard error	Standard Deviation	%RSD
Cu %	0.011 ± 0.002	0.001	11.9
Ni %	0.126 ± 0.006	0.005	4.2
Cr %	22.1 ± 0.5	0.595	2.7
SG g/ml	3.95 ± 0.09	0.096	2.4

CERTIFICATE OF ANALYSIS

G8 at a 95% confidence limit

Merensky Ore

Certified Values

Lead Collection Fire Assay			
Element	Mean ± standard error	Standard Deviation	%RSD
Au (g/t)	0.242 ± 0.011	0.016	6.7
Pt (g/t)	3.9 ± 0.04	0.075	1.9
Pd (g/t)	1.98 ± 0.04	0.045	2.3
Rh (g/t)	0.286 ± 0.021	0.010	3.5
Nickel Sulfide Collection Fire Assay			
Element	Mean ± standard error	Standard Deviation	%RSD
Au (g/t)	0.245 ± 0.007	0.012	4.9
Pt (g/t)	3.89 ± 0.23	0.144	3.7
Pd (g/t)	1.99 ± 0.03	0.038	1.9
Rh (g/t)	0.286 ± 0.025	0.021	7.4
Totals			
Element	Mean ± standard error	Standard Deviation	%RSD
Cu %	0.133 ± 0.004	0.005	3.7
Ni %	0.246 ± 0.009	0.013	5.2
Cr %	0.576 ± 0.014	0.020	3.5
SG g/ml	3.01 ± 0.16	0.094	3.1

Figure 72. Standard Certificates G4, G6 and G8

CERTIFICATE OF ANALYSIS

G9 at a 95% confidence limit

UG2 Bulk Ore

Certified Values

Lead Collection Fire Assay			
Element	**Mean ± standard error**	**Standard Deviation**	**%RSD**
Au (g/t)	0.041 ± 0.004	0.006	13.6
Pt (g/t)	2.91 ± 0.15	0.120	4.1
Pd (g/t)	1.86 ± 0.09	0.108	5.8
Rh (g/t)	0.554 ± 0.052	0.018	3.3
Nickel Sulfide Collection Fire Assay			
Element	**Mean ± standard error**	**Standard Deviation**	**%RSD**
Au (g/t)	0.035 ± 0.011	0.011	30.8
Pt (g/t)	2.93 ± 0.16	0.110	3.8
Pd (g/t)	1.94 ± 0.08	0.051	2.6
Rh (g/t)	0.596 ± 0.073	0.045	7.6
Totals			
Element	**Mean ± standard error**	**Standard Deviation**	**%RSD**
Cu %	0.01 ± 0	0.0005	4.5
Ni %	0.113 ± 0.004	0.005	4.7
Cr %	14.219 ± 0.484	0.738	5.2
SG g/ml	3.57 ± 0.2	0.143	4.0

CERTIFICATE OF ANALYSIS

G10 at a 95% confidence limit

Merensky Barren Ore

Certified Values

Combined Methods G10			
Element	**Mean ± standard error**	**Standard Deviation**	**%RSD**
Au (g/t)	0.036 ± 0.004	0.004	12.3
Pt (g/t)	0.57 ± 0.04	0.055	9.7
Pd (g/t)	0.28 ± 0.01	0.018	6.5
Rh (g/t)	0.047 ± 0.005	0.005	10.1
Recommended Values			
Element	**Mean ± standard error**	**Standard Deviation**	**%RSD**
Cu %	0.018 ± 0	0.001	5.8
Ni %	0.053 ± 0.003	0.002	4.1
Cr %	0.538 ± 0.024	0.020	3.8
SG g/ml	2.94 ± 0.11	0.052	1.7

CERTIFICATE OF ANALYSIS

G11 UG2 Barren Reference Material

Certified Values

Constituent	Certified Value ± standard error	Standard Deviation	% RSD	Median
Precious Metals				
Au (g/t)	0.010 ± 0.001	0.002	24.2	0.011
Pt (g/t)	0.060 ± 0.002	0.006	10.6	0.062
Pd (g/t)	0.031 ± 0.001	0.005	17.5	0.030
Rh (g/t)	0.020 ± 0.001	0.003	13.2	0.019
Base Metals				
Ni (%)	0.094 ± 0.001	0.003	3.3	0.093
Cr (%)	29.9 ± 0.22	0.75	2.5	29.7
SG (g/cm^3)	4.54 ± 0.03	0.09	2.1	4.49

Figure 73. Standard Certificates G9, G10 and G11

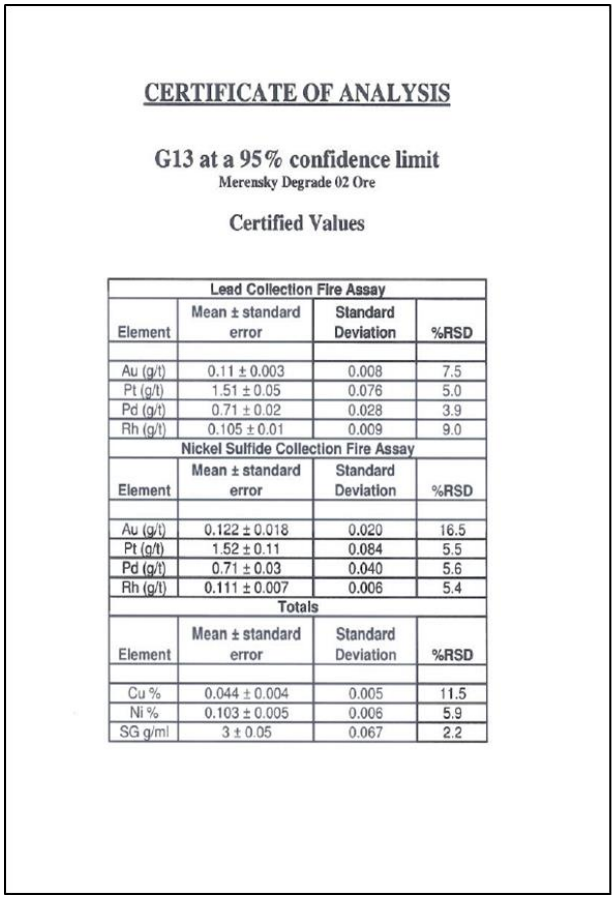

CERTIFICATE OF ANALYSIS

G13 at a 95% confidence limit

Merensky Degrade 02 Ore

Certified Values

Lead Collection Fire Assay			
Element	Mean ± standard error	Standard Deviation	%RSD
Au (g/t)	0.11 ± 0.003	0.008	7.5
Pt (g/t)	1.51 ± 0.05	0.076	5.0
Pd (g/t)	0.71 ± 0.02	0.028	3.9
Rh (g/t)	0.105 ± 0.01	0.009	9.0
Nickel Sulfide Collection Fire Assay			
Element	Mean ± standard error	Standard Deviation	%RSD
Au (g/t)	0.122 ± 0.018	0.020	16.5
Pt (g/t)	1.52 ± 0.11	0.084	5.5
Pd (g/t)	0.71 ± 0.03	0.040	5.6
Rh (g/t)	0.111 ± 0.007	0.006	5.4
Totals			
Element	Mean ± standard error	Standard Deviation	%RSD
Cu %	0.044 ± 0.004	0.005	11.5
Ni %	0.103 ± 0.005	0.006	5.9
SG g/ml	3 ± 0.05	0.067	2.2

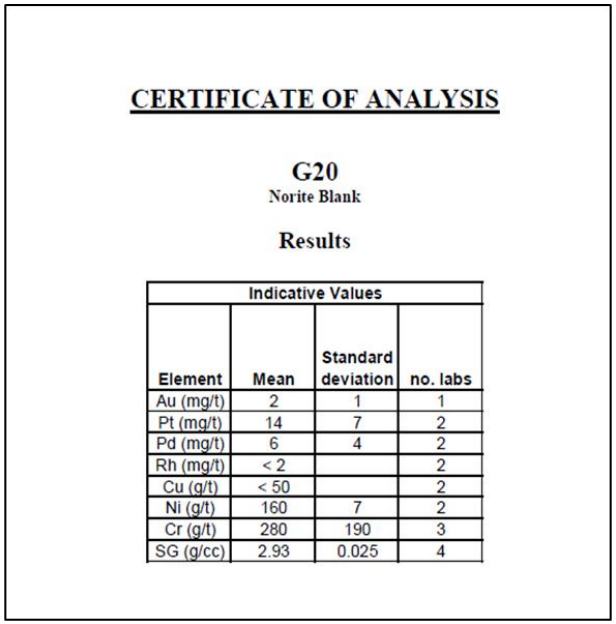

CERTIFICATE OF ANALYSIS

G20

Norite Blank

Results

Indicative Values			
Element	Mean	Standard deviation	no. labs
Au (mg/t)	2	1	1
Pt (mg/t)	14	7	2
Pd (mg/t)	6	4	2
Rh (mg/t)	< 2		2
Cu (g/t)	< 50		2
Ni (g/t)	160	7	2
Cr (g/t)	280	190	3
SG (g/cc)	2.93	0.025	4

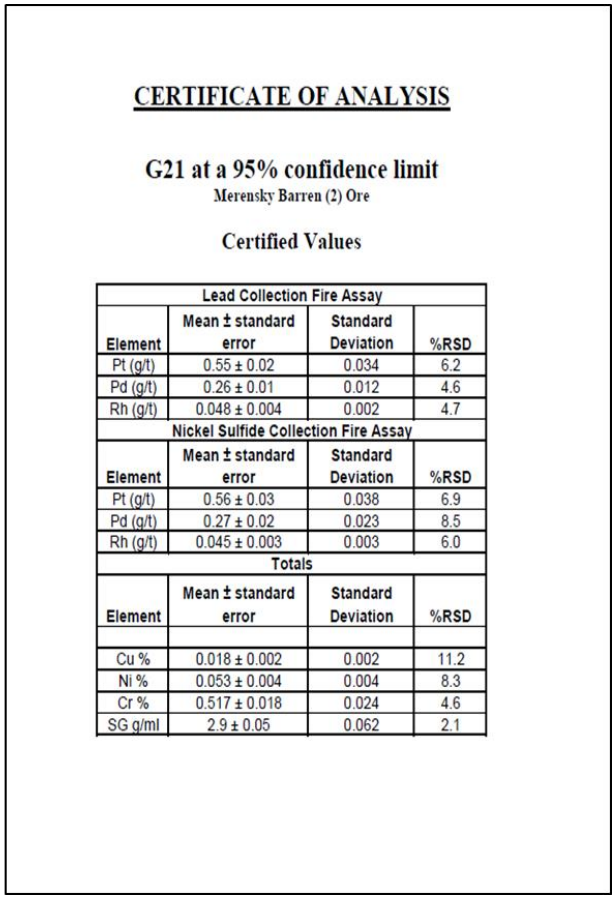

CERTIFICATE OF ANALYSIS

G21 at a 95% confidence limit

Merensky Barren (2) Ore

Certified Values

Lead Collection Fire Assay			
Element	Mean ± standard error	Standard Deviation	%RSD
Pt (g/t)	0.55 ± 0.02	0.034	6.2
Pd (g/t)	0.26 ± 0.01	0.012	4.6
Rh (g/t)	0.048 ± 0.004	0.002	4.7
Nickel Sulfide Collection Fire Assay			
Element	Mean ± standard error	Standard Deviation	%RSD
Pt (g/t)	0.56 ± 0.03	0.038	6.9
Pd (g/t)	0.27 ± 0.02	0.023	8.5
Rh (g/t)	0.045 ± 0.003	0.003	6.0
Totals			
Element	Mean ± standard error	Standard Deviation	%RSD
Cu %	0.018 ± 0.002	0.002	11.2
Ni %	0.053 ± 0.004	0.004	8.3
Cr %	0.517 ± 0.018	0.024	4.6
SG g/ml	2.9 ± 0.05	0.062	2.1

Figure 74. Standard Certificates G13 and blanks G20 and G21

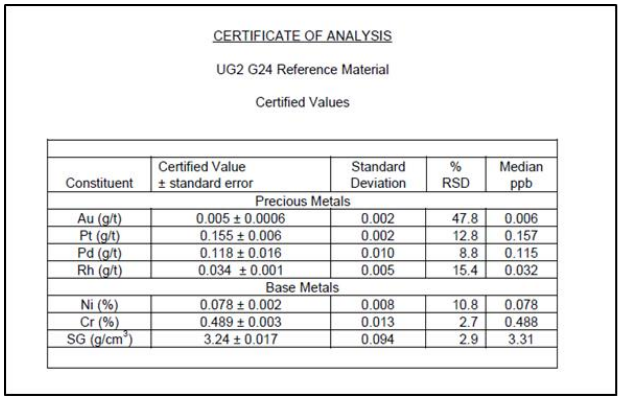

CERTIFICATE OF ANALYSIS

UG2 G24 Reference Material

Certified Values

Constituent	Certified Value ± standard error	Standard Deviation	% RSD	Median ppb
Precious Metals				
Au (g/t)	0.005 ± 0.0006	0.002	47.8	0.006
Pt (g/t)	0.155 ± 0.006	0.002	12.8	0.157
Pd (g/t)	0.118 ± 0.016	0.010	8.8	0.115
Rh (g/t)	0.034 ± 0.001	0.005	15.4	0.032
Base Metals				
Ni (%)	0.078 ± 0.002	0.008	10.8	0.078
Cr (%)	0.489 ± 0.003	0.013	2.7	0.488
SG (g/cm^3)	3.24 ± 0.017	0.094	2.9	3.31

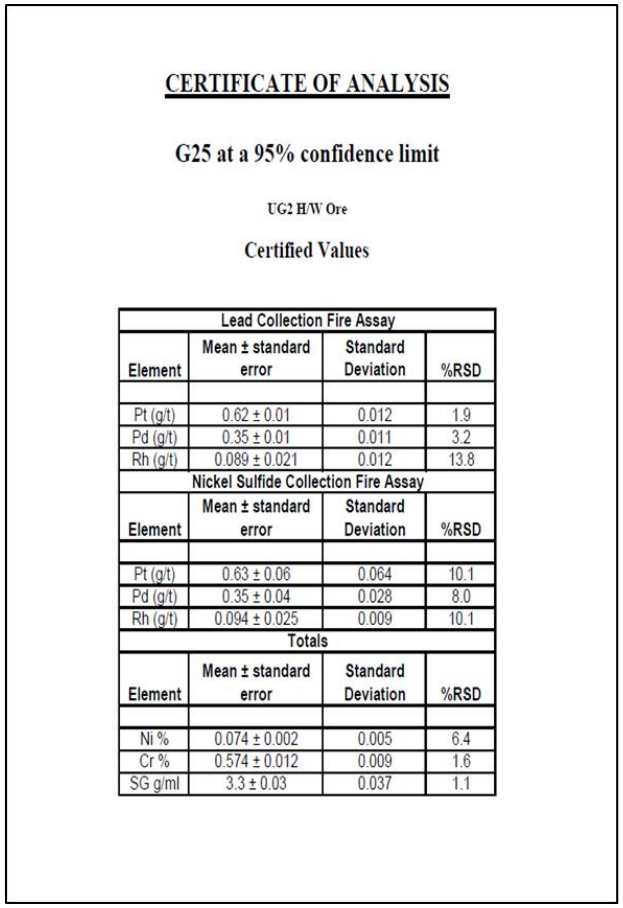

CERTIFICATE OF ANALYSIS

G25 at a 95% confidence limit

UG2 H/W Ore

Certified Values

Lead Collection Fire Assay			
Element	Mean ± standard error	Standard Deviation	%RSD
Pt (g/t)	0.62 ± 0.01	0.012	1.9
Pd (g/t)	0.35 ± 0.01	0.011	3.2
Rh (g/t)	0.089 ± 0.021	0.012	13.8
Nickel Sulfide Collection Fire Assay			
Element	Mean ± standard error	Standard Deviation	%RSD
Pt (g/t)	0.63 ± 0.06	0.064	10.1
Pd (g/t)	0.35 ± 0.04	0.028	8.0
Rh (g/t)	0.094 ± 0.025	0.009	10.1
Totals			
Element	Mean ± standard error	Standard Deviation	%RSD
Ni %	0.074 ± 0.002	0.005	6.4
Cr %	0.574 ± 0.012	0.009	1.6
SG g/ml	3.3 ± 0.03	0.037	1.1

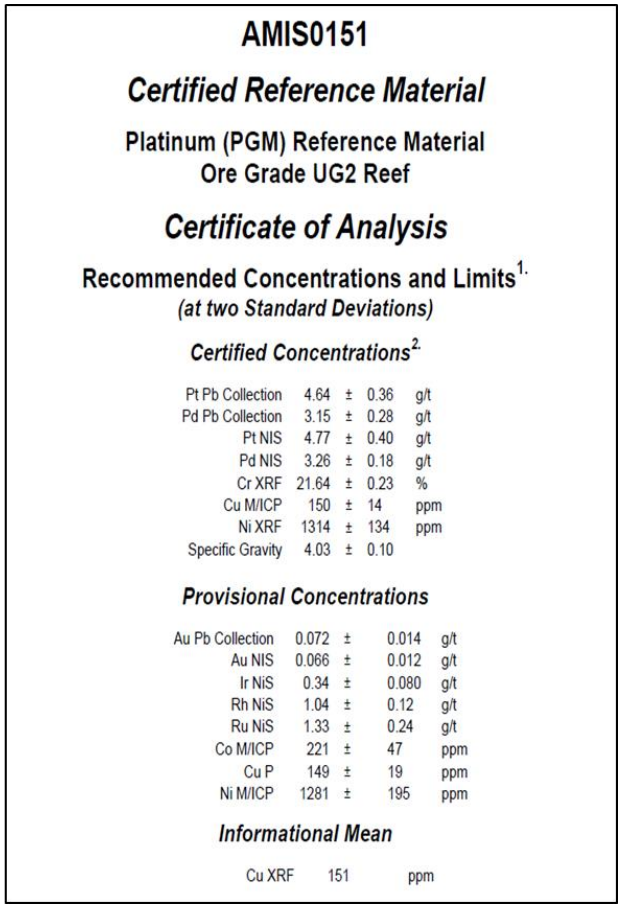

AMIS0151

Certified Reference Material

Platinum (PGM) Reference Material
Ore Grade UG2 Reef

Certificate of Analysis

Recommended Concentrations and Limits[1.]
(at two Standard Deviations)

Certified Concentrations[2.]

Pt Pb Collection	4.64	±	0.36	g/t
Pd Pb Collection	3.15	±	0.28	g/t
Pt NIS	4.77	±	0.40	g/t
Pd NIS	3.26	±	0.18	g/t
Cr XRF	21.64	±	0.23	%
Cu M/ICP	150	±	14	ppm
Ni XRF	1314	±	134	ppm
Specific Gravity	4.03	±	0.10	

Provisional Concentrations

Au Pb Collection	0.072	±	0.014	g/t
Au NIS	0.066	±	0.012	g/t
Ir NiS	0.34	±	0.080	g/t
Rh NiS	1.04	±	0.12	g/t
Ru NiS	1.33	±	0.24	g/t
Co M/ICP	221	±	47	ppm
Cu P	149	±	19	ppm
Ni M/ICP	1281	±	195	ppm

Informational Mean

Cu XRF	151	ppm

Figure 75. Standard Certificates G24, G25 and AMIS0151

7.2 Appendix B: CRM Result Graphs

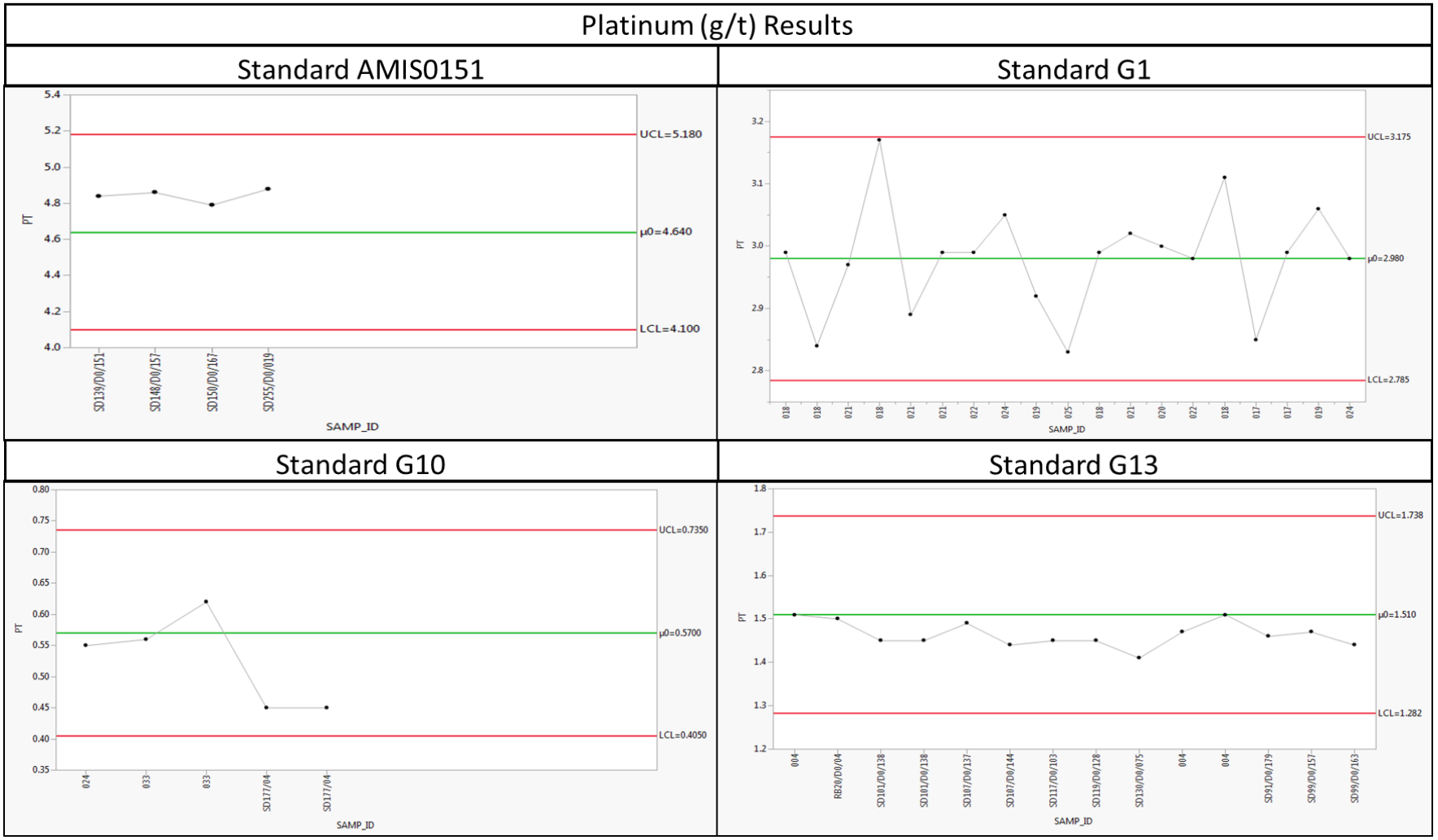

Figure 76. Platinum results of standards AMIS0151, G1, G10 and G13

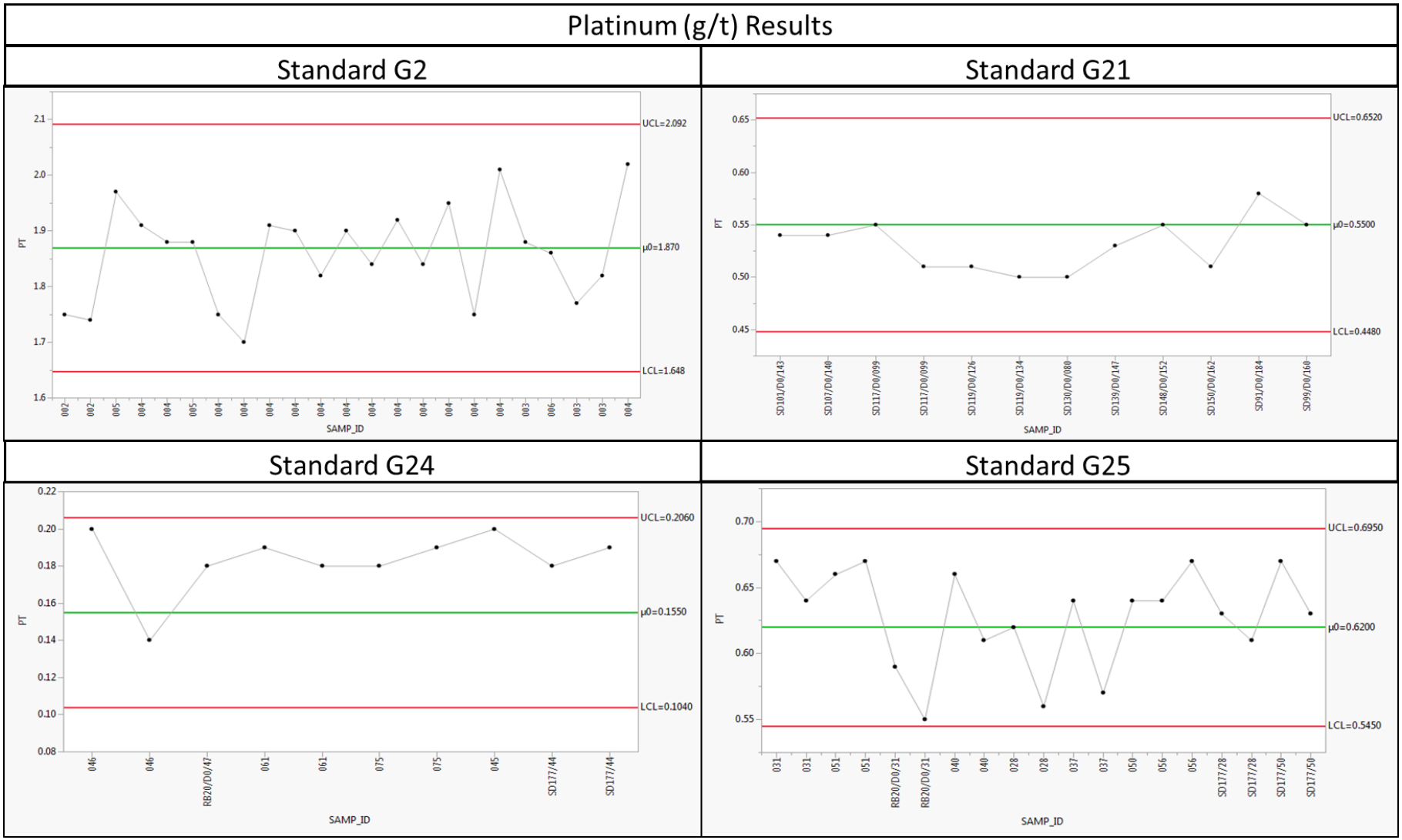

Figure 77. Platinum results of standards G2, G21, G24 and G25

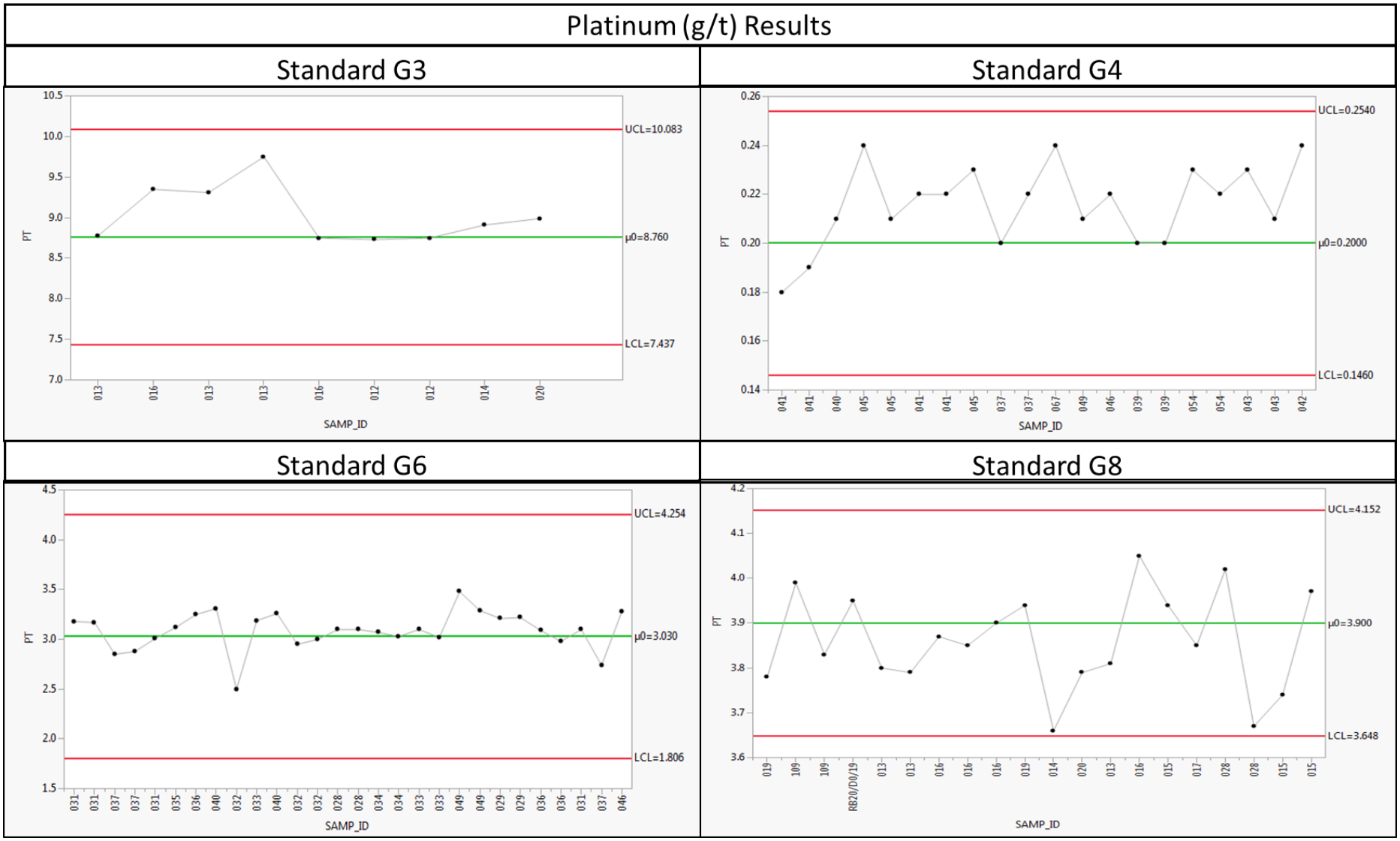

Figure 78. Platinum results of standards G3, G4, G6 and G8

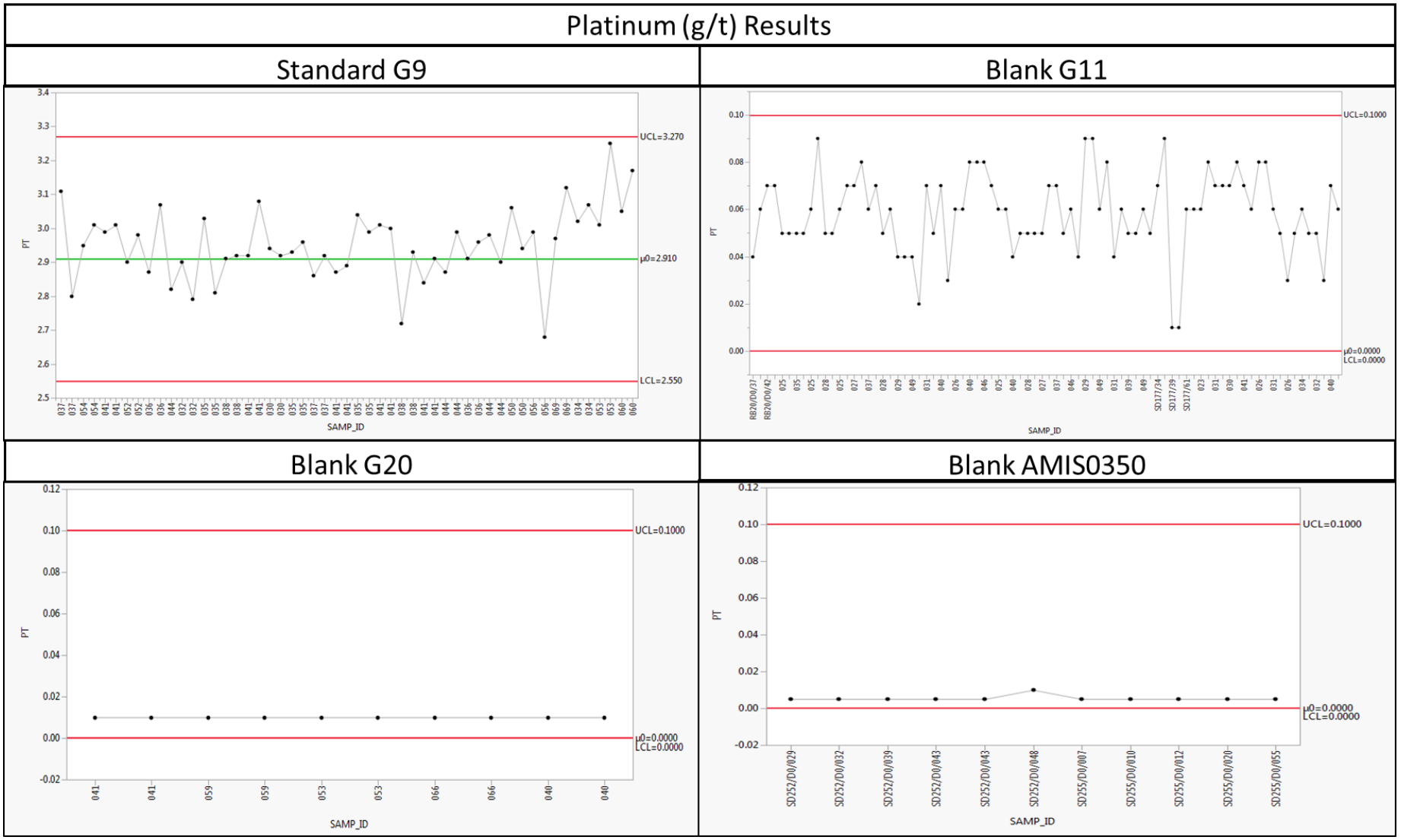

Figure 79. Platinum results of standard G9 and blanks G11, G20 and AMIS0350

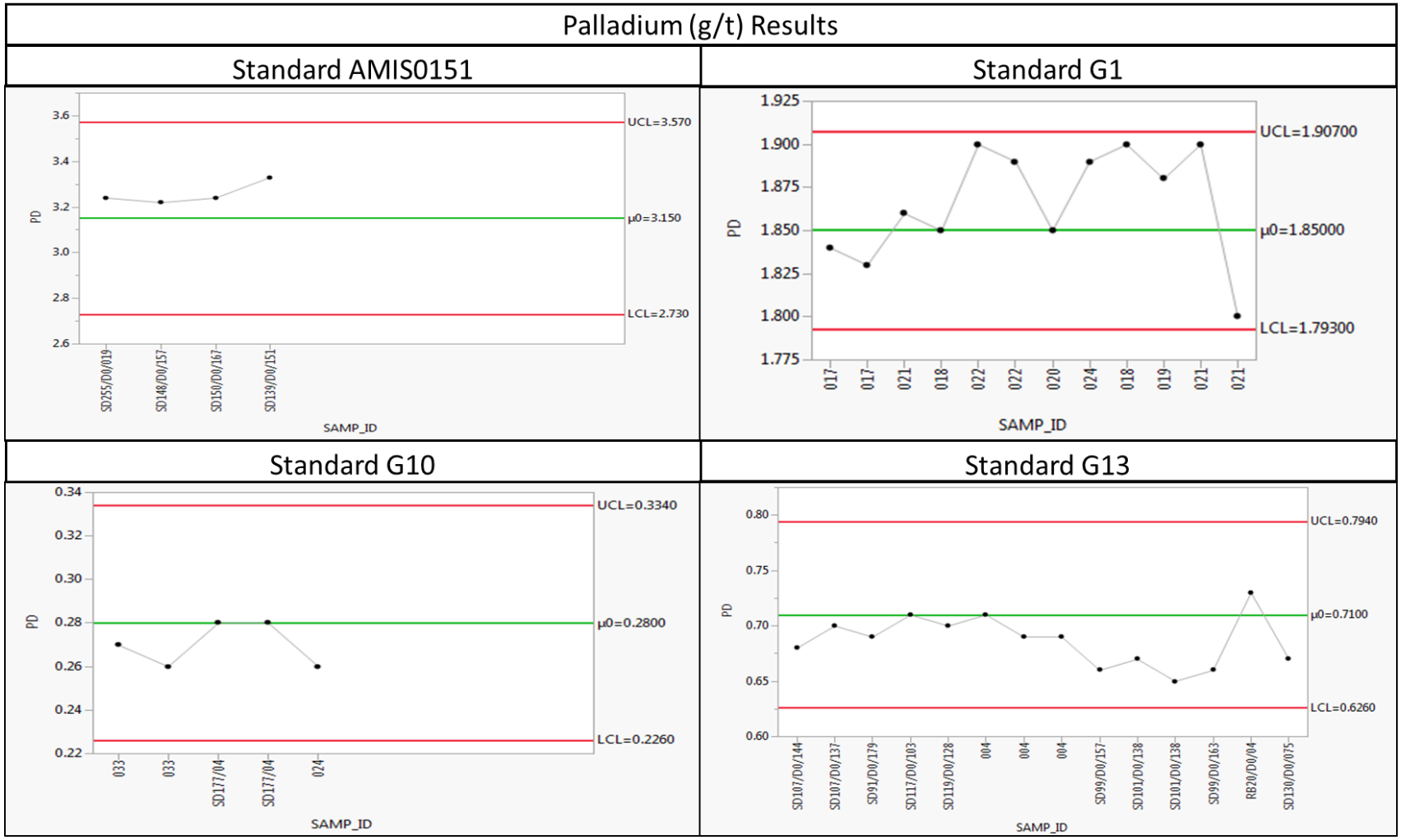

Figure 80. Palladium results of standards AMIS0151, G1, G10 and G13

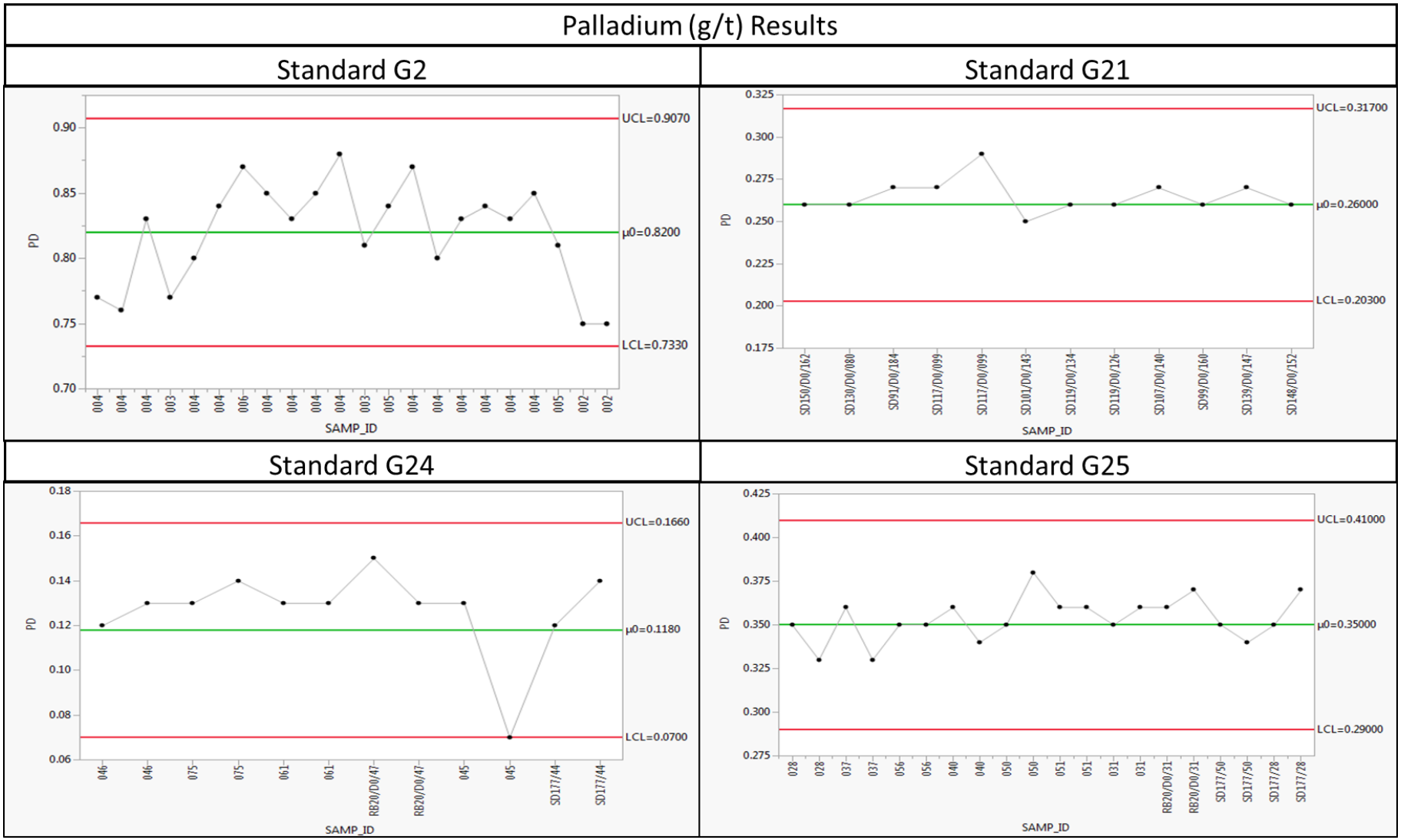

Figure 81. Palladium results of standards G2, G21, G24 and G25

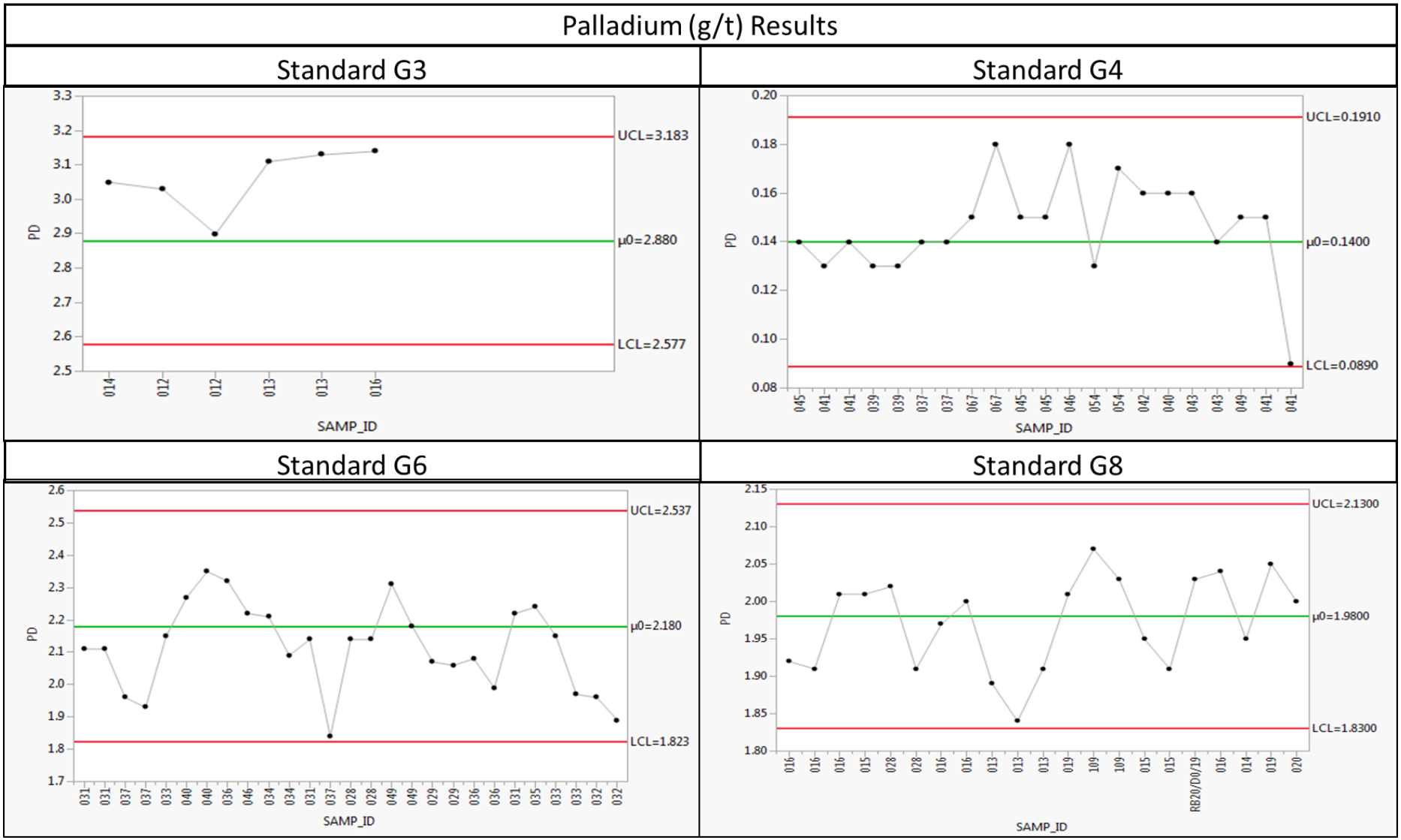

Figure 82. Palladium results of standards G3, G4, G6 and G8

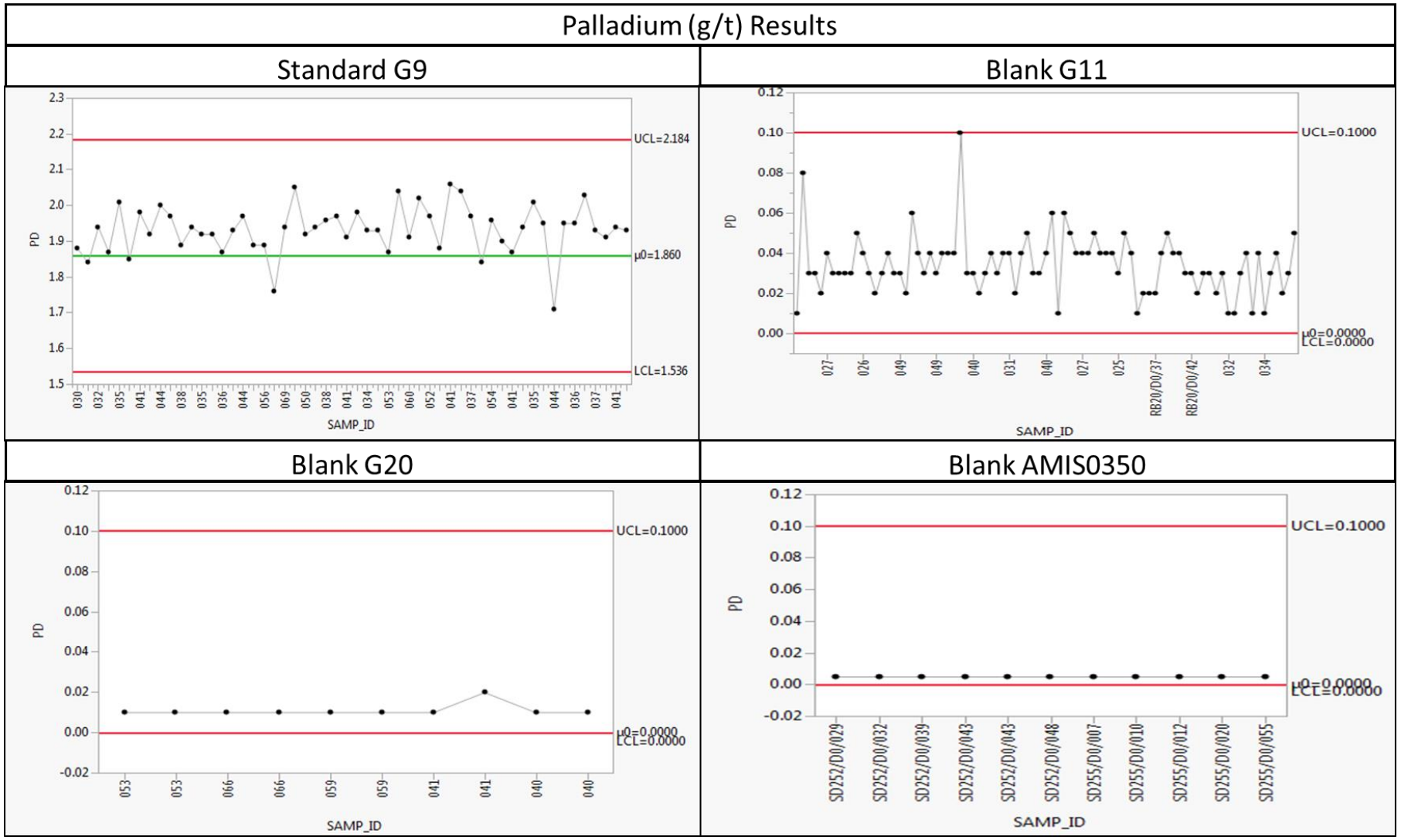

Figure 83. Palladium results of standards G9, G11, G20 and AMIS0350

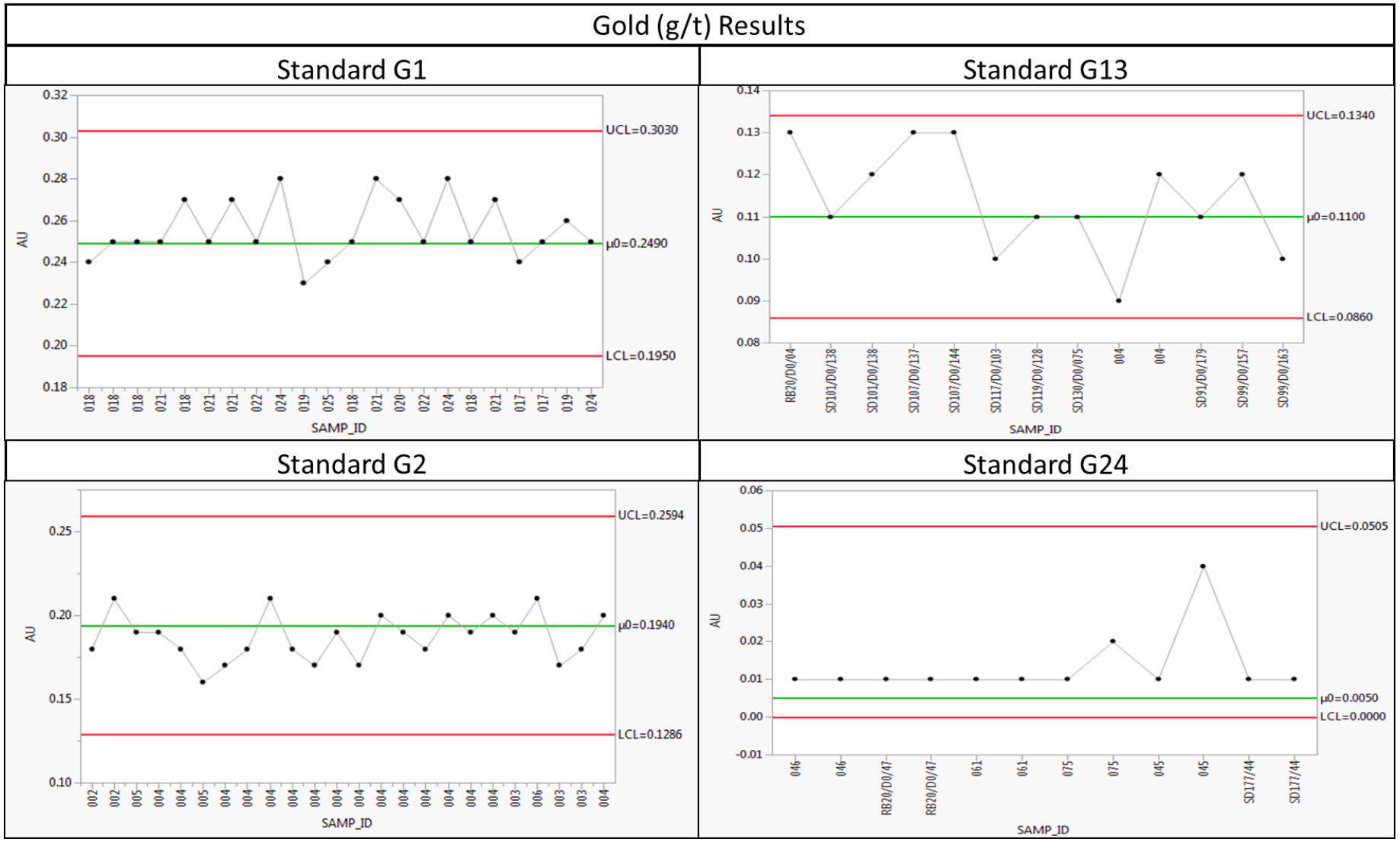

Figure 84. Gold results of standards G1, G13, G2 and G24

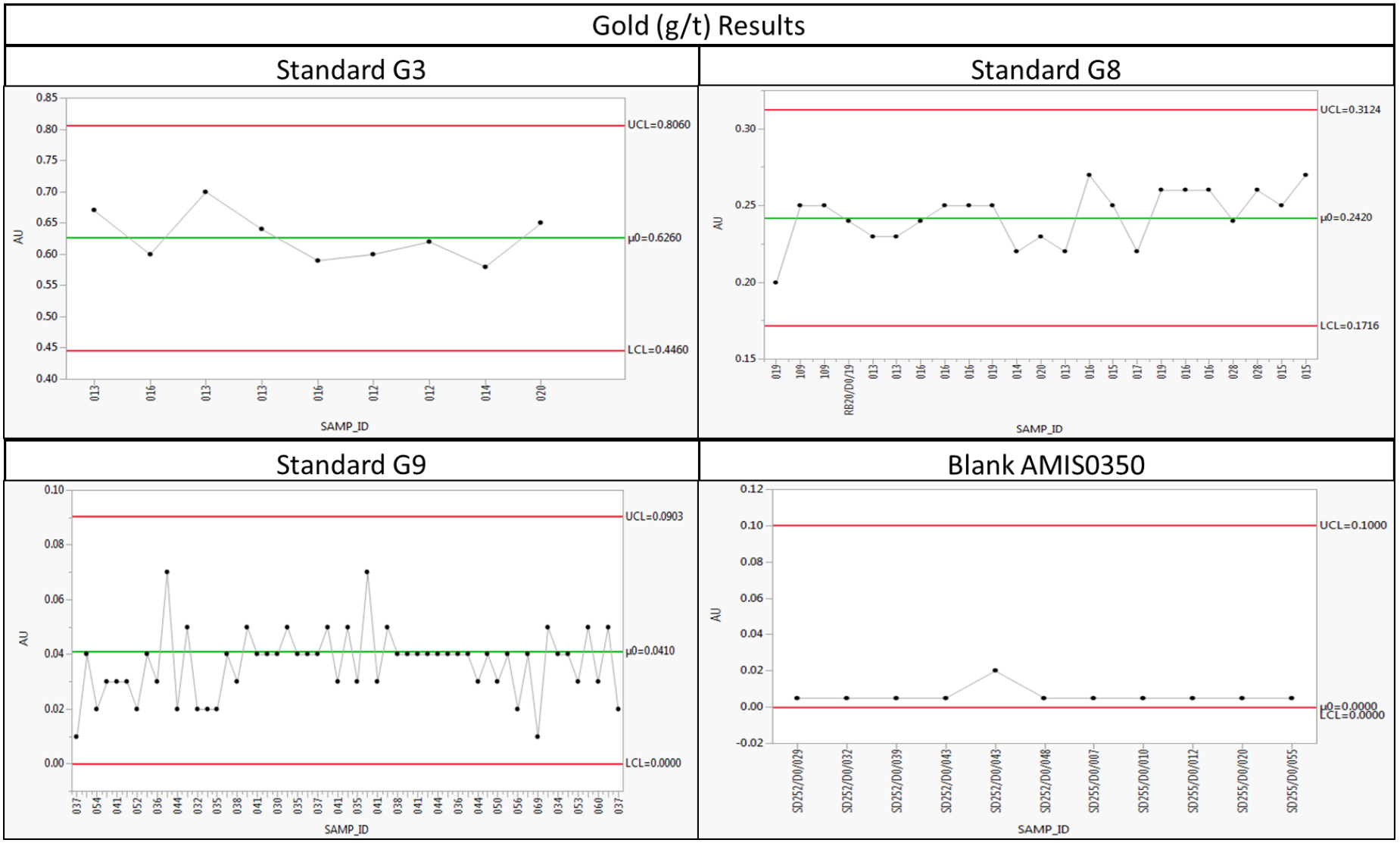

Figure 85. Gold results of standards G3, G8, G9 and blank AMIS0350

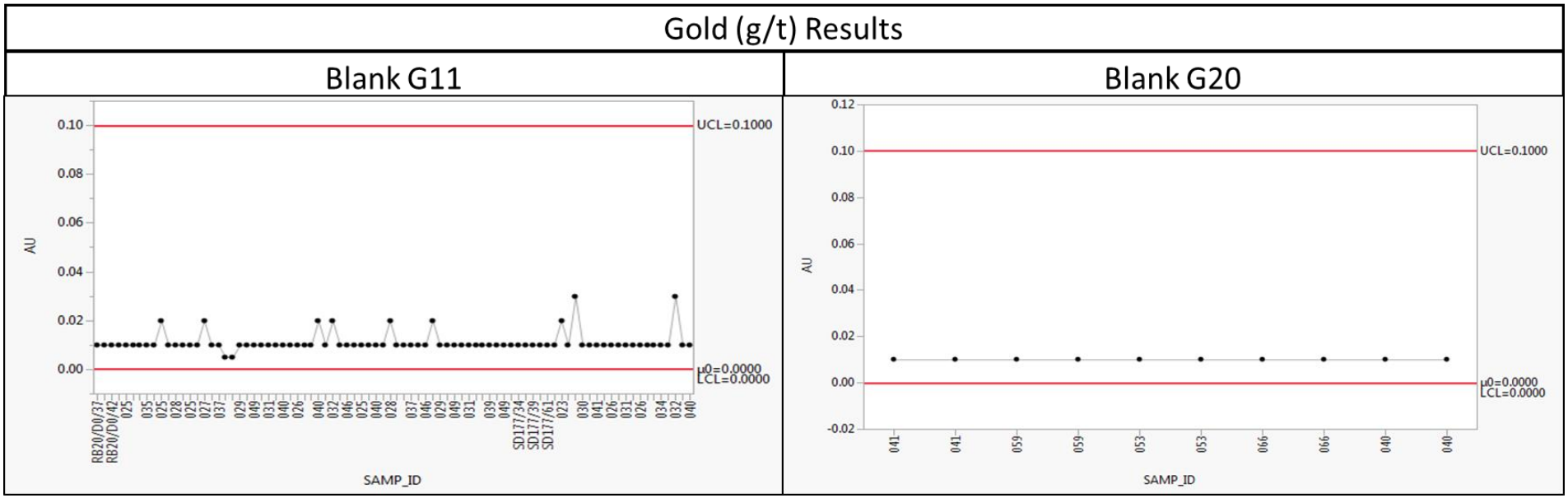

Figure 86. Gold results of blanks G11 and G20

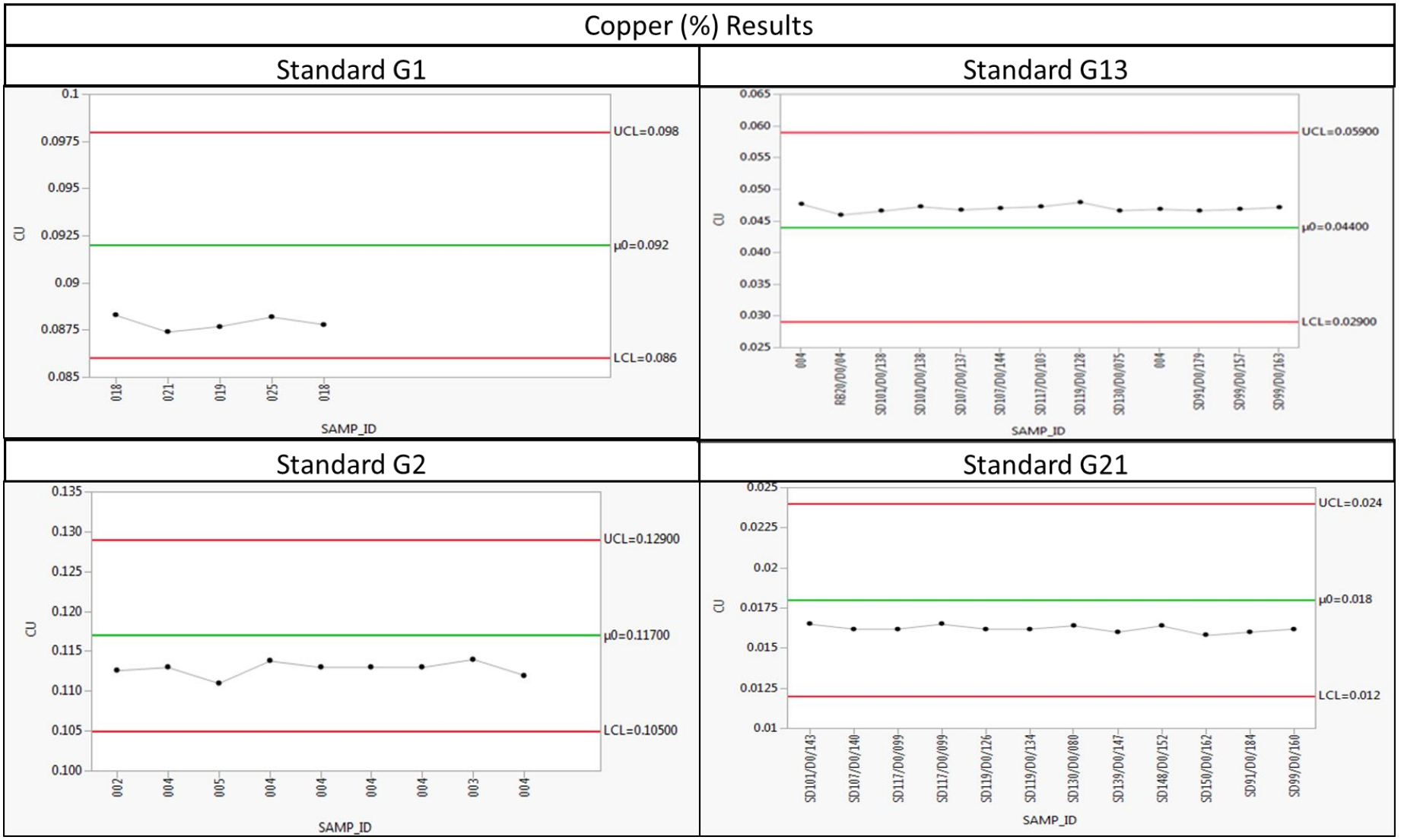

Figure 87. Copper results of standards G1, G13, G2 and G21

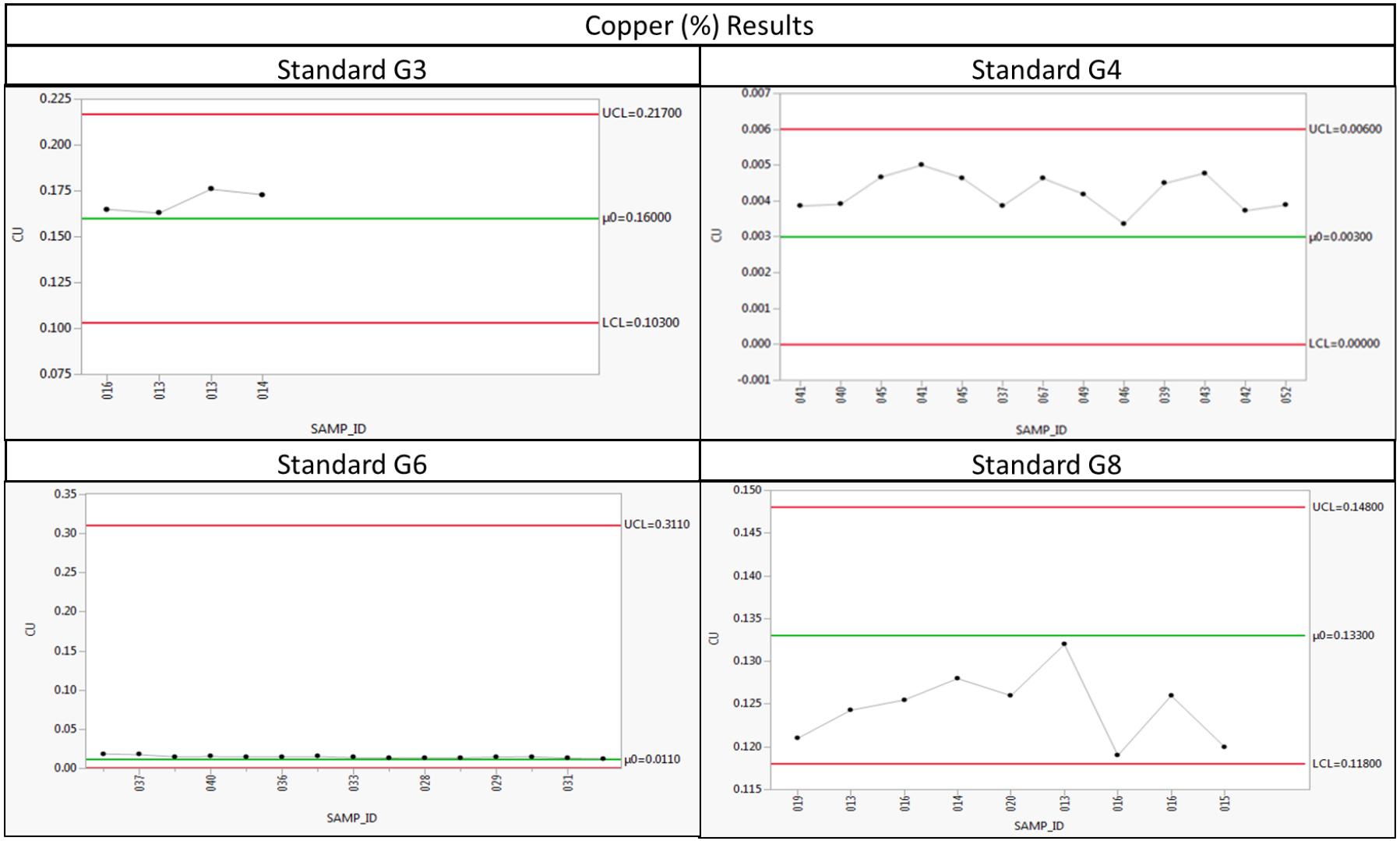

Figure 88. Copper results of standards G3, G4, G6 and G8

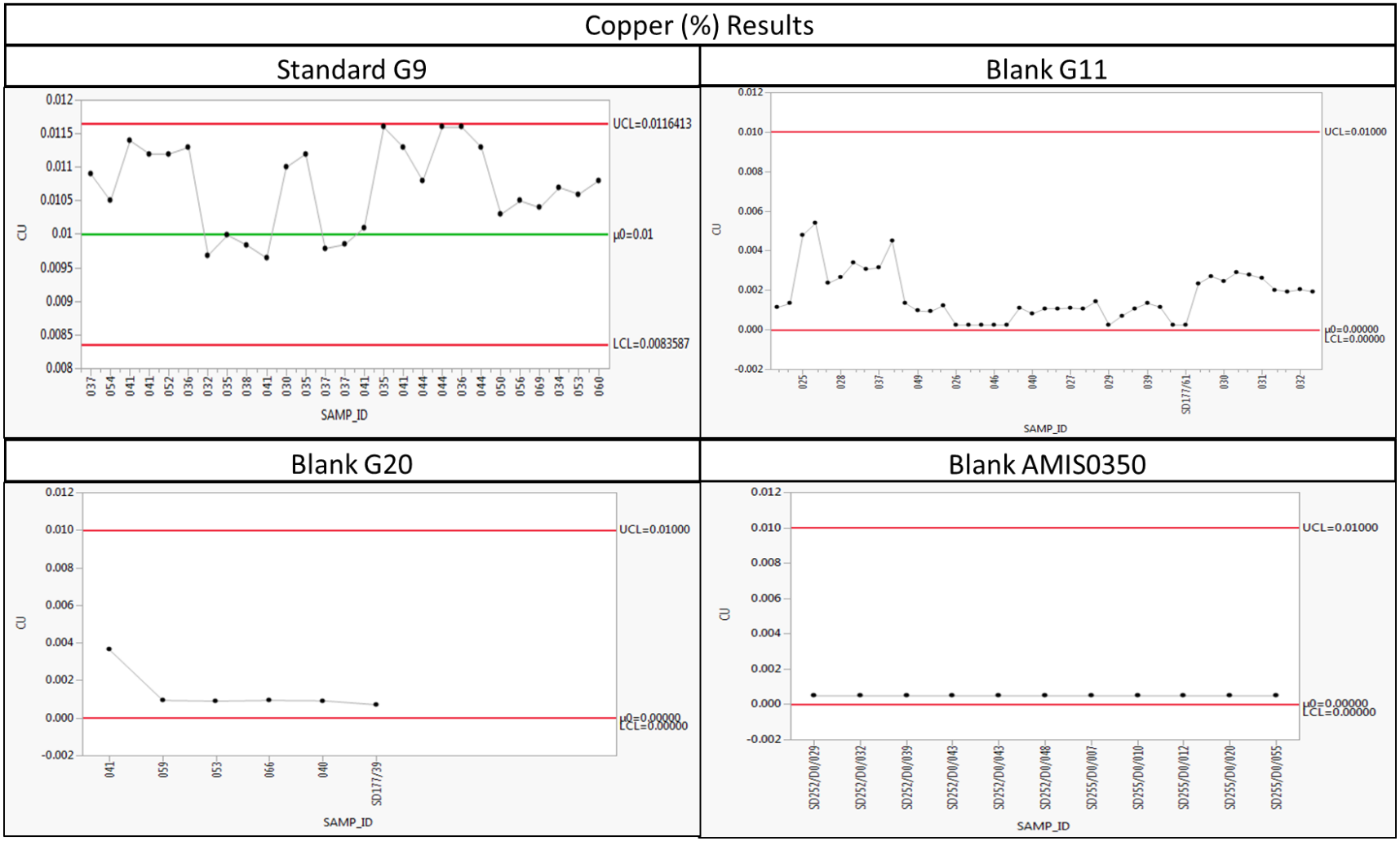

Figure 89. Copper results of standards G9 and blanks G11, G20 and AMIS0350

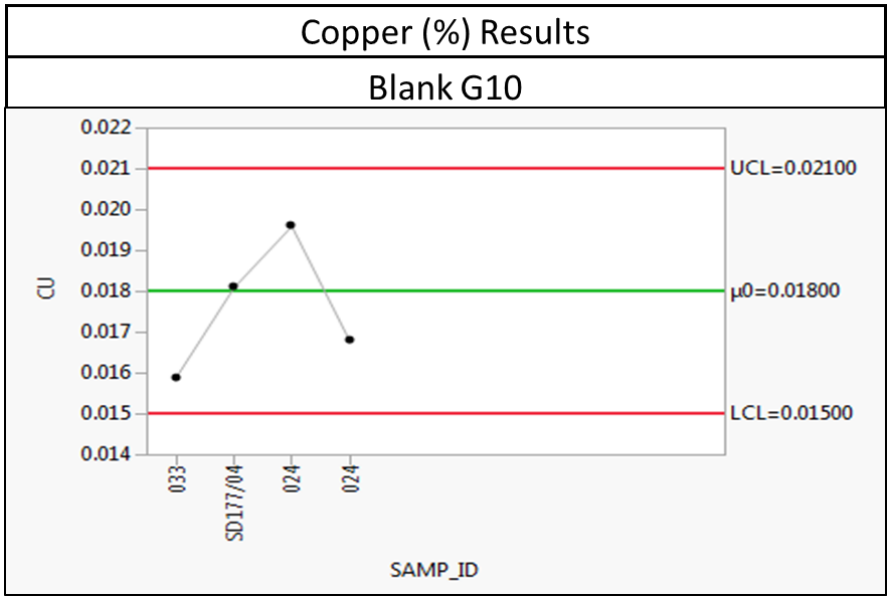

Figure 90. Copper results of blank G10

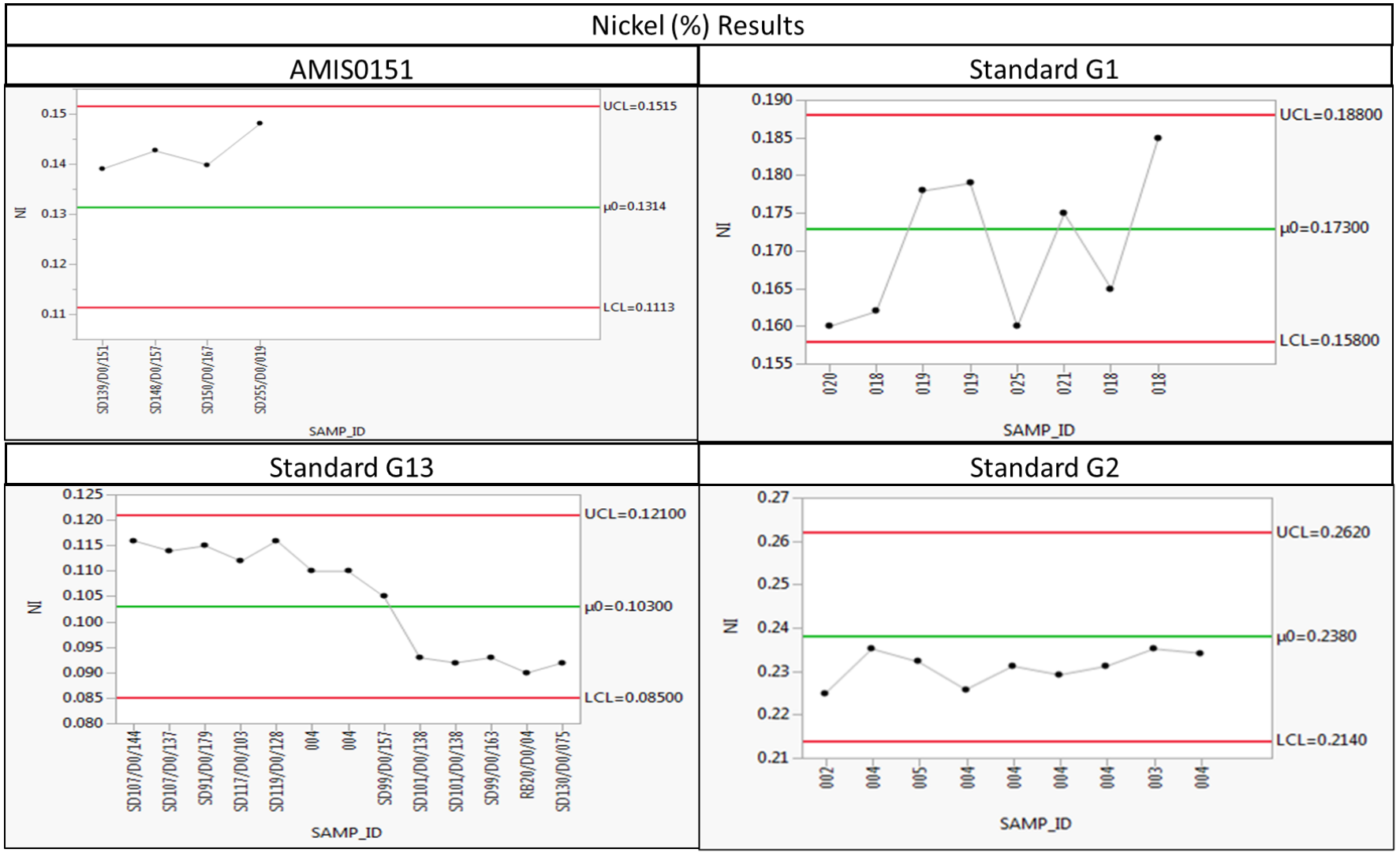

Figure 91. Nickel results of standards AMIS0151, G1, G13 and G2

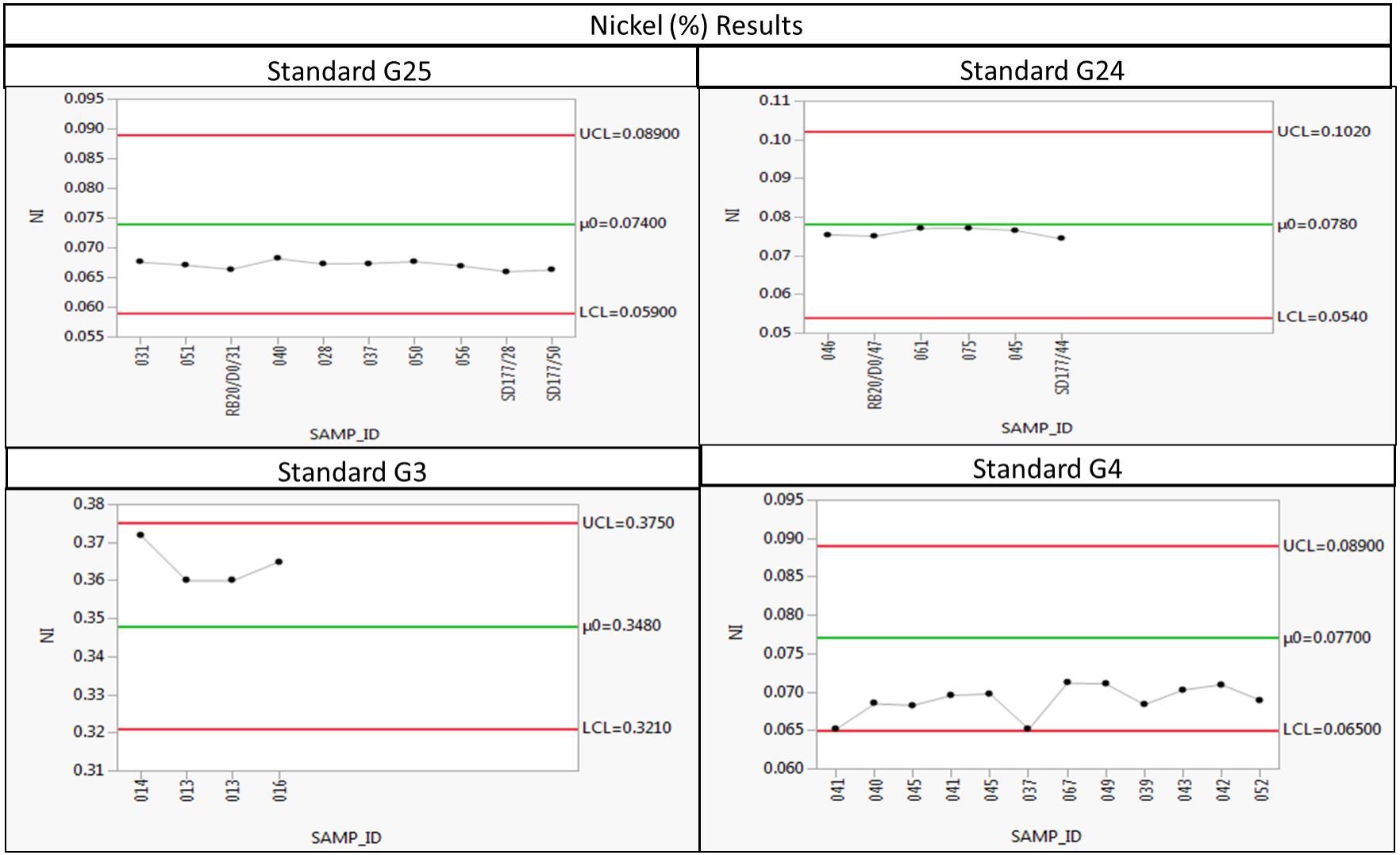

Figure 92. Nickel results of standards G25, G24, G3 and G4

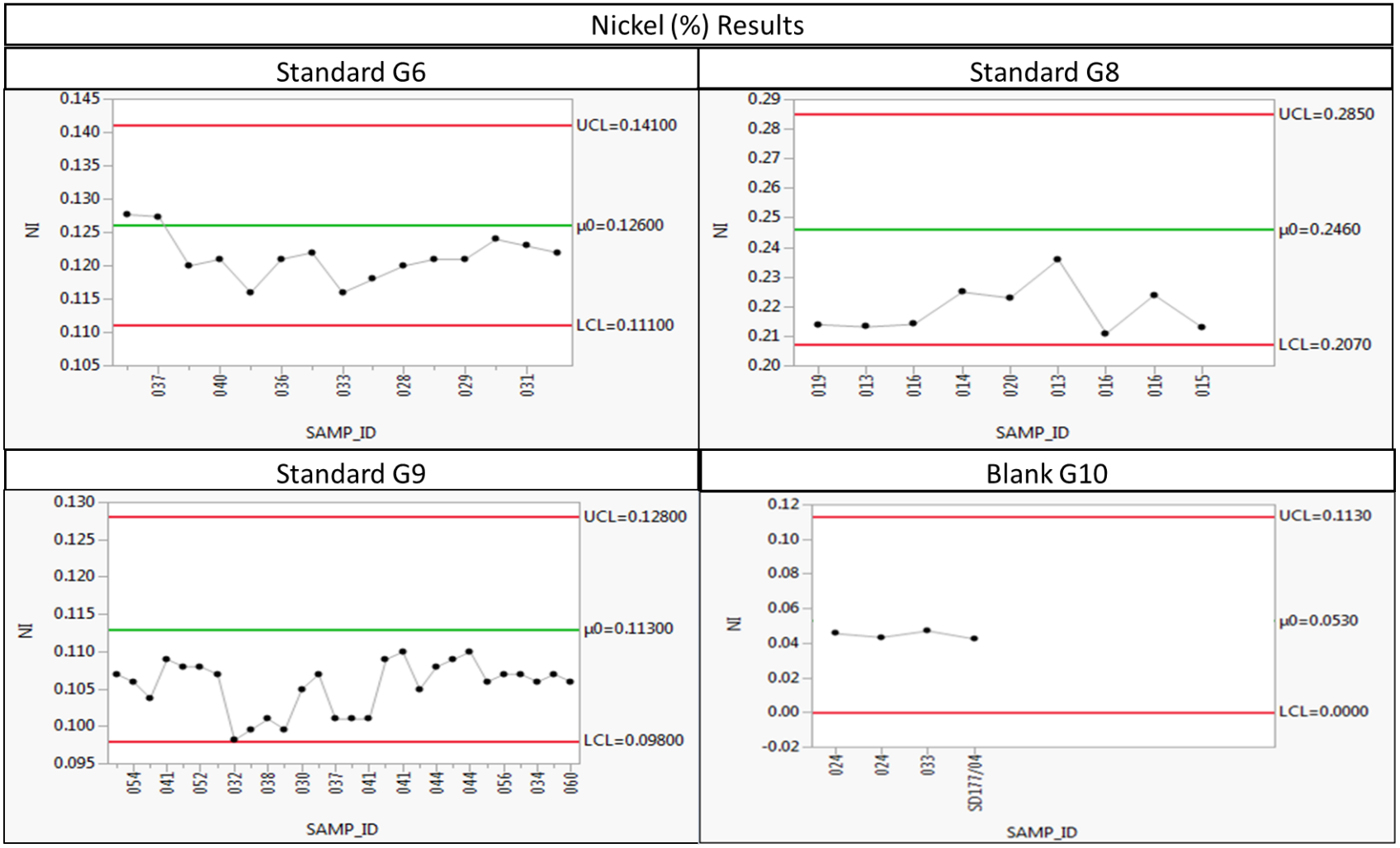

Figure 93. Nickel results of standards G6, G8, G9 and blank G10

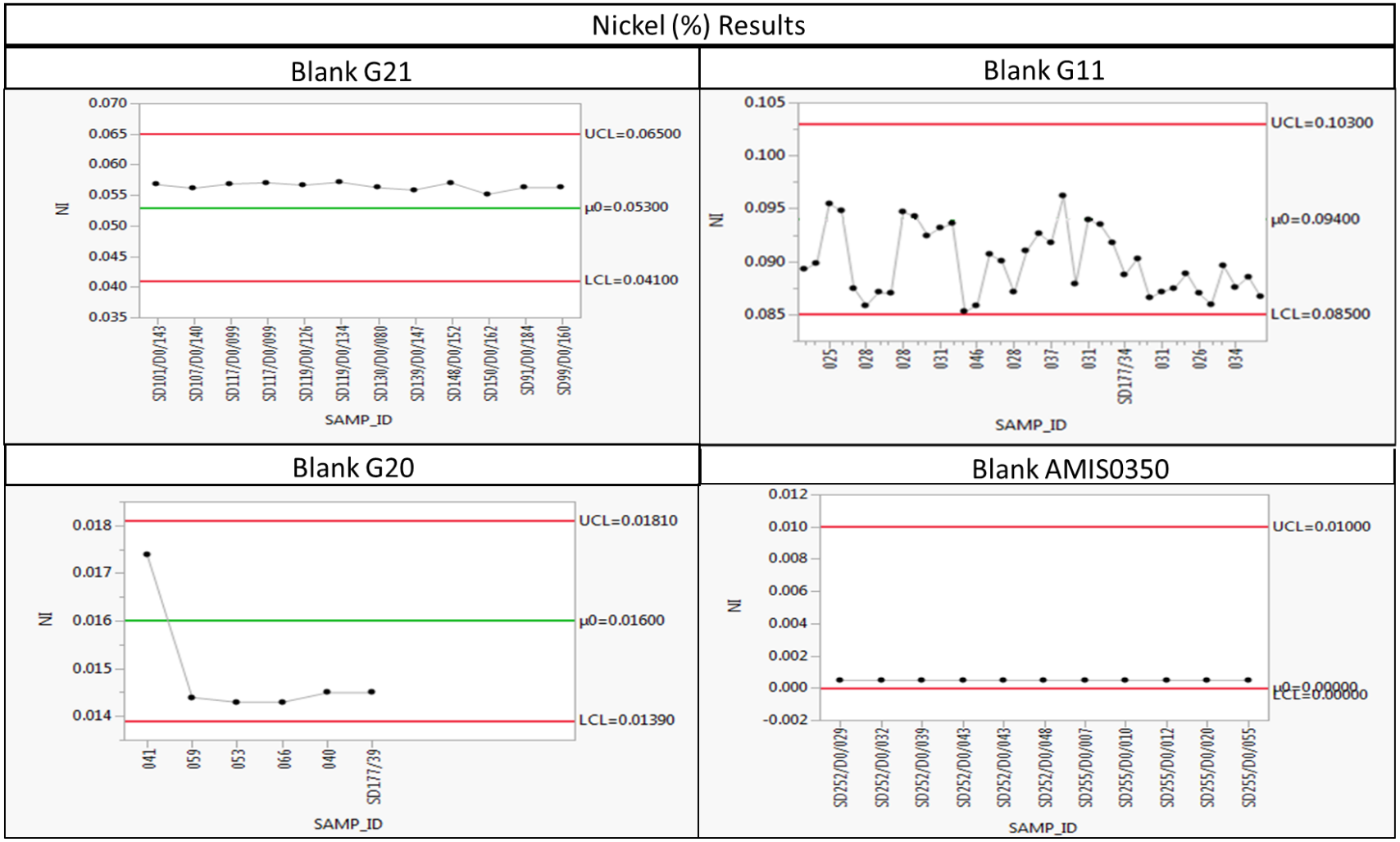

Figure 94. Nickel results of blanks G21, G11, G20 and AMIS0350

7.3. Appendix C: Niton XL3T GOLDD pXRF Specifications

Table 12: Niton XL3t GOLDD pXRF Analyser specifications (Thermo Scientific, 2017)

Weight	**< 3.0 lbs (< 1.3 kg)**
Dimensions	**9.60 x 9.05 x 3.75 in. (244 x 230 x 95.5 mm)**
Tube	**Au anode (9-50 kV, 0-40 µA max)**
Detector	**Geometrically Optimized Large Area Drift Detector (GOLDD)** **Proprietary detector with 180,000 throughput cps** **Resolution: < 185 eV @ 60,000 cps @ 4µ sec shaping time**
System Electronics	**533 MHz ARM 11 CPU** **300 MHz dedicated DSP** **80 MHz ASICS DSP for signal processing** **4096 channel MCA** **32 MB internal system memory/128 MB internal user storage**
Display	**Tilting, color, touch-screen display**
Standard Analytical Range	**Up to 30 elements from S – U (varies by application)**
Data Storage	**Internal >10,000 readings with spectra**
Data Transfer	**USB, Bluetooth, and RS-232 serial communication**
Security	**Password-protected user security**
Mode **(Varies by application)**	**Alloy Modes: Electronics Alloy** **Bulk Modes: Soil, Mining, TestAll™** **Plastic Modes: RoHS Plastics, Toy & Consumer Goods Plastics, TestAll,** **Custom Modes: Upon request (based on application feasibility)**
Data Entry	**Touch-screen keyboard** **User-programmable pick lists** **Optional wireless remote barcode reader**
Standard Accessories	**Integrated CCD camera for locating and storing images** **Locking shielded carrying caser** **Shielded belt holster** **Two lithium-ion battery packs** **110/220 VAC battery charger/AC adaptor** **PC connection cables (USB and RS-232)** **Niton Data Transfer (NDT) PC software** **Safety lanyard** **Check samples/standards**
Optional Features and Accessories	**3 mm small-spot collimation** **Thermo Scientific SmartStand™ portable test stand, stationary (bench-top) test stand, mobile test stand, Field Mate™** **Thermo Scientific Extend-a-Pole™ extension pole** **Soil testing guard**
Licensing/Registration	**Varies by region. Contact your local distributor.**
Compliance	**CE, RoHS**

7.3 Appendix D: Drillholes Analysed for pXRF Accuracy Test

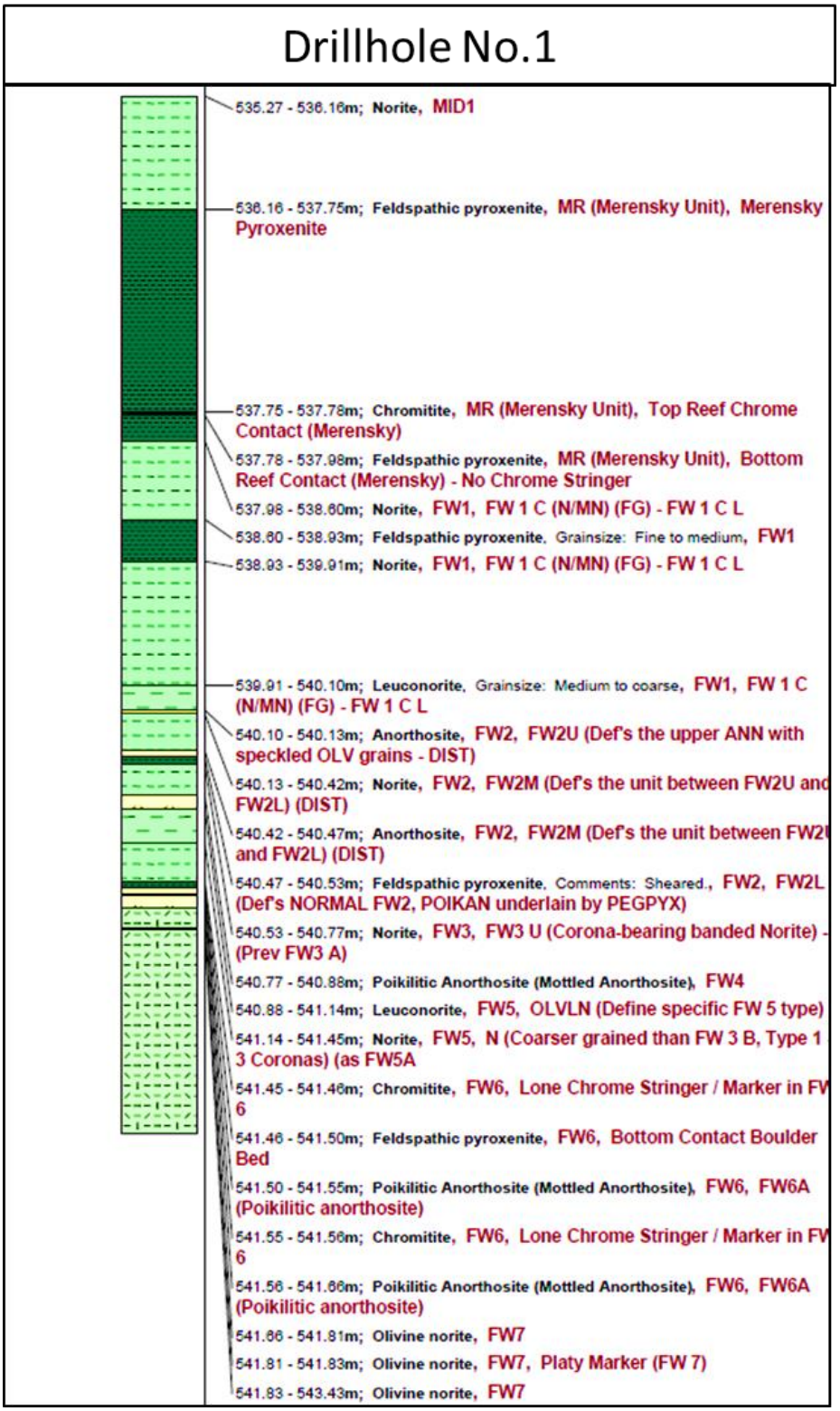

Figure 95. Drillhole No.1 used for Core Analysis

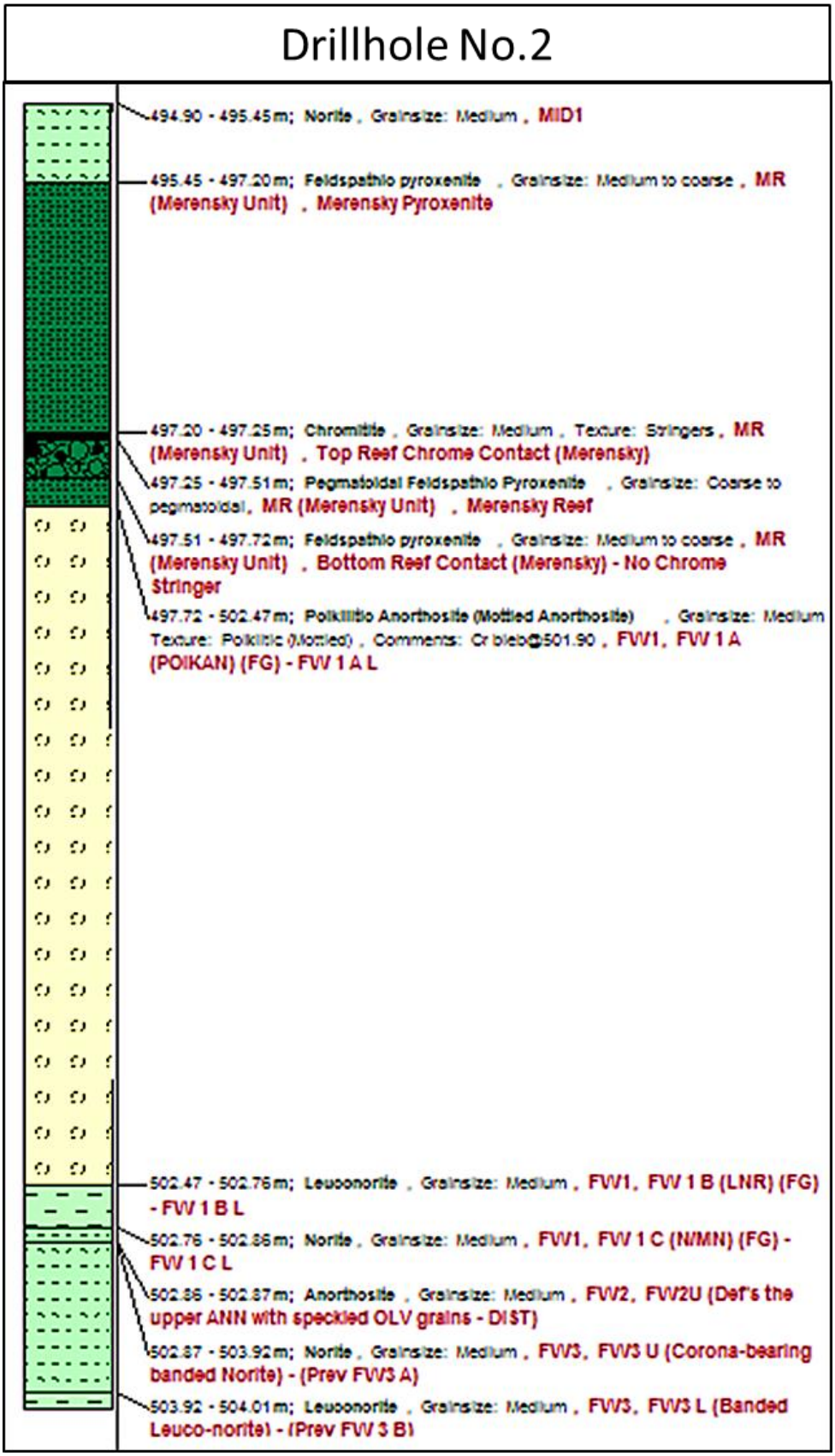

Figure 96. Drillhole No.2 used for Core Analysis

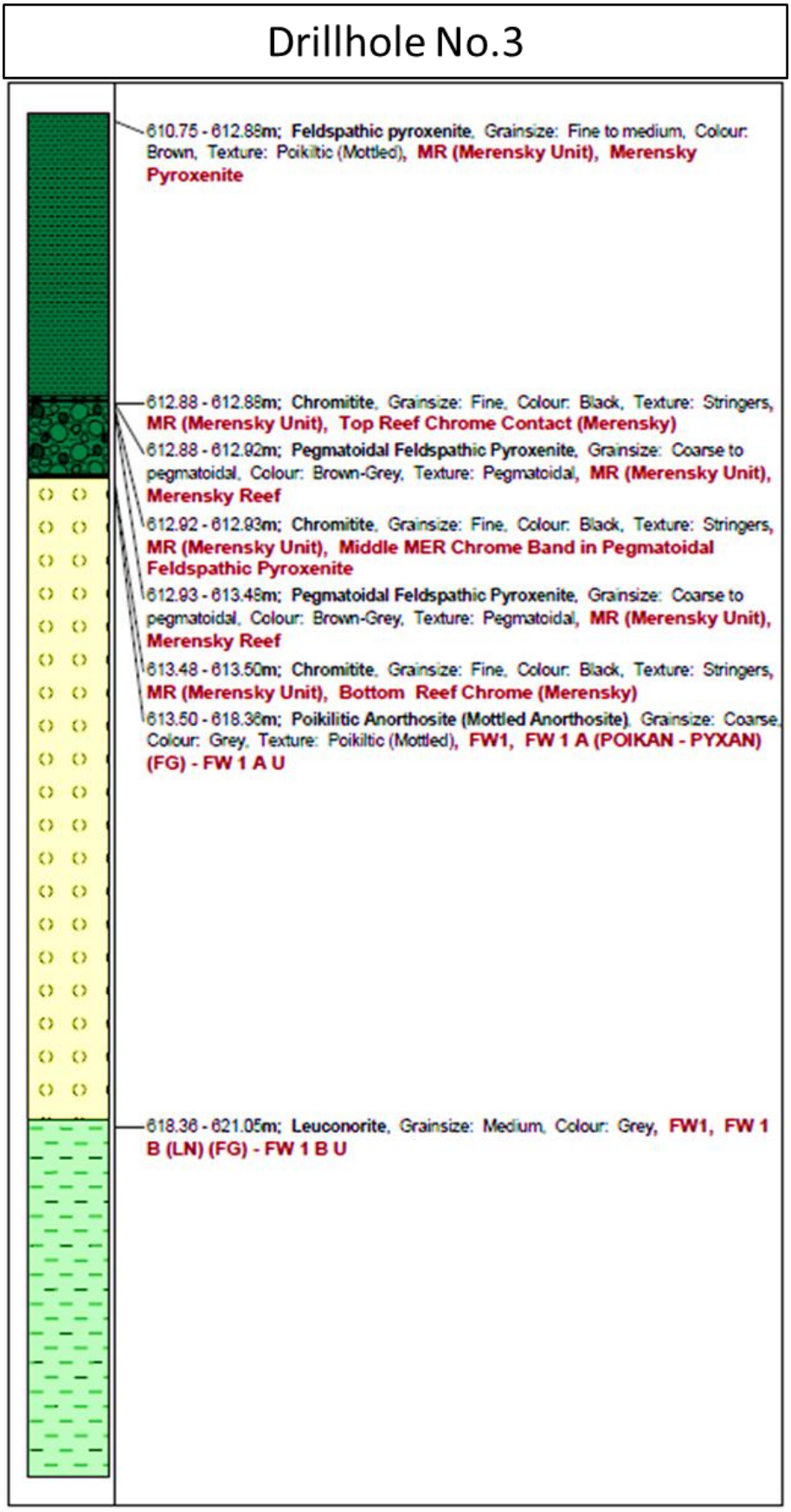

Figure 97. Drillhole No.3 used for Core Analysis

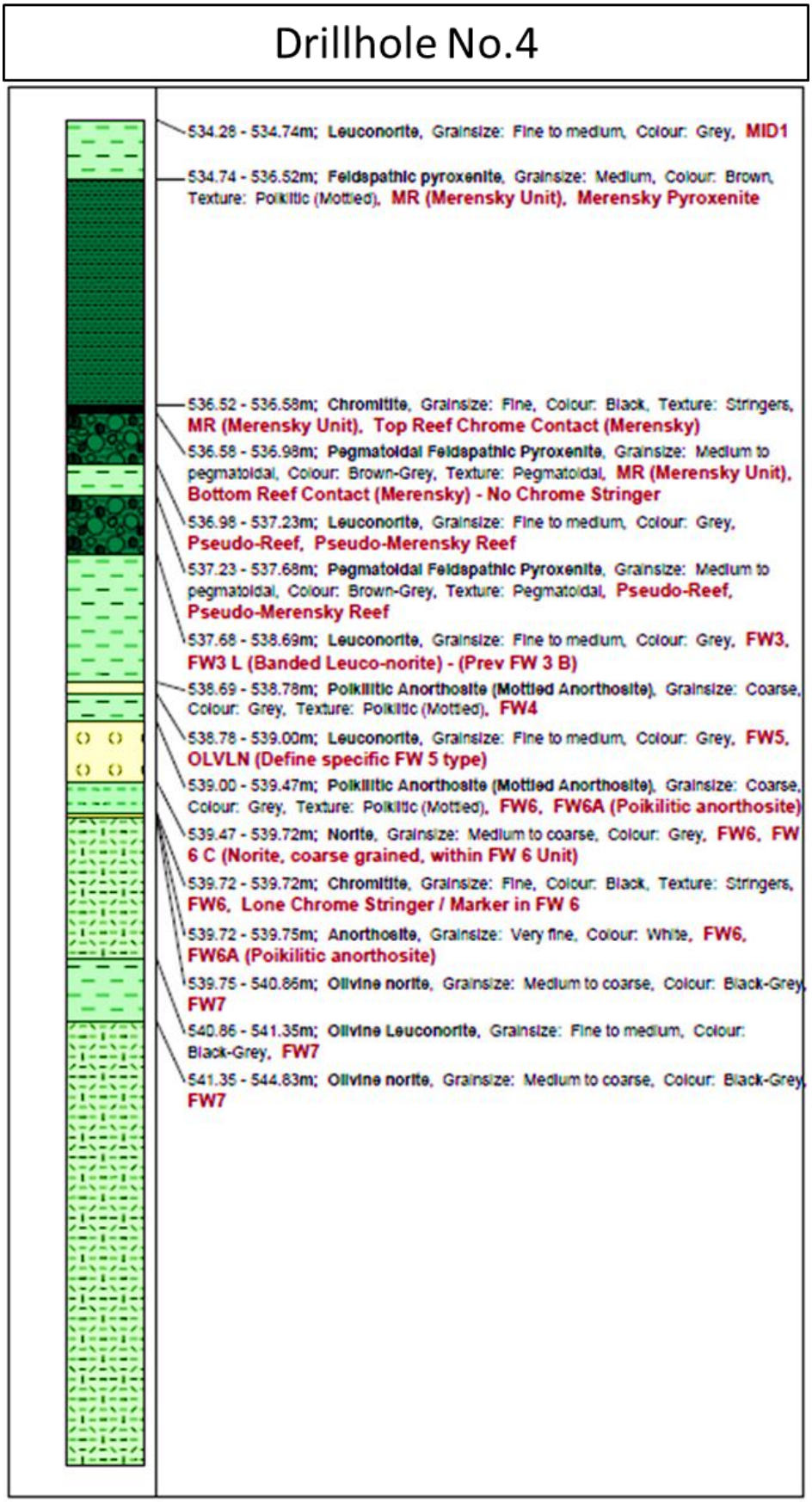

Figure 98. Drillhole No.4 used for Core Analysis

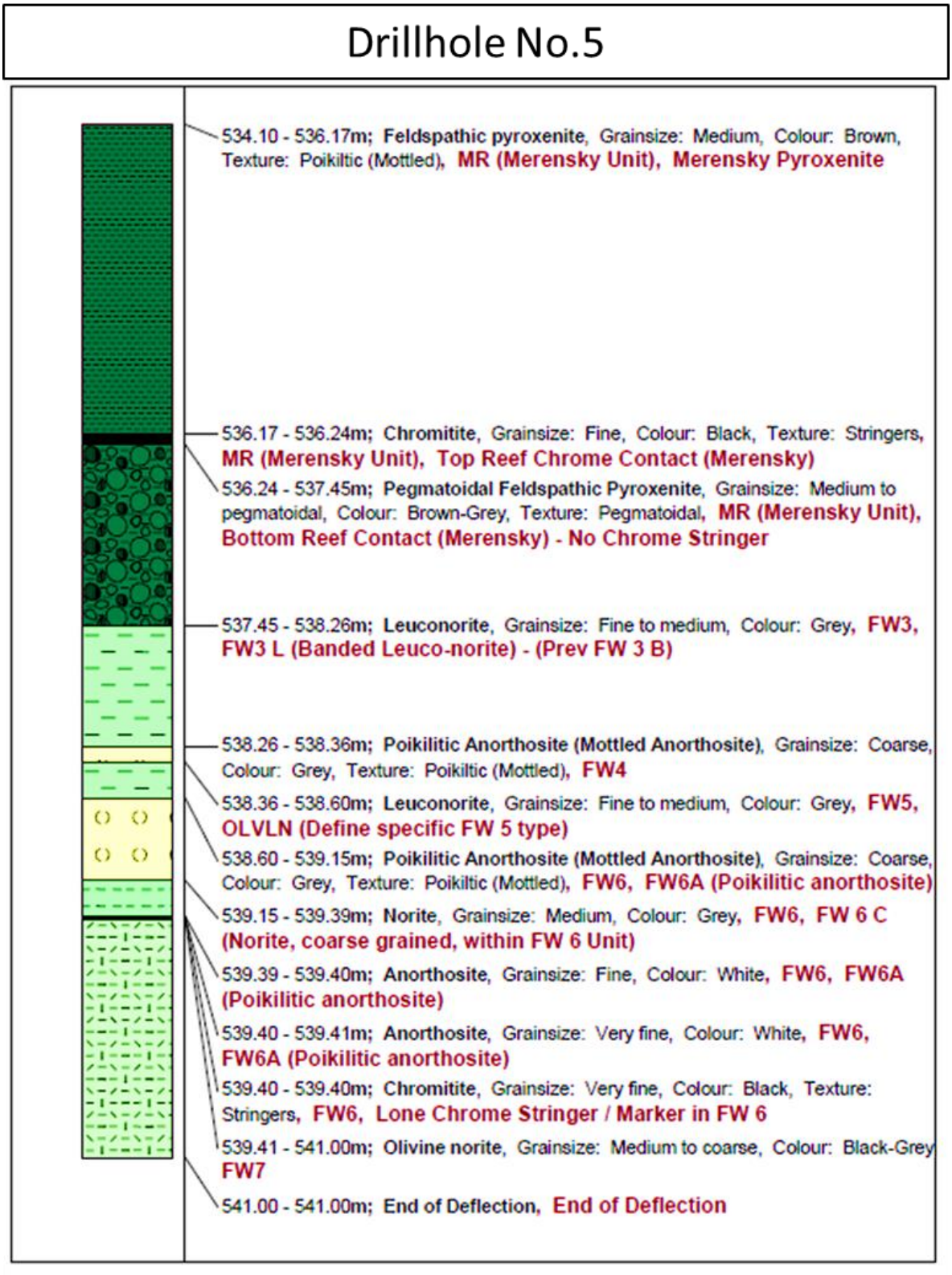

Figure 99. Drillhole No.5 used for Core Analysis